Federated Learning under Covariate Shifts with Generalization Guarantees

Anonymous authors
Paper under double-blind review

Abstract

This paper addresses intra-client and inter-client covariate shifts in federated learning (FL) with a focus on the overall generalization performance. To handle covariate shifts, we formulate a new global model training paradigm and propose Federated Importance-weighteD Empirical risk Minimization (FIDEM) along with improving density ratio matching methods without requiring perfect knowledge of the supremum over true ratios. We also propose the communication-efficient variant FIIDEM with the same level of privacy guarantees as those of classical ERM in FL. We theoretically show that FIDEM achieves smaller generalization error than classical ERM under certain settings. Experimental results demonstrate the superiority of FIDEM over existing FL baselines in challenging imbalanced federated settings in terms of data distribution shifts across clients.

1 Introduction

Federated learning (FL) (Li et al., 2020; Kairouz et al., 2021; Wang et al., 2021) is an efficient and powerful paradigm to collaboratively train a shared machine learning model among multiple clients, such as hospitals and cellphones, without sharing local data.

Existing FL literature mainly focuses on training a model under the classical empirical risk minimization (ERM) paradigm in learning theory, with implicitly assuming that the training and test data distributions of each client are the same. However, this stylized setup overlooks the specific requirements of each client. Statistical heterogeneity is a major challenge for FL, which has been mainly studied in terms of non-identical data distributions across clients, i.e., inter-client distribution shifts (Li et al., 2020; Kairouz et al., 2021; Wang et al., 2021). Even for a single client, the distribution shift between training and test data, i.e., intra-client distribution shift, has been a major challenge for decades (Wang & Deng 2018; Kouw & Loog 2019, and references therein). For instance, scarce disease data for training and test in a local hospital can be different. To adequately address the statistical heterogeneity challenge in FL, we need to handle both intra-client and inter-client distribution shifts under stringent requirements in terms of privacy and communication costs.

We focus on the *overall generalization performance* on multiple clients by considering both intra-client and inter-client distribution shifts. There exist three major challenges to tackle this problem: 1) how to modify the classical ERM to obtain an unbiased estimate of an overall true risk minimizer under intra-client and inter-client distribution shifts; 2) how to develop an efficient density ratio estimation method under stringent privacy requirements of FL; 3) are there theoretical guarantees for the modified ERM under the improved density ratio method in FL?

We aim to address the above challenges in our new paradigm for FL. For description simplicity, in our problem setting, we focus on covariate shift, which is the *most commonly used and studied* in *theory* and *practice* in distribution shifts (Sugiyama et al., 2007; Kanamori et al., 2009; Kato & Teshima, 2021; Uehara et al., 2020; Tripuraneni et al., 2021; Zhou & Levine, 2021).[1] To be specific, for any client k, covariate shift assumes the conditional distribution $p_k^{\mathrm{tr}}(\mathbf{y}|\mathbf{x}) = p_k^{\mathrm{te}}(\mathbf{y}|\mathbf{x}) := p(\mathbf{y}|\mathbf{x})$ remains the same; while marginal distributions $p_k^{\mathrm{tr}}(\mathbf{x})$ and $p_k^{\mathrm{te}}(\mathbf{x})$ can be arbitrarily different, which gives rise to intra-client and inter-client *covariate shifts*. Handling covariate shift is a challenging issue, especially in federated settings (Kairouz et al., 2021).

[1] Our results can be extended to other typical distribution shifts, e.g., target shift (Azizzadenesheli, 2022). We provide experimental results on target shift in Section 5.

To this end, motivated by Sugiyama et al. (2007) under the classical covariate shift setting, we propose Federated Importance-weighteD Empirical risk Minimization (FIDEM), that considers covariate shifts across multiple clients in FL. We show that the learned global model under intra/inter-client covariate shifts is still unbiased in terms of minimizing the overall true risk, i.e., FIDEM is *consistent* in FL. To handle covariate shifts accurately, we propose a histogram-based density ratio matching method (DRM) under both intra/inter-client distribution shifts. Our method unifies well-known DRMs in FL, which has its own interest in the distribution shift community for ratio estimation (Zadrozny, 2004; Huang et al., 2006; Sugiyama et al., 2007; Kanamori et al., 2009; Sugiyama et al., 2012; Zhang et al., 2020; Kato & Teshima, 2021). To fully eliminate *any privacy risks*, we introduce another variant of FIDEM, termed as Federated Independent Importance-weighteD Empirical risk Minimization (FIIDEM). It does not require any form of data sharing among clients and preserves the *same level of privacy* and *same communication costs* as those of baseline federated averaging (FedAvg) (McMahan et al., 2017). An overview of FIDEM is shown in Fig. 1.

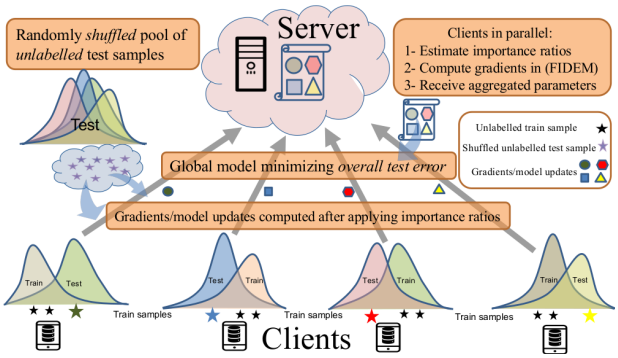

Figure 1: An overview of FIDEM. Marginal train and test distributions of clients are arbitrarily different leading to intra-client and inter-client *covariate shifts*. To control privacy leakage, the server *randomly shuffles* unlabelled test samples and broadcasts to the clients.

1.1 Technical challenges and contributions

Learning on multiple clients in FL under covariate shifts via importance-weighted ERM is challenging due to multiple data owners with own learning objectives, multiple potential but unpredictable train/test shift scenarios, privacy, and communication costs (Kairouz et al., 2021). To be specific,
1) It is non-trivial to control privacy leakage to other clients while estimating ratios and relax the requirement to have perfect estimates of the supremum over true ratios, which is a key step for non-negative BD (nnBD) DRM. Our work is the first step towards handling inter/inter-client distribution shifts in FL;
2) It is challenging to obtain per-client bounds on ratio estimation error for a general nnBD DRM with multiple clients and imperfect estimates of the supremum due to intra/inter-client couplings in ratios. Note that, even if we have access to perfect estimates of density ratios, it is still unclear whether importance-weighted ERM results in smaller excess risk compared to classical ERM. Our work gives an initial attempt by providing an affirmative answer for ridge regression;
3) While well-established benchmarks for multi-client FL have been used, they are usually designed in a way that each client's test samples are drawn uniformly from a set of classes. However, we believe this might not be the case in real-world applications and then design realistic experimental settings in our work.

To address those technical challenges, we

- Algorithmically propose an intuitive framework to minimize average *test error* in FL, design efficient mechanisms to control privacy leakage while estimating ratios (FIDEM) along with a privacy-preserving and communication-efficient variant (FIIDEM), and improve nnBD DRM under FL without requiring perfect knowledge of the supremum over true ratios.

- Theoretically establish high-probability guarantees on ratio estimation error for general nnBD DRM with multiple clients under imperfect estimates of the supremum, which unifies a number of DRMs, and show benefits of importance weighting in terms of excess risk decoupled from density ratio estimation through bias-variance decomposition.

- Experimentally demonstrate more than 16% overall test accuracy improvement over existing FL baselines when training ResNet-18 (He et al., 2016) on CIFAR10 (Krizhevsky) in challenging imbalanced federated settings in terms of data distribution shifts across clients.

In conclusion, we expand the concept and application scope of FL to a general setting under intra/inter-client covariate shifts, provide an in-depth theoretical understanding of learning with FIDEM via a general DRM, and experimentally validate the utility of the proposed framework. We hope that our work opens the door to a new FL paradigm.

1.2 Related work

In this section, we overview a summary of related work. See Appendix B for complete discussion.

Federated learning. The current FL literature largely focuses on minimizing the empirical risk, under the same training/test data distribution assumption over each client (Li et al., 2020; Kairouz et al., 2021; Wang et al., 2021). Statistical heterogeneity across clients in training-time is handled using heuristics-based personalization methods that typically do not have a statistical learning theoretical support (Smith et al., 2017; Khodak et al., 2019; Li et al., 2021b). In contrast, we focus on learning under both intra-client and inter-client covariate shifts. Communication-efficient, robust, and secure aggregations can be viewed as complementary technologies, which can be used along with FIDEM to improve FIDEM's scalability and security while addressing overall generalization. Our theory focuses on cross-silo FL where a number of trustworthy and available clients under intra/inter-client covariate shifts learn a global model collaboratively, and our experiments extend to scenarios with 100 clients and client partial participation.

Importance-weighted ERM and density ratio matching. Shimodaira (2000) introduced covariate shift where the input train and test distributions are different while the conditional distribution of the output variable given the input variable remains unchanged. Importance-weighted ERM is widely used to improve generalization performance under covariate shift (Zadrozny, 2004; Sugiyama & Müller, 2005; Huang et al., 2006; Sugiyama et al., 2007; Kanamori et al., 2009; Sugiyama et al., 2012; Fang et al., 2020; Zhang et al., 2020; Kato & Teshima, 2021). Sugiyama et al. (2012) proposed a Bregman divergence-based DRM, which unifies various DRMs. Kato & Teshima (2021) proposed a non-negative Bregman divergence-based DRM when using deep neural networks for density ratio estimation. Our work largely differs from Kato & Teshima (2021) in our *problem setting* that allows multiple clients, *algorithm design* to estimate different ratios across clients while controlling privacy leakage, and *theoretical analyses* to show the benefit of importance weighting in generalization.

Domain adaptation. Distribution shifts between a source and a target domain have been a prominent problem in machine learning for several decades (Wang & Deng, 2018; Kouw & Loog, 2019). The premise behind such shifts is that data is frequently biased, and this results in distribution shifts that can be estimated by assuming some (unlabelled) knowledge of the target distribution. The following two categories of domain adaptation methods are most closely related to our work: a) sample-based, and b) feature-based methods. In feature-based methods, the goal is to find a transformation that maps the source samples to target samples (Ganin et al., 2016; Bousmalis et al., 2017; Das & Lee, 2018; Damodaran et al., 2018). Sample-based methods aim at minimizing the target risk through data in the source domain. Importance weighting is often used in sample-based methods (Shimodaira, 2000; Jiang & Zhai, 2007; Baktashmotlagh et al., 2014). However, the focus on domain adaptation has been mainly to adapt to a single target distribution, not the overall generalization performance on multiple clients, which is addressed in this paper.

Statistical generalization and excess risk bounds. Understanding generalization performance of learning algorithms is one essential topic in modern machine learning. Typical techniques to establish generalization guarantees include uniform convergence by Rademacher complexity (Bartlett, 1998), and its variants (Bartlett et al., 2005), bias-variance decomposition (Geman et al., 1992; Adlam & Pennington, 2020), PAC-Bayes (McAllester, 1999), and stability-based analysis (Bousquet & Elisseeff, 2002; Shalev-Shwartz et al., 2010). Our work employs the first two techniques to analyze our density ratio estimation method in a federated setting and establish generalization guarantees for FIDEM, respectively. Rademacher complexity has been used in FL to obtain theoretical guarantees on the centralized model (Mohri et al., 2019) and personalized model (Mansour et al., 2020). These work are different from our setting our setting where we consider multiple test distributions under different training/test data distributions for clients and focus on the

overall test error. Bias-variance decomposition is typically studied in two settings, i.e., the fixed and random design setting, which is categorized by whether the (training) data are fixed or random. This technique has been extensively applied in least squares (Hsu et al., 2012; Dieuleveut et al., 2017), analysis of SGD (Jain et al., 2018; Zou et al., 2021), and double descent (Adlam & Pennington, 2020).

Notation: We use $\mathbb{E}[\cdot]$ to denote the expectation and $\|\cdot\|$ to represent the Euclidean norm of a vector. We use lower-case bold font to denote vectors. Sets and scalars are represented by calligraphic and standard fonts, respectively. We use $[n]$ to denote $\{1,\dots,n\}$ for an integer n. We use $\lesssim$ to ignore terms up to constants and logarithmic factors.

2 Covariate shift and FIDEM for FL

We first provide the problem setting under intra/inter client covariate shifts, and then describe the proposed FIDEM as an unbiased estimate in terms of minimizing the overall true risk[2].

2.1 Problem setting

Let $\mathcal{X} \subseteq \mathbb{R}^{d_{\mathbf{x}}}$ be a compact metric space, $\mathcal{Y} \subseteq \mathbb{R}^{d_{\mathbf{y}}}$, and K be the number of clients in an FL setting. Let $\mathcal{S}_k = \{(\mathbf{x}^{\text{tr}}_{k,i}, \mathbf{y}^{\text{tr}}_{k,i})\}_{i=1}^{n^{\text{tr}}_k}$ denote the training set of client k with n^{tr}_k samples drawn i.i.d from an unknown probability distribution p^{tr}_k on $\mathcal{X} \times \mathcal{Y}$.[3] The test data of client k, is drawn from another unknown probability distribution p^{te}_k on $\mathcal{X} \times \mathcal{Y}$. Under the covariate shift setting (Sugiyama et al., 2007; Kanamori et al., 2009; Kato & Teshima, 2021; Uehara et al., 2020; Tripuraneni et al., 2021; Zhou & Levine, 2021), the conditional distribution $p^{\text{tr}}_k(\mathbf{y}|\mathbf{x}) = p^{\text{te}}_k(\mathbf{y}|\mathbf{x}) := p(\mathbf{y}|\mathbf{x})$ is assumed to be the same for all k, while $p^{\text{tr}}_k(\mathbf{x})$ and $p^{\text{te}}_k(\mathbf{x})$ can be arbitrarily different, which gives rise to intra-client and inter-client covariate shifts. We consider supervised learning where the goal is to find a hypothesis $h_{\mathbf{w}} : \mathcal{X} \to \mathcal{Y}$, parameterized by $\mathbf{w} \in \mathbb{R}^d$ e.g., weights and biases of a neural network, such that $h_{\mathbf{w}}(\mathbf{x})$ (for short $h(\mathbf{x})$) is a good approximation of the label $\mathbf{y} \in \mathcal{Y}$ corresponding to a new sample $\mathbf{x} \in \mathcal{X}$. Let $\ell : \mathcal{X} \times \mathcal{Y} \to \mathbb{R}_+$ denote a loss function. In our FL setting, the true (expected) risk of client k is given by $R_k(h_{\mathbf{w}}) = \mathbb{E}_{(\mathbf{x},\mathbf{y})\sim p^{\text{te}}_k(\mathbf{x},\mathbf{y})}[\ell(h_{\mathbf{w}}(\mathbf{x}), \mathbf{y})]$.

2.2 FIDEM for FL under covariate shift

For a scenario with K clients, we first focus on minimizing R_l ($l \in [K]$) under intra/inter-client covariate shifts, i.e., $p^{\text{tr}}_k(\mathbf{x}) \neq p^{\text{te}}_l(\mathbf{x})$ for all k. We then formulate FIDEM to minimize the average test error over K clients under covariate shifts by optimizing a global model under our FL setting.

FIDEM for one client. Under $p^{\text{tr}}_k(\mathbf{x}) \neq p^{\text{te}}_l(\mathbf{x})$ $\forall k$, FIDEM focusing on minimizing R_l is given by:

$$\min_{\mathbf{w}\in\mathbb{R}^d} \sum_{k=1}^{K} \frac{1}{n^{\text{tr}}_k} \sum_{i=1}^{n^{\text{tr}}_k} \frac{p^{\text{te}}_l(\mathbf{x}^{\text{tr}}_{k,i})}{p^{\text{tr}}_k(\mathbf{x}^{\text{tr}}_{k,i})} \ell(h_{\mathbf{w}}(\mathbf{x}^{\text{tr}}_{k,i}), \mathbf{y}^{\text{tr}}_{k,i}) \,. \tag{2.1}$$

In Appendix C, we elaborate on four special cases of the above scenario, i.e., $p^{\text{tr}}_k(\mathbf{x}) \neq p^{\text{te}}_l(\mathbf{x})$ $\forall k$, focusing on one client under various covariate shifts and formulate their FIDEM's.

Proposition 1. *Let $l \in [K]$. FIDEM in Eq. (2.1) is consistent. i.e., the learned function converges in probability to the optimal function in terms of minimizing R_l.*

See Appendix C for the proof. Proposition 1 implies that, under intra/inter-client covariate shifts, FIDEM outputs an unbiased estimate of a true risk minimizer of client l. In Appendix C.1, we show usefulness of importance weighting under no intra-client covariate shifts but inter-client covariate shifts, which is a special and important case of our setting.

Building on Eq. (2.1) that aims to minimize R_l, we now formulate FIDEM to minimize the average test error over all clients and explain its costs and benefits for federated settings.

[2]Notations are provided in Appendix A.

[3]For notational simplicity, we use the same notation for probability distributions and density functions.

FIDEM for K clients. Let $\mathbf{w}$ be the global model. For K clients under intra/inter-clinet covariate shifts, FIDEM minimizes the average test error over all clients and is formulated as:

$$\min_{\mathbf{w}\in\mathbb{R}^d} F(\mathbf{w}) := \sum_{k=1}^{K} F_k(\mathbf{w}) \ , \tag{FIDEM}$$

where

$$F_k(\mathbf{w}) = \frac{1}{n_k^{\mathrm{tr}}} \sum_{i=1}^{n_k^{\mathrm{tr}}} \frac{\sum_{l=1}^{K} p_l^{\mathrm{te}}(\mathbf{x}_{k,i}^{\mathrm{tr}})}{p_k^{\mathrm{tr}}(\mathbf{x}_{k,i}^{\mathrm{tr}})} \ell(h_{\mathbf{w}}(\mathbf{x}_{k,i}^{\mathrm{tr}}), \mathbf{y}_{k,i}^{\mathrm{tr}}). \tag{2.2}$$

Each client requires an estimate of a ratio in the form of sum test over own train. We emphasize that $F_k(\mathbf{w})$ should *not* be viewed as the local loss function of client k. Our formulation FIDEM is meant to minimize the overall test error over all clients given intra/inter-client covariate shifts. To solve FIDEM, we employ the stochastic gradient descent (SGD) algorithm for T iterations starting from an initial parameter $\mathbf{w}_0$: $\mathbf{w}_{t+1} = \mathbf{w}_t - \eta_t \sum_{k=1}^{K} \mathbf{g}_k(\mathbf{w}_t)$ where $\eta_t > 0$ is the step size, $\mathbf{g}_k(\mathbf{w}_t)$ is an unbiased estimate of $\nabla_{\mathbf{w}} F_k(\mathbf{w}_t)$, and $\mathbf{w}_T$ is the output.

Under no covariate shift, both FIDEM and classical ERM result in the same solution, which is a minimizer of the overall *empirical risk*. The main difference happens under intra-client and inter-client covariate shifts. In those challenging settings, FIDEM's solution is an unbiased estimate of a minimizer of the overall *true risk*, while the solution of ERM minimizes the overall *empirical risk*.

2.3 Privacy, communication, and computation in FL

Privacy and communication efficiency are major concerns in FL (Kairouz et al., 2021). We elaborate on them and introduce another variant of FIDEM with the same guarantees and costs as FedAvg.

Communication/computational costs and security benefits. Compared to classical ERM, the communication/computational overhead of FIDEM is negligible.[4] To solve FIDEM, client k should compute an unbiased estimate of the weighted gradient $\nabla_{\mathbf{w}} F_k(\mathbf{w}_t)$, which requires a single backward pass at a single parameter $\mathbf{w} = \mathbf{w}_t$. Hence, given the ratios, there is no extra computational/communication overhead compared to classical ERM. Clients compute the ratios in parallel. In Appendix E, we provide a concrete example and show that the number of communication bits needed during training in standard FL is usually many orders of magnitudes larger than the size of samples shared for estimating the ratios. To further reduce communication costs of density ratio estimation and gradient aggregation, compression methods such as quantization, sparsification, and local updating rules, can be used along with FIDEM on the fly. More importantly, due to *importance weighting*, $\mathbf{g}_k(\mathbf{w})$ can be arbitrarily different from an unbiased stochastic gradient of classical ERM for client k, *i.e.,* $\frac{1}{n_k^{\mathrm{tr}}} \sum_{i=1}^{n_k^{\mathrm{tr}}} \nabla_{\mathbf{w}} \ell(h_{\mathbf{w}}(\mathbf{x}_{k,i}^{\mathrm{tr}}), \mathbf{y}_{k,i}^{\mathrm{tr}})$. The formulation FIDEM makes it impossible for an adversary to apply gradient inversion attack and obtain private training data of clients (Zhu et al., 2019). In particular, the attacker cannot find the vanilla (stochastic) gradients and reconstructs data unless the attacker has a perfect knowledge of the ratio $r_k(\mathbf{x}) = \sum_{l=1}^{K} p_l^{\mathrm{te}}(\mathbf{x}) / p_k^{\mathrm{tr}}(\mathbf{x})$.

Privacy. Given $\{r_k(\mathbf{x})\}_{k=1}^{K}$, FIDEM efficiently minimizes the overall test error over all clients in a privacy-preserving manner. To estimate those ratios, if clients can tolerate some level of privacy leakage, clients send unlabelled samples $\mathbf{x}_{l,j}^{\mathrm{te}}$ for $l \in [K]$ and $j \in [n^{\mathrm{te}}]$ from their test distributions. To control privacy leakage to other clients, we propose that the server *randomly shuffles* these unlabelled samples before broadcasting to clients. In Appendix Q, we discuss an alternative method instead of sending original unlabelled samples and discuss its limitations.

To fully *eliminate any privacy risks* compared to classical ERM, clients may opt to minimize the following surrogate objective, which we name *Federated Independent Importance-weighteD Empirical risk Minimization*

[4] The analyses of computational/communication overheads are provided in Appendices P and E, respectively.

(FIIDEM):

$$\min_{\mathbf{w}} \tilde{F}(\mathbf{w}) := \sum_{k=1}^{K} \frac{1}{n_k^{\mathrm{tr}}} \sum_{i=1}^{n_k^{\mathrm{tr}}} \frac{p_k^{\mathrm{te}}(\mathbf{x}_{k,i}^{\mathrm{tr}})}{p_k^{\mathrm{tr}}(\mathbf{x}_{k,i}^{\mathrm{tr}})} \ell(h_{\mathbf{w}}(\mathbf{x}_{k,i}^{\mathrm{tr}}), \mathbf{y}_{k,i}^{\mathrm{tr}}). \tag{FIIDEM}$$

The formulation FIIDEM preserves the *same level of privacy* and *same communication costs* as those of classical ERM, e.g., FedAvg. However, to exploit the entire data distributed among all clients and achieve the optimal global model in terms of overall test error, clients need to compromise some level of privacy and share unlabelled test samples with the server. Hence, in this paper, we focus on the original objective in FIDEM.

3 Ratio estimation for FL under covariate shift

To solve FIDEM, client k should have access to an accurate estimate of this ratio

$$r_k(\mathbf{x}) = \frac{\sum_{l=1}^{K} p_l^{\mathrm{te}}(\mathbf{x})}{p_k^{\mathrm{tr}}(\mathbf{x})}. \tag{3.1}$$

Ratio estimation is a key step for importance weighting (Sugiyama et al., 2007; 2012). The discrepancy between the true ratio r_k^* for client k in Eq. (3.1) and the estimated one r_k using our ratio model can be measured by $\mathbb{E}_{p_k^{\mathrm{tr}}}[\mathrm{BD}_f(r_k^*(\mathbf{x}) \parallel r_k(\mathbf{x}))]$ where the Bregman divergence (BD) associated with a strictly convex f leads to BD-based DRMs (Kato & Teshima, 2021; Kiryo et al., 2017):

Definition 1 (Bregman 1967)**.** *Let $\mathcal{B}_f \subset [0, \infty)$ and $f : \mathcal{B}_f \to \mathbb{R}$ be a strictly convex function with bounded gradient. The BD associated with f from $\tilde{z}$ to z is given by* $\mathrm{BD}_f(\tilde{z} \parallel z) = f(\tilde{z}) - f(z) - \nabla f(z)(\tilde{z} - z)$.

Note that $\mathrm{BD}_f(\tilde{z} \parallel z)$ is a convex function w.r.t. $\tilde{z}$; however, it is not necessarily convex w.r.t. z. Motivated by Kato & Teshima (2021); Kiryo et al. (2017), we propose a new histogram-based DRM (HDRM) for FL with multiple clients. HDRM overcomes the over-fitting issue (Kiryo et al., 2017; Kato & Teshima, 2021) while providing an estimate for the upper bound $\overline{r}_k = \sup_{\mathbf{x} \in \mathcal{X}^{\mathrm{tr}}} r_k^*(\mathbf{x})$, which is a key step for non-negative BD (nnBD) DRM. We now extend nnBD DRM to FL settings.

3.1 Extension of nnBD DRM to FL

We assume that $p_k^{\mathrm{tr}}(\mathbf{x}^{\mathrm{tr}}) > 0$ for $k \in [K]$ and all $\mathbf{x}^{\mathrm{tr}} \in \mathcal{X}^{\mathrm{tr}} \subseteq \mathcal{X}$ with $\mathcal{X}^{\mathrm{te}} \subseteq \mathcal{X}^{\mathrm{tr}}$, i.e., we need a common data domain with strictly positive train density, which is a common assumption (Kanamori et al., 2009; Kato & Teshima, 2021). Let $\mathcal{H}_r \subset \{r : \mathcal{X} \to \mathcal{B}_f\}$ denote a hypothesis class for our ratios r_k, e.g., neural networks with a given architecture. Our goal is to estimate r_k by minimizing the discrepancy $\mathbb{E}_{p_k^{\mathrm{tr}}}[\mathrm{BD}_f(r_k^*(\mathbf{x}) \parallel r_k(\mathbf{x}))]$, which leads to BD-based DRM for FL and is formulated in Appendix D.2. Let $\{\mathbf{x}_{k,i}^{\mathrm{tr}}\}_{i=1}^{n_k^{\mathrm{tr}}}$ and $\{\mathbf{x}_{l,j}^{\mathrm{te}}\}_{j=1}^{n^{\mathrm{te}}}$ denote unlabelled samples drawn i.i.d from distributions p_k^{tr} and p_l^{te}, respectively, for $l \in [K]$. Standard BD-based DRM is shown to suffer from an over-fitting issue where $-\frac{1}{n^{\mathrm{te}}} \sum_{j=1}^{n^{\mathrm{te}}} \nabla f(r_k(\mathbf{x}_{l,j}^{\mathrm{te}}))$ diverges if there is no lower bound on this term (Kiryo et al., 2017; Kato & Teshima, 2021). To resolve this issue in FL, we consider non-negative BD (nnBD) DRM for client k, *i.e.,* $\min_{r_k \in \mathcal{H}_r} \hat{\mathcal{E}}_f^+(r_k)$ where

$$\hat{\mathcal{E}}_f^+(r_k) = \mathrm{ReLU}\Big(\frac{1}{n_k^{\mathrm{tr}}} \sum_{i=1}^{n_k^{\mathrm{tr}}} \ell_1(r_k(\mathbf{x}_{k,i}^{\mathrm{tr}})) - \frac{C_k}{n^{\mathrm{te}}} \sum_{j=1}^{n^{\mathrm{te}}} \sum_{l=1}^{K} \ell_1(r_k(\mathbf{x}_{l,j}^{\mathrm{te}}))\Big) + \frac{1}{n^{\mathrm{te}}} \sum_{j=1}^{n^{\mathrm{te}}} \sum_{l=1}^{K} \ell_2(r_k(\mathbf{x}_{l,j}^{\mathrm{te}})), \tag{3.2}$$

$\mathrm{ReLU}(z) = \max\{0, z\}$, $0 < C_k < \frac{1}{\overline{r}_k}$, $\overline{r}_k = \sup_{\mathbf{x} \in \mathcal{X}^{\mathrm{tr}}} r_k^*(\mathbf{x})$, $\ell_1(z) = \nabla f(z) z - f(z)$, and $\ell_2(z) = C(\nabla f(z) z - f(z)) - \nabla f(z)$. Intuitively, ReLU is used for non-negativity and $0 < C_k < \frac{1}{\overline{r}_k}$ acts as a regularization parameter. Substituting different f's into Eq. (3.2) leads to different variants of nnBD, which covers previous work (Basu et al., 1998; Hastie et al., 2001; Gretton et al., 2009; Nguyen et al., 2010; Kato et al., 2019). We provide explicit expressions of those variants for client k in Appendix H. In this work, we focus on $f(z) = \frac{(z-1)^2}{2}$ leading to the well-known least-squares importance fitting (LSIF) variant of nnBD for client k.

Input: Samples $\{\{\mathbf{x}_{k,i}^{\mathrm{tr}}\}_{i=1}^{n_k^{\mathrm{tr}}}\}_{k=1}^{K}$, $\{\{\mathbf{x}_{l,j}^{\mathrm{te}}\}_{j=1}^{n^{\mathrm{te}}}\}_{l=1}^{K}$, learning rate α, regularization $\Lambda(r)$ and regularization coefficient λ.

Output: Ratio model parameters $\{\boldsymbol{\theta}_{r_k}\}_{k=1}^{K}$.

for $k = 1$ ***to*** K *(in parallel)* **do**
  Send n^{te} samples to the server ;
Server randomly shuffles and broadcasts samples $\{\{\mathbf{x}_{l,j}^{\mathrm{te}}\}_{j=1}^{n^{\mathrm{te}}}\}_{l=1}^{K}$ to clients ;
for $k = 1$ ***to*** K *(in parallel)* **do**
  Create M bins and compute $\tilde{r}_{k,m} = \frac{1/n^{\mathrm{te}} \sum_{j=1}^{n^{\mathrm{te}}} \sum_{l=1}^{K} \mathbb{1}(\mathbf{x}_{l,j}^{\mathrm{te}} \in \mathcal{B}_m)}{1/n_k^{\mathrm{tr}} \sum_{i=1}^{n_k^{\mathrm{tr}}} \mathbb{1}(\mathbf{x}_{k,i}^{\mathrm{tr}} \in \mathcal{B}_m)}$;
  Estimate $C_k = \frac{1}{\max\{\tilde{r}_{k,1},\ldots,\tilde{r}_{k,M}\}}$;
for $t = 1$ ***to*** T **do**
  for $k = 1$ ***to*** K *(in parallel)* **do**
    for $n = 1$ ***to*** N_k **do**
      if $\frac{1}{B_k^{\mathrm{tr}}} \sum_{i=1}^{B_k^{\mathrm{tr}}} \ell_1(r_k(\mathbf{x}_{k,n,i}^{\mathrm{tr}})) - \frac{KC_k}{B_k^{\mathrm{te}}} \sum_{j=1}^{B_k^{\mathrm{te}}} \ell_1(r_k(\mathbf{x}_{k,n,j}^{\mathrm{te}})) \geq 0$ **then**
        $\mathbf{g}_k = -\nabla_{\boldsymbol{\theta}_r} \Big(\frac{1}{B_k^{\mathrm{tr}}} \sum_{i=1}^{B_k^{\mathrm{tr}}} \ell_1(r_k(\mathbf{x}_{k,n,i}^{\mathrm{tr}})) - \frac{KC_k}{B_k^{\mathrm{te}}} \sum_{j=1}^{B_k^{\mathrm{te}}} \ell_1(r_k(\mathbf{x}_{k,n,j}^{\mathrm{te}})) + \frac{K}{B_k^{\mathrm{te}}} \sum_{j=1}^{B_k^{\mathrm{te}}} \ell_2(r_k(\mathbf{x}_{k,n,j}^{\mathrm{te}})) + \frac{\lambda}{2}\Lambda(r_k) \Big)$;
      else
        $\mathbf{g}_k = \nabla_{\boldsymbol{\theta}_r} \Big(\frac{1}{B_k^{\mathrm{tr}}} \sum_{i=1}^{B_k^{\mathrm{tr}}} \ell_1(r_k(\mathbf{x}_{k,n,i}^{\mathrm{tr}})) - \frac{KC_k}{B_k^{\mathrm{te}}} \sum_{j=1}^{B_k^{\mathrm{te}}} \ell_1(r_k(\mathbf{x}_{k,n,j}^{\mathrm{te}})) + \frac{\lambda}{2}\Lambda(r_k) \Big)$;
      Update ratio model parameters $\boldsymbol{\theta}_{r_k} = \boldsymbol{\theta}_{r_k} + \alpha \mathbf{g}_k$;

Algorithm 1: Histogram-based density ratio matching. Loops are executed in parallel on each client.

3.2 Estimation of the upper bound $\overline{r}_k$

Estimating $\overline{r}_k = \sup_{\mathbf{x} \in \mathcal{X}^{\mathrm{tr}}} r_k^*(\mathbf{x})$ is a key step for nnBD DRM. For a single train and test distribution, it is shown that overestimating $\overline{r}$ leads to significant performance degradation (Kato & Teshima, 2021, Section 5). Kato & Teshima (2021) considered C as a hyper-parameter, which can be tuned. However, obtaining an efficient estimate of $\overline{r}_k$ is desirable, in particular when training a deep model. Here we propose a histogram-based method for estimation of $\overline{r}_k$.

Let $\mathcal{B} \subset \mathcal{X}^{\mathrm{tr}}$, and assume p_k^{tr} and p_l^{te} are continuous for $l \in [K]$. Since $\mathcal{B}$ is connected and Lebesgue-measurable with finite measure, by applying intermediate value theorem (Russ, 1980), there exist $\tilde{\mathbf{x}}^{\mathrm{tr}}$ and $\hat{\mathbf{x}}^{\mathrm{te}}$ such that $\Pr\{X_k^{\mathrm{tr}} \in \mathcal{B}\} = p_k^{\mathrm{tr}}(\tilde{\mathbf{x}}^{\mathrm{tr}})\mathrm{Vol}(\mathcal{B})$ and $\sum_{l=1}^{K} \Pr\{X_l^{\mathrm{te}} \in \mathcal{B}\} = \sum_{l=1}^{K} p_l^{\mathrm{te}}(\hat{\mathbf{x}}^{\mathrm{te}})\mathrm{Vol}(\mathcal{B})$ where $\mathrm{Vol}(\mathcal{B}) = \int_{\mathbf{x} \in \mathcal{B}} \mathrm{d}\mathbf{x}$. We note that $\sup_{\mathbf{x} \in \mathcal{B}} r_k^*(\mathbf{x}) \leq \frac{\sup_{\mathbf{x} \in \mathcal{B}} \sum_{l=1}^{K} p_l^{\mathrm{te}}(\mathbf{x})}{\inf_{\mathbf{x} \in \mathcal{B}} p_k^{\mathrm{tr}}(\mathbf{x})}$ and $\frac{\sum_{l=1}^{K} p_l^{\mathrm{te}}(\hat{x}^{\mathrm{te}})}{p_k^{\mathrm{tr}}(\tilde{x}^{\mathrm{tr}})} \leq \frac{\sup_{\mathbf{x} \in \mathcal{B}} \sum_{l=1}^{K} p_l^{\mathrm{te}}(\mathbf{x})}{\inf_{\mathbf{x} \in \mathcal{B}} p_k^{\mathrm{tr}}(\mathbf{x})}$. To estimate $\overline{r}_k$, we first partition $\mathcal{X}^{\mathrm{tr}}$ into M bins where for each bin $\mathcal{B}_m$, if there exists some $\mathbf{x}_{k,i}^{\mathrm{tr}} \in \mathcal{B}_m$, then we define $\tilde{r}_{k,m} := \frac{\sum_{l=1}^{K} \Pr\{X_l^{\mathrm{te}} \in \mathcal{B}_m\}}{\Pr\{X_k^{\mathrm{tr}} \in \mathcal{B}_m\}} \simeq \frac{\frac{1}{n^{\mathrm{te}}} \sum_{j=1}^{n^{\mathrm{te}}} \sum_{l=1}^{K} \mathbb{1}(\mathbf{x}_{l,j}^{\mathrm{te}} \in \mathcal{B}_m)}{\frac{1}{n_k^{\mathrm{tr}}} \sum_{i=1}^{n_k^{\mathrm{tr}}} \mathbb{1}(\mathbf{x}_{k,i}^{\mathrm{tr}} \in \mathcal{B}_m)}$ for $m \in [M]$. Otherwise, $\tilde{r}_{k,m} = 0$. Finally, we propose to use $C_k = \frac{1}{\tilde{r}_k}$ where $\tilde{r}_k = \max\{\tilde{r}_{k,1}, \ldots, \tilde{r}_{k,M}\}$. Convergence of $\tilde{r}_k$ to $\overline{r}_k$ is established in Appendix G. Furthermore, for high-dimensional data, an efficient implementation of HDRM using k-means clustering is provided in Appendix G.

In HDRM, K clients estimate their ratios in parallel. To be specific, clients first share unlabelled test samples with the server. The server returns the randomly shuffled pool of samples to all clients. Then clients find C_k's in parallel. Given C_k's, clients estimate their corresponding ratios in parallel. To handle high-dimensional data samples and deep ratio estimation models, we adopt a variant of SGD. For client k, we divide unlabelled samples $\{\mathbf{x}_{k,i}^{\mathrm{tr}}\}_{i=1}^{n_k^{\mathrm{tr}}}$ and $\{\mathbf{x}_{l,j}^{\mathrm{te}}\}_{j=1}^{n^{\mathrm{te}}}$ for $l \in [K]$ into N_k batches $\{\mathbf{x}_{k,n,i}^{\mathrm{tr}}\}_{i=1}^{B_k^{\mathrm{tr}}}$ and $\{\mathbf{x}_{k,n,j}^{\mathrm{te}}\}_{j=1}^{B_k^{\mathrm{te}}}$ for $n \in [N_k]$. Client k first computes $\frac{1}{B_k^{\mathrm{tr}}} \sum_{i=1}^{B_k^{\mathrm{tr}}} \ell_1(r_k(\mathbf{x}_{k,n,i}^{\mathrm{tr}})) - \frac{KC_k}{B_k^{\mathrm{te}}} \sum_{j=1}^{B_k^{\mathrm{te}}} \ell_1(r_k(\mathbf{x}_{k,n,j}^{\mathrm{te}}))$. If it becomes negative, then we apply a

gradient ascent step to increase this term. We may also opt to apply 1-norm or 2-norm regularizations. The details of the HDRM algorithm are shown in Algorithm 1.

4 Theoretical guarantees

To address learning on multiple clients in FL, it is essential to obtain per-client generalization bounds for a general nnBD DRM with imperfect estimates of $\overline{r}_k$'s. Even if we have access to perfect estimates of density ratios, it is still unclear the usefulness of importance weighting. In this section, we firstly study the high-probability guarantees on ratio estimation error of nnBD DRM under imperfect estimate of $\overline{r}_k$ in terms of BD risk. We then show the benefit of importance weighting in term of excess risk through a refined bias-variance decomposition on a ridge regression problem. Theorem 1, Lemma 1, Theorem 2 are proved in Appendix I, Appendix L, and Appendix M, respectively.

4.1 Ratio estimation error in terms of BD risk

We establish a high-probability bound on the ratio estimation error of nnBD DRM with an arbitrary f for client k in terms of BD risk given by

$$\mathcal{E}_f(r_k) = \tilde{\mathbb{E}}_k(\mathbf{x})[\ell_1(r_k(\mathbf{x}))] + \sum_{l=1}^{K} \mathbb{E}_{p_l^{\text{te}}}[\ell_2(r_k(\mathbf{x}))]\,, \tag{4.1}$$

where $\tilde{\mathbb{E}}_k := \mathbb{E}_{p_k^{\text{tr}}} - C_k \sum_{l=1}^{K} \mathbb{E}_{p_l^{\text{te}}}$. Our bound for client k depends on the Rademacher complexity (Shalev-Shwartz & Ben-David, 2014) of the hypothesis class for our density ratio model $\mathcal{H}_r \subset \{r : \mathcal{X} \to \mathcal{B}_f\}$ w.r.t. client k train distribution p_k^{tr} and all client's test distributions p_l^{te} for $l \in [K]$. Let $R_n^p(\mathcal{H})$ denotes the Rademacher complexity of function class $\mathcal{H}$ w.r.t. distribution p, formally defined as follows:

Definition 2. *Let $n \in \mathbb{Z}_+$ and p be a distribution, $\mathcal{S} = \{\mathbf{x}_1, \ldots, \mathbf{x}_n\}$ be i.i.d. random variables drawn from p, and $\mathcal{H}$ be a function class. The Rademacher complexity of $\mathcal{H}$ w.r.t. p is given by:*

$$R_n^p(\mathcal{H}) = \mathbb{E}_{\mathcal{S}}\mathbb{E}_{\boldsymbol{\sigma}}\left[\sup_{r\in\mathcal{H}} \left|\frac{1}{n}\sum_{i=1}^{n} \sigma_i r(\mathbf{x}_i)\right|\right]$$

where $\{\sigma_i\}_{i=1}^n$ are Rademacher variables uniformly chosen from $\{-1, 1\}$.

We first make the following assumptions on $\ell_1(z) = \nabla f(z)z - f(z)$ and $\ell_2(z) = C(\nabla f(z)z - f(z)) - \nabla f(z)$.

Assumption 1 (Basic assumptions on ℓ_1 and ℓ_2)**.** We assume 1) $\sup_{z\in\mathcal{B}_f} \max_{i\in\{1,2\}} |\ell_i(z)| < \infty$; 2) ℓ_1 is L_1-Lipschitz and ℓ_2 is L_2-Lipschitz on $\mathcal{X}$; 3) $\inf_{r\in\mathcal{H}_r} \tilde{\mathbb{E}}_k[\ell_1(r_k(\mathbf{x}))] > 0$ for $k \in [K]$.

The first two assumptions are satisfied if $\inf\{z|z \in \mathcal{B}_f\} > 0$ for commonly used loss functions, e.g., unnormalized Kullback– Leibler and logistic regression. The third assumption is mild, commonly used in DRM literature (Kiryo et al., 2017; Lu et al., 2020; Kato & Teshima, 2021).

Theorem 1 (High-probability ratio estimation error bound for client k)**.** *Let f be a strictly convex function with bounded gradient. Denote $\Delta_\ell := \sup_{z\in\mathcal{B}_f} \max_{i\in\{1,2\}} |\ell_i(z)|$, $\hat{r}_k := \arg\min_{r_k\in\mathcal{H}_r} \hat{\mathcal{E}}_f^+(r_k)$ and $r_k^* := \arg\min_{r_k\in\mathcal{H}_r} \mathcal{E}_f(r_k)$ where $\hat{\mathcal{E}}_f^+$ and $\mathcal{E}_f$ are defined in Eqs. (3.2) and (4.1), respectively. Suppose that ℓ_1 and ℓ_2 satisfy Assumption 1, then for any $0 < \delta < 1$, with probability at least $1 - \delta$:*

$$\mathcal{E}_f(\hat{r}_k) - \mathcal{E}_f(r_k^*) \lesssim R_{n_k^{\text{tr}}}^{p_k^{\text{tr}}}(\mathcal{H}_r) + C_k \sum_{l=1}^{K} R_{n^{\text{te}}}^{p_l^{\text{te}}}(\mathcal{H}_r) + \sqrt{\Upsilon \log \frac{1}{\delta}} + KC_k\Delta_\ell \exp\left(\frac{-1}{\Upsilon}\right) \tag{4.2}$$

where $\Upsilon = \Delta_\ell^2(1/n_k^{\text{tr}} + C_k^2 K/n^{\text{te}})$.

Remark 1. Theorem 1 provides generalization guarantees for a general nnBD DRM in a federated setting under a strictly convex f with bounded gradient. We make the following remarks.
1) Our results are general to cover various ratio models. For example, in Corollary 1 of Appendix J, we consider

neural networks with depth L and bounded Frobenius norm $\|\mathbf{W}_i\|_F \leq \Delta_{\mathbf{W}_i}$ and establish explicit ratio estimation error bounds for client k in $\mathcal{O}\big(\sqrt{L}\prod_{i=1}^{L}\Delta_{\mathbf{W}_i}(1/\sqrt{n_k^{\mathrm{tr}}}+K/\sqrt{n^{\mathrm{te}}})+\sqrt{\Upsilon\log\frac{1}{\delta}}+KC_k\Delta_\ell\exp\left(\frac{-1}{\Upsilon}\right)\big)$.
2) If the additional error due to estimation of $\bar{r}_k$ with HDRM in Section 3 using M bins is considered, it leads to $\mathcal{O}(K\Delta_\ell\big(\frac{1}{M}+\sqrt{\frac{M}{n_k^{\mathrm{tr}}}}\big))$ under mild assumptions. Refer to Appendix K for details.
3) Our error bound increases with K due to the structure of BD risk. Note that K is in a constant order. Our goal is to show that nnBD DRM is guaranteed to generalize in a general federated setting.

4.2 Excess risk and benefit of FIDEM

In this section, we aim to demonstrate the benefit of importance weighting in term of excess risk through bias-variance decomposition. We consider the classical least squares problem, a good starting point to understand the superiority of FIDEM over ERM with generalization guarantees. We consider the single client setting $K = 1$ for the ease of description, and our results can be extended to the multiple clients setting.

Let $(\mathbf{x}, y)$ denote the (test) data sampled from an unknown probability measure ρ. The least squares problem is to estimate the true parameter $\boldsymbol{\theta}_*$, which is assumed to be the unique solution that minimizes the *population risk* in a Hilbert space $\mathcal{H}$: $L(\boldsymbol{\theta}_*) = \min_{\boldsymbol{\theta}\in\mathcal{H}} L(\boldsymbol{\theta})$ where $L(\boldsymbol{\theta}) := \frac{1}{2}\mathbb{E}_{(\mathbf{x},y)\sim\rho}[(y-\boldsymbol{\theta}^\top\mathbf{x})]^2$. Moreover, we have $L(\boldsymbol{\theta}_*) = \sigma_\epsilon^2$ corresponding to the noise level. For an estimate $\boldsymbol{\theta}$ found by a learning algorithm such as ridge regression, its performance is measured by the expected *excess risk*, $\mathbb{E}[L(\boldsymbol{\theta})] - L(\boldsymbol{\theta}_*)$, where the expectation is over the random noise, randomness of the algorithm, and training data. In the following, we consider two settings: random-design setting and fixed-design settings where the training data matrix is random and given, respectively.

Bias variance decomposition. We need the following noise assumption for our proof.

Assumption 2 (Dhillon et al. 2013; Zou et al. 2021, bounded variance)**.** Let $\epsilon := y - \boldsymbol{\theta}_*^\top\mathbf{x}$. We assume that $\mathbb{E}[\epsilon] = 0$ and $\mathbb{E}[\epsilon^2] = \sigma_\epsilon^2$.

We have the following lemma on the bias-variance decomposition of the ridge regression FIDEM estimate in the random-design setting.

Lemma 1. *Let $\mathbf{X} \in \mathbb{R}^{n\times d}$ be the training data matrix. Let $\mathbf{W} = \mathrm{diag}(w_1, \ldots, w_n)$ with $w_i = p^{\mathrm{te}}(\mathbf{x}_i)/p^{\mathrm{tr}}(\mathbf{x}_i)$ for $i \in [n]$, $\hat{\boldsymbol{\theta}}$ be the regularized least square estimate with importance weighting: $\hat{\boldsymbol{\theta}} = \arg\min_{\boldsymbol{\theta}} \sum_{i=1}^{n} w_i(\boldsymbol{\theta}^\top\mathbf{x}_i - y_i)^2 + \lambda\|\boldsymbol{\theta}\|_2^2$ where λ is the regularization parameter. Denote $\boldsymbol{\theta}_*$ be the true estimate, then the excess risk can be decomposed as the bias $\mathtt{B}$ and the variance $\mathtt{V}$: $\mathbb{E}[L(\hat{\boldsymbol{\theta}})] - L(\boldsymbol{\theta}_*) = \mathtt{B} + \mathtt{V}$, with*

$$\mathtt{B} := \lambda^2\mathbb{E}\left[\boldsymbol{\theta}_*^\top\boldsymbol{\Sigma}_{\mathbf{W},\lambda}^{-1}\boldsymbol{\Sigma}^{\mathrm{te}}\boldsymbol{\Sigma}_{\mathbf{W},\lambda}^{-1}\boldsymbol{\theta}_*\right], \quad \mathtt{V} := \sigma_\epsilon^2\mathbb{E}\left[\mathrm{tr}\left(\boldsymbol{\Sigma}_{\mathbf{W},\lambda}^{-1}\mathbf{X}^\top\mathbf{W}^2\mathbf{X}\boldsymbol{\Sigma}_{\mathbf{W},\lambda}^{-1}\boldsymbol{\Sigma}^{\mathrm{te}}\right)\right],$$

where $\boldsymbol{\Sigma}_{\mathbf{W},\lambda} := \mathbf{X}^\top\mathbf{W}\mathbf{X} + \lambda\mathbf{I}$, and $\boldsymbol{\Sigma}^{\mathrm{te}} = \mathbb{E}_{\mathbf{x}}[\mathbf{x}\mathbf{x}^\top]$. Note that the expectation is taken over the randomness of the training data matrix $\mathbf{X}$ and label noise.

Remark 2. Our results in Lemma 1 hold under the fixed-design setting where the training data are given (Dhillon et al., 2013; Hsu et al., 2012), by omitting the expectations from $\mathtt{B}$ and $\mathtt{V}$.

One-hot case. To theoretically prove that FIDEM outperforms ERM in non-trivial settings, we start from the one-hot case, along the lines of Zou et al. (2021), and strictly show that, under which level of covariate shift, the excess risk of FIDEM is always smaller than the classical ERM.

To be specific, in the one-hot case, every training data $\mathbf{x}$ is sampled from the set of natural basis $\{\mathbf{e}_1, \mathbf{e}_2, \ldots, \mathbf{e}_d\}$ according to the data distribution given by $\Pr\{\mathbf{x} = \mathbf{e}_i\} = \lambda_i$ where $0 < \lambda_i \leq 1$ and $\sum_i \lambda_i = 1$. The class of one-hot least square instances is characterized by the following problem set: $\left\{(\boldsymbol{\theta}_*; \lambda_1, \ldots, \lambda_d) : \boldsymbol{\theta}_* \in \mathcal{H}, \sum_i\lambda_i = 1\right\}$. It is not difficult to show that the population second momentum matrix is $\boldsymbol{\Sigma}^{\mathrm{tr}} = \mathbb{E}[\mathbf{x}_i\mathbf{x}_i^\top] = \mathrm{diag}(\lambda_1, \ldots, \lambda_d)$ for $i \in [n]$. Similarly, we assume that each test data follows the same scheme but with different probabilities $\Pr\{\mathbf{x} = \boldsymbol{e}_i\} = \lambda_i'$, and hence, we have $\boldsymbol{\Sigma}^{\mathrm{te}} = \mathrm{diag}(\lambda_1', \ldots, \lambda_d')$. This is a relatively simple setting, which admits covariate shift.Take $\{\mu_1, \mu_2, \ldots, \mu_d\}$ as the eigenvalues of $\mathbf{X}^\top\mathbf{X}$. Since $\mathbf{x}_i$ can only take on natural basis, the eigenvalue μ_i can be understood as the number of training data that equals $\mathbf{e}_i$. For notational simplicity, we

Table 1: Fashion MNIST with label shift across five clients, where each client receives different fractions of examples from each class. In this case, FIDEM achieves a better average accuracy than the baselines.

	FIDEM	**FIIDEM**	**FedAvg**
Average accuracy	**0.8245** $\pm$ 0.0111	0.7942 $\pm$ 0.0096	0.5475 $\pm$ 0.0093
Client 1 accuracy	**0.8627** $\pm$ 0.0175	0.8336 $\pm$ 0.0066	0.3978 $\pm$ 0.0215
Client 2 accuracy	**0.9308** $\pm$ 0.0057	0.8896 $\pm$ 0.0124	0.9143 $\pm$ 0.0048
Client 3 accuracy	**0.7742** $\pm$ 0.0618	0.7275 $\pm$ 0.0261	0.3677 $\pm$ 0.0297
Client 4 accuracy	0.7933 $\pm$ 0.0598	**0.8204** $\pm$ 0.0152	0.6566 $\pm$ 0.0447
Client 5 accuracy	**0.7616** $\pm$ 0.0593	0.6998 $\pm$ 0.0649	0.4009 $\pm$ 0.0642

Table 2: Average, worst-case, and best-case client accuracies of CIFAR10 target shift experiment across 100 clients where 5 randomly sampled clients participate in every round of training.

	FIDEM	**FedAvg**
Average client accuracy	**0.7658**	0.7237
Worst client accuracy	**0.6163**	0.5403
Best client accuracy	**0.9016**	0.8904

rearrange the order of the training data following the decreasing order of the ratio, such that the i-th sample $\mathbf{x}_i$ corresponds to the ratio w_i as the exact i-th largest value.

Theorem 2. *Let $\hat{\boldsymbol{\theta}}$ be the estimate of FIDEM, $\boldsymbol{\theta}^{\mathrm{v}}$ be the classical ERM, and $\xi_i := \frac{\lambda}{\lambda+\mu_i}$. Under the fixed-design setting in the one-hot case, label noise assumption, and data correlation assumption, if the ratio $w_i := p^{\mathrm{te}}(\mathbf{x}_i)/p^{\mathrm{tr}}(\mathbf{x}_i)$ satisfies*

$$\sqrt{\frac{\lambda_i'}{\lambda_i}} - 1 \leq w_i \leq \xi_i \sqrt{\frac{\lambda_i}{\lambda_i'}}\,, \tag{4.3}$$

then we have $R(\hat{\boldsymbol{\theta}}) \leqslant R(\boldsymbol{\theta}^{\mathrm{v}})$.

Remark 3. We have the following remarks:

1) The condition (4.3) is equivalent to $\sqrt{\frac{\lambda_i'}{\lambda_i}} \in \left(0, \frac{1+\sqrt{1+4\xi_i}}{2}\right)$, which requires the training and test data to behave similarly in terms of eigenvalues, avoiding significant differences under distribution shifts for learnability. Other metrics, e.g., similarity on eigenvectors (Tripuraneni et al., 2021) also coincide with the spirit of our assumption.

2) The ratio matrix is $\mathbf{W} \in \mathbb{R}^{n\times n}$. However, we only need its top d eigenvalue, i.e., the top-d ratios. In particular, the last $n-d$ ratios have no effect on the final excess risk. This makes our algorithm robust to noise and domain shift.

3) For the special case by taking the ratio as $w_i := \sqrt{\frac{\lambda_i'}{\lambda_i}}$, we have

$$\mathtt{B}(\hat{\boldsymbol{\theta}}) = \lambda^2 \sum_{i=1}^{d} \frac{[(\boldsymbol{\theta}_*)_i]^2 \lambda_i'}{[\mu_i w_i + \lambda]^2} = \lambda^2 \sum_{i=1}^{d} \frac{[(\boldsymbol{\theta}_*)_i]^2 \lambda_i}{\left[\mu_i + \sqrt{\frac{\lambda_i}{\lambda_i'}}\lambda\right]^2}\,,$$

which implies that the ratio can be regarded as an implicit regularization (Zou et al., 2021).

5 Experimental evaluation

In this section we illustrate conditions under which FIDEM is favored over both Federated Averaging without ratio estimation (FedAvg) (McMahan et al., 2017) and FIIDEM. For MNIST-based experiments we use a LeNet (LeCun et al., 1989) with cross entropy loss and compute standard deviations over *5 independent executions*. For CIFAR10-based experiments we use the larger ResNet-18 network (He et al., 2016). Further implementation details can be found in Appendix O.

Table 3: A challenging binary classification task on Colored MNIST with covariate shift across two clients. FIDEM is close to the idealised baseline that ignores the spurious correlation (Grayscale).

	Upper Bound (Grayscale)	**FIDEM**	**FIIDEM**	**FedAvg**
Average accuracy	0.68 ± 0.01	**0.66** ± 0.01	0.63 ± 0.00	0.58 ± 0.01

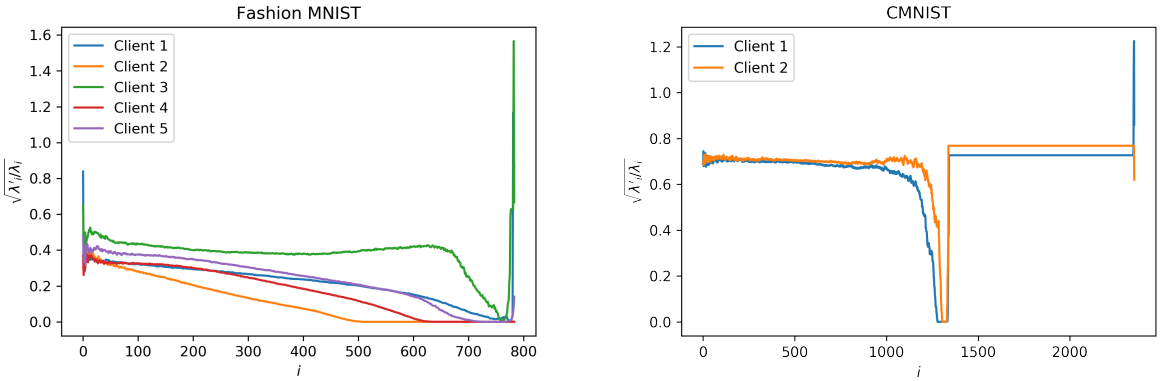

Figure 2: The squared ratio of eigenvalues ordered in descending order are all below 1 thus satisfying $\sqrt{\frac{\lambda'_i}{\lambda_i}} \in \left(0, \frac{1+\sqrt{1+4\xi_i}}{2}\right)$ in Theorem 2. The sudden increase in the ratio for the lowest eigenvalues are most likely due to numerical error occuring when the eigenvalues are close to zero (cf. Figure 3).

Target shift. We consider the case of target shift where the label distribution $p(y)$ changes but the conditional distribution $p(\mathbf{x}|y)$ remains invariant. We split the 10-class Fashion MNIST dataset between 5 clients and simulate a target shift by including different fractions of examples from each class across the training data and test data. We further consider the separable case in order to compute the exact ratio for FIDEM and FIIDEM in closed form. The specific distribution and the construction of the ratio can be found in Appendix O.1. The results in Table 1 illustrate that FIIDEM can outperform FedAvg on average while preserving the same level of privacy. By relaxing the privacy slightly the proposed FIDEM improves on FedAvg uniformly across all clients. Even though the proportions of the classes have been artificially created, we believe that this demonstrates a realistic scenario where clients have a different fraction of samples per class. Additional experiments using larger models on the CIFAR10 dataset under a challenging target shift setting can be found in Appendix O.1 where FIDEM is observed to improve uniformly over FedAvg.

To model a scenario closer to real-world FL, we consider a setting with 100 clients on CIFAR10 under challenging distribution shifts and partial participation of clients, which is a requirement for cross-device FL (Kairouz et al., 2021; Wang et al., 2021). We sub-sample 5 clients uniformly at random at every round for $200,000$ iterations. The target distribution is described in Table 6 and experimental results can be found in Table 2. We observe that FIDEM uniformly improves the test accuracy when compared with FedAvg and that the gap is especially large between the worst-performing clients.

Covariate shift. We now focus on covariate shift, where $p(\mathbf{x})$ undergoes a shift while $p(y|\mathbf{x})$ remains unchanged. For this setting, we extend the Colored MNIST dataset in Arjovsky et al. (2019) to the multi-client setting. The dataset is constructed by first assigning a binary label 0 to digits from 0-4 and label 1 for digits between 5-9. The label is then flipped with probability 0.25 to make the dataset non-separable. A spurious correlation is introduced by coloring the digits according to their assigned labels and then flipping the colors according to a different probability for each distribution (see Appendix O.2). For this experimental setup, we introduce an idealized scheme, which ignores the color and thus the spurious correlation, i.e., provides an upper bound, and is referred to as *Grayscale*. FIDEM outperforms both baselines in terms of the average accuracy even in a two-client setting. FIDEM is also close to Grayscale upper bound that by construction ignores the spurious correlations.

Verifying assumptions. Consider the two datasets used for the main experiments in Table 1 and Table 3. We verify in Figure 3 that the eigenvalues of the training distribution and test distribution for each client satisfy $\sqrt{\frac{\lambda_i'}{\lambda_i}} \in \left(0, \frac{1+\sqrt{1+4\xi_i}}{2}\right)$ in Theorem 2.

6 Conclusions and future work

In this work, we focus on FL under both intra-client and inter-client distribution shifts and propose FIDEM to improve the overall generalization performance. We establish high-probability ratio estimation guarantees for a general DRM method in a federated setting. We further show the benefit of importance weighting in term of excess risk through bias-variance decomposition in a ridge regression problem. Our theoretical guarantees indicate how FIDEM can provably solve a learning task under distribution shifts. We experimentally evaluate FIDEM under both label shift and covariate shift cases. Our experimental results validate that under certain covariate and target shifts, the proposed method can learn the task, while baselines such as vanilla federated averaging fails to do so. We anticipate that our methods to be applicable in learning from e.g., medical data, where there might be arbitrary skews on the distribution. In addition, we believe our study can further encourage the investigation of distribution shifts in FL, as this is a critical subject for learning across clients.

References

Ben Adlam and Jeffrey Pennington. Understanding double descent requires a fine-grained bias-variance decomposition. *Advances in Neural Information Processing Systems*, 33, 2020.

Dan Alistarh, Demjan Grubic, Jerry Li, Ryota Tomioka, and Milan Vojnovic. QSGD: Communication-efficient SGD via gradient quantization and encoding. In *Proc. Advances in Neural Information Processing Systems (NeurIPS)*, 2017.

Martin Arjovsky, Léon Bottou, Ishaan Gulrajani, and David Lopez-Paz. Invariant risk minimization. *arXiv preprint arXiv:1907.02893*, 2019.

Kamyar Azizzadenesheli. Importance weight estimation and generalization in domain adaptation under label shift. *IEEE Transactions on Pattern Analysis and Machine Intelligence (T-PAMI)*, 44(10):6578–6584, 2022.

Mahsa Baktashmotlagh, Mehrtash T Harandi, Brian C Lovell, and Mathieu Salzmann. Domain adaptation on the statistical manifold. In *Conference on Computer Vision and Pattern Recognition (CVPR)*, pp. 2481–2488, 2014.

Peter L Bartlett. The sample complexity of pattern classification with neural networks: the size of the weights is more important than the size of the network. *IEEE transactions on Information Theory*, 44(2):525–536, 1998.

Peter L Bartlett and Shahar Mendelson. Rademacher and gaussian complexities: Risk bounds and structural results. *Journal of Machine Learning Research (JMLR)*, 3(Nov.):463–482, 2002.

Peter L Bartlett, Olivier Bousquet, and Shahar Mendelson. Local rademacher complexities. *Annals of Statistics*, 33(4):1497–1537, 2005.

Ayanendranath Basu, Ian R Harris, Nils L Hjort, and MC Jones. Robust and efficient estimation by minimising a density power divergence. *Biometrika*, 85(3):549–559, 1998.

Steffen Bickel and Tobias Scheffer. Dirichlet-enhanced spam filtering based on biased samples. In *Advances in Neural Information Processing Systems (NeurIPS)*, 2007.

Konstantinos Bousmalis, Nathan Silberman, David Dohan, Dumitru Erhan, and Dilip Krishnan. Unsupervised pixel-level domain adaptation with generative adversarial networks. In *Conference on Computer Vision and Pattern Recognition (CVPR)*, pp. 3722–3731, 2017.

Olivier Bousquet and André Elisseeff. Stability and generalization. *Journal of Machine Learning Research (JMLR)*, 2:499–526, 2002.

Lev M. Bregman. The relaxation method of finding the common point of convex sets and its application to the solution of problems in convex programming. *USSR computational mathematics and mathematical physics*, 7(3):200–217, 1967.

Sebastian Caldas, Sai Meher Karthik Duddu, Peter Wu, Tian Li, Jakub Konečnỳ, H Brendan McMahan, Virginia Smith, and Ameet Talwalkar. LEAF: A benchmark for federated settings. In *Advances in Neural Information Processing Systems (NeurIPS)*, 2019.

Kuang Fu Cheng and Chih-Kang Chu. Semiparametric density estimation under a two-sample density ratio model. *Bernoulli*, 10(4):583–604, 2004.

Bharath Bhushan Damodaran, Benjamin Kellenberger, Rémi Flamary, Devis Tuia, and Nicolas Courty. Deepjdot: Deep joint distribution optimal transport for unsupervised domain adaptation. pp. 447–463, 2018.

Debasmit Das and CS George Lee. Unsupervised domain adaptation using regularized hyper-graph matching. In *2018 25th IEEE International Conference on Image Processing (ICIP)*, pp. 3758–3762. IEEE, 2018.

Paramveer S. Dhillon, Dean P. Foster, Sham M. Kakade, and Lyle H. Ungar. A risk comparison of ordinary least squares vs ridge regression. *Journal of Machine Learning Research*, 14(1):1505–1511, 2013.

Aymeric Dieuleveut, Nicolas Flammarion, and Francis Bach. Harder, better, faster, stronger convergence rates for least-squares regression. *Journal of Machine Learning Research*, 18(1):3520–3570, 2017.

Jian-Hui Duan, Wenzhong Li, and Sanglu Lu. FedDNA: Federated learning with decoupled normalization-layer aggregation for non-IID data. In *Joint European Conference on Machine Learning and Knowledge Discovery in Databases*, 2021.

Tongtong Fang, Nan Lu, Gang Niu, and Masashi Sugiyama. Rethinking importance weighting for deep learning under distribution shift. In *Advances in Neural Information Processing Systems (NeurIPS)*, 2020.

Yaroslav Ganin, Evgeniya Ustinova, Hana Ajakan, Pascal Germain, Hugo Larochelle, François Laviolette, Mario Marchand, and Victor Lempitsky. Domain-adversarial training of neural networks. *The journal of machine learning research*, 17(1):2096–2030, 2016.

Elnur Gasanov, Ahmed Khaled, Samuel Horváth, and Peter Richtárik. FLIX: A simple and communication-efficient alternative to local methods in federated learning. In *International Conference on Artificial Intelligence and Statistics (AISTATS)*, 2022.

Stuart Geman, Elie Bienenstock, and René Doursat. Neural networks and the bias/variance dilemma. *Neural computation*, 4(1):1–58, 1992.

Noah Golowich, Alexander Rakhlin, and Ohad Shamir. Size-independent sample complexity of neural networks. In *Conference On Learning Theory*, pp. 297–299, 2018.

Ian Goodfellow, Jean Pouget-Abadie, Mehdi Mirza, Bing Xu, David Warde-Farley, Sherjil Ozair, Aaron Courville, and Yoshua Bengio. Generative adversarial networks. *Communications of the ACM*, 63(11): 139–144, 2020.

Arthur Gretton, Alex Smola, Jiayuan Huang, Marcel Schmittfull, Karsten Borgwardt, and Bernhard Schölkopf. Covariate shift by kernel mean matching. *Dataset shift in machine learning*, 3(4):5, 2009.

Hirotaka Hachiya, Masashi Sugiyama, and Naonori Ueda. Importance-weighted least-squares probabilistic classifier for covariate shift adaptation with application to human activity recognition. *Neurocomputing*, 80: 93–101, 2012.

Boris Hanin and David Rolnick. Deep ReLU networks have surprisingly few activation patterns. In *Advances in Neural Information Processing Systems (NeurIPS)*, 2019.

Filip Hanzely, Slavomír Hanzely, Samuel Horváth, and Peter Richtárik. Lower bounds and optimal algorithms for personalized federated learning. In *Advances in Neural Information Processing Systems (NeurIPS)*, 2020.

Trevor Hastie, Robert Tibshirani, and Jerome Friedman. *The elements of statistical learning: data mining, inference and prediction*. Springer, 2001.

Kaiming He, Xiangyu Zhang, Shaoqing Ren, and Jian Sun. Deep residual learning for image recognition. In *Proceedings of the IEEE conference on computer vision and pattern recognition*, pp. 770–778, 2016.

Shohei Hido, Yuta Tsuboi, Hisashi Kashima, Masashi Sugiyama, and Takafumi Kanamori. Statistical outlier detection using direct density ratio estimation. *Knowledge and Information Systems*, 26(2):309–336, 2011.

Daniel Hsu, Sham M. Kakade, and Tong Zhang. Random design analysis of ridge regression. In *Conference on Learning Theory*, 2012.

Jiayuan Huang, Arthur Gretton, Karsten Borgwardt, Bernhard Schölkopf, and Alex Smola. Correcting sample selection bias by unlabeled data. In *Advances in Neural Information Processing Systems (NeurIPS)*, 2006.

Prateek Jain, Sham Kakade, Rahul Kidambi, Praneeth Netrapalli, and Aaron Sidford. Parallelizing stochastic gradient descent for least squares regression: mini-batching, averaging, and model misspecification. *Journal of Machine Learning Research*, 18, 2018.

Jing Jiang and ChengXiang Zhai. Instance weighting for domain adaptation in nlp. In *Proceedings of the 45th annual meeting of the association of computational linguistics*, pp. 264–271, 2007.

Suwicha Jirayucharoensak, Setha Pan-Ngum, and Pasin Israsena. EEG-based emotion recognition using deep learning network with principal component based covariate shift adaptation. *The Scientific World Journal*, 2014, 2014.

P. Kairouz, H. B. McMahan, B. Avent, A. Bellet, M. Bennis, A. N. Bhagoji, K. Bonawitz, Z. Charles, G. Cormode, R. Cummings, R. G. L. D'Oliveira, S. E. Rouayheb, D. Evans, J. Gardner, Z. Garrett, A. Gascón, B. Ghazi, P. B. Gibbons, M. Gruteser, Z. Harchaoui, C. He, L. He, Z. Huo, B. Hutchinson, J. Hsu, M. Jaggi, T. Javidi, G. Joshi, M. Khodak, J. Konečný, A. Korolova, F. Koushanfar, S. Koyejo, T. Lepoint, Y. Liu, P., M. Mohri, R. Nock, A. Özgür, R. Pagh, M. Raykova, H. Qi, D. Ramage, R. Raskar, D. Song, W. Song, S. U. Stich, Z. Sun, A. T. Suresh, F. Tramèr, P. Vepakomma, J. Wang, L. Xiong, Z. Xu, Q. Yang, F. X. Yu, H. Yu, and S. Zhao. Advances and open problems in federated learning. *Foundations and Trends® in Machine Learning*, 14(1–2):1–210, 2021.

Takafumi Kanamori, Shohei Hido, and Masashi Sugiyama. A least-squares approach to direct importance estimation. *Journal of Machine Learning Research*, 10:1391–1445, 2009.

Takafumi Kanamori, Taiji Suzuki, and Masashi Sugiyama. f-divergence estimation and two-sample homogeneity test under semiparametric density-ratio models. *IEEE Transactions on Information Theory*, 58(2): 708–720, 2011.

Masahiro Kato and Takeshi Teshima. Non-negative Bregman divergence minimization for deep direct density ratio estimation. In *International Conference on Machine Learning (ICML)*, 2021.

Masahiro Kato, Takeshi Teshima, and Junya Honda. Learning from positive and unlabeled data with a selection bias. In *International Conference on Learning Representations (ICLR)*, 2019.

Yoshinobu Kawahara and Masashi Sugiyama. Change-point detection in time-series data by direct density-ratio estimation. In *Proceedings of the SIAM international conference on data mining*, 2009.

Amor Keziou and Samuela Leoni-Aubin. Test of homogeneity in semiparametric two-sample density ratio models. *Comptes Rendus Mathématique*, 340(12):905–910, 2005.

Mikhail Khodak, Maria-Florina Balcan, and Ameet Talwalkar. Adaptive gradient-based meta-learning methods. In *Advances in Neural Information Processing Systems (NeurIPS)*, 2019.

Ryuichi Kiryo, Gang Niu, Marthinus C. du Plessis, and Masashi Sugiyama. Positive-unlabeled learning with non-negative risk estimator. In *Advances in Neural Information Processing Systems (NeurIPS)*, 2017.

Pang Wei Koh, Shiori Sagawa, Henrik Marklund, Sang Michael Xie, Marvin Zhang, Akshay Balsubramani, Weihua Hu, Michihiro Yasunaga, Richard Lanas Phillips, Irena Gao, et al. WILDS: A benchmark of in-the-wild distribution shifts. In *International Conference on Machine Learning (ICML)*, 2021.

Wouter M Kouw and Marco Loog. A review of domain adaptation without target labels. *IEEE Transactions on Pattern Analysis and Machine Intelligence (T-PAMI)*, 43(3):766–785, 2019.

A. Krizhevsky. Learning multiple layers of features from tiny images. Technical report, University of Toronto, 2009.

Alex Krizhevsky, Geoffrey Hinton, et al. Learning multiple layers of features from tiny images. 2009.

Yann LeCun, Bernhard Boser, John S. Denker, Donnie Henderson, Richard E. Howard, Wayne Hubbard, and Lawrence D. Jackel. Backpropagation applied to handwritten zip code recognition. *Neural computation*, 1 (4):541–551, 1989.

Yann LeCun, Léon Bottou, Yoshua Bengio, Patrick Haffner, et al. Gradient-based learning applied to document recognition. *Proceedings of the IEEE*, 86(11):2278–2324, 1998.

Michel Ledoux and Michel Talagrand. *Probability in Banach Spaces: Isoperimetry and Processes*, volume 23. Springer Science & Business Media, 1991.

Tian Li, Anit Kumar Sahu, Ameet Talwalkar, and Virginia Smith. Federated learning: Challenges, methods, and future directions. *IEEE Signal Processing Magazine*, 37:50–60, 2020.

Tian Li, Ahmad Beirami, Maziar Sanjabi, and Virginia Smith. Tilted empirical risk minimization. In *International Conference on Learning Representations (ICLR)*, 2021a.

Tian Li, Shengyuan Hu, Ahmad Beirami, and Virginia Smith. Ditto: Fair and robust federated learning through personalization. In *International Conference on Machine Learning (ICML)*, 2021b.

Xiaoxiao Li, Meirui Jiang, Xiaofei Zhang, Michael Kamp, and Qi Dou. FedBN: Federated learning on non-IID features via local batch normalization. In *International Conference on Learning Representations (ICLR)*, 2021c.

Yan Li, Hiroyuki Kambara, Yasuharu Koike, and Masashi Sugiyama. Application of covariate shift adaptation techniques in brain–computer interfaces. *IEEE Transactions on Biomedical Engineering*, 57(6):1318–1324, 2010.

Tongliang Liu and Dacheng Tao. Classification with noisy labels by importance reweighting. *IEEE Transactions on Pattern Analysis and Machine Intelligence (T-PAMI)*, 38(3):447–461, 2015.

Stuart Lloyd. Least squares quantization in PCM. *IEEE Transactions on Information Theory*, 28(2):129–137, 1982.

Nan Lu, Tianyi Zhang, Gang Niu, and Masashi Sugiyama. Mitigating overfitting in supervised classification from two unlabeled datasets: A consistent risk correction approach. In *International Conference on Artificial Intelligence and Statistics (AISTATS)*, 2020.

Yishay Mansour, Mehryar Mohri, Jae Ro, and Ananda Theertha Suresh. Three approaches for personalization with applications to federated learning. *arXiv preprint arXiv:2002.10619*, 2020.

David A McAllester. Some pac-bayesian theorems. *Machine Learning*, 37(3):355–363, 1999.

Colin McDiarmid et al. On the method of bounded differences. *Surveys in combinatorics*, 141(1):148–188, 1989.

H. B. McMahan, E. Moore, D. Ramage, S. Hampson, and B. A. y Arcas. Communication-efficient learning of deep networks from decentralized data. In *Proc. International Conference on Artificial Intelligence and Statistics (AISTATS)*, 2017.

Mehryar Mohri, Gary Sivek, and Ananda Theertha Suresh. Agnostic federated learning. In *International Conference on Machine Learning*, pp. 4615–4625. PMLR, 2019.

Arkadi Nemirovski. *Topics in Non-parametric Statistics*. Ecole d'Eťe de Probabilíťes de Saint-Flour XXVIII, 1998.

XuanLong Nguyen, Martin J Wainwright, and Michael I Jordan. Estimating divergence functionals and the likelihood ratio by convex risk minimization. *IEEE Transactions on Information Theory*, 56(11):5847–5861, 2010.

Jing Qin. Inferences for case-control and semiparametric two-sample density ratio models. *Biometrika*, 85(3): 619–630, 1998.

Sashank Reddi, Barnabas Póczos, and Alex Smola. Doubly robust covariate shift correction. In *AAAI Conference on Artificial Intelligence*, 2015.

SB Russ. A translation of Bolzano's paper on the intermediate value theorem. *Historia Mathematica*, 7(2): 156–185, 1980.

Shai Shalev-Shwartz and Shai Ben-David. *Understanding machine learning: From theory to algorithms*. Cambridge university press, 2014.

Shai Shalev-Shwartz, Ohad Shamir, Nathan Srebro, and Karthik Sridharan. Learnability, stability and uniform convergence. *Journal of Machine Learning Research (JMLR)*, 11:2635–2670, 2010.

Hidetoshi Shimodaira. Improving predictive inference under covariate shift by weighting the log-likelihood function. *Journal of Statistical Planning and Inference*, 90(2):227–244, 2000.

Virginia Smith, Chao-Kai Chiang, Maziar Sanjabi, and Ameet S. Talwalkar. Federated multi-task learning. In *Advances in Neural Information Processing Systems (NeurIPS)*, 2017.

Alex Smola, Le Song, and Choon Hui Teo. Relative novelty detection. In *International Conference on Artificial Intelligence and Statistics (AISTATS)*, 2009.

Masashi Sugiyama and Klaus-Robert Müller. Input-dependent estimation of generalization error under covariate shift. *Statistics & Decisions*, 2005.

Masashi Sugiyama, Matthias Krauledat, and Klaus-Robert Müller. Covariate shift adaptation by importance weighted cross validation. *Journal of Machine Learning Research*, 8(5), 2007.

Masashi Sugiyama, Taiji Suzuki, Yuta Itoh, Takafumi Kanamori, and Manabu Kimura. Least-squares two-sample test. *Neural networks*, 24(7):735–751, 2011.

Masashi Sugiyama, Taiji Suzuki, and Takafumi Kanamori. Density-ratio matching under the Bregman divergence: a unified framework of density-ratio estimation. *Annals of the Institute of Statistical Mathematics*, 64(5):1009–1044, 2012.

Nilesh Tripuraneni, Ben Adlam, and Jeffrey Pennington. Overparameterization improves robustness to covariate shift in high dimensions. In *Advances in Neural Information Processing Systems (NeurIPS)*, 2021.

Alexandre B. Tsybakov. *Introduction to Nonparametric Estimation*. Springer Series in Statistics, 2008.

Masatoshi Uehara, Masahiro Kato, and Shota Yasui. Off-policy evaluation and learning for external validity under a covariate shift. In *Advances in Neural Information Processing Systems (NeurIPS)*, 2020.

Vladimir N Vapnik. An overview of statistical learning theory. *IEEE Transactions on Neural Networks and Learning Systems (T-NN)*, 10(5):988–999, 1999.

Jianyu Wang, Zachary Charles, Zheng Xu, Gauri Joshi, H. Brendan McMahan, Blaise Aguera y Arcas, Maruan Al-Shedivat, Galen Andrew, Salman Avestimehr, Katharine Daly, Deepesh Data, Suhas Diggavi, Hubert Eichner, Advait Gadhikar, Zachary Garrett, Antonious M. Girgis, Filip Hanzely, Andrew Hard, Chaoyang He, Samuel Horvath, Zhouyuan Huo, Alex Ingerman, Martin Jaggi, Tara Javidi, Peter Kairouz, Satyen Kale, Sai Praneeth Karimireddy, Jakub Konecny, Sanmi Koyejo, Tian Li, Luyang Liu, Mehryar Mohri, Hang Qi, Sashank J. Reddi, Peter Richtarik, Karan Singhal, Virginia Smith, Mahdi Soltanolkotabi, Weikang Song, Ananda Theertha Suresh, Sebastian U. Stich, Ameet Talwalkar, Hongyi Wang, Blake Woodworth, Shanshan Wu, Felix X. Yu, Honglin Yuan, Manzil Zaheer, Mi Zhang, Tong Zhang, Chunxiang Zheng, Chen Zhu, and Wennan Zhu. A field guide to federated optimization. *arXiv preprint arXiv:2107.06917*, 2021.

Mei Wang and Weihong Deng. Deep visual domain adaptation: A survey. *Neurocomputing*, 312:135–153, 2018.

Larry Wasserman. *All of nonparametric statistics*. Springer Science & Business Media, 2006.

Han Xiao, Kashif Rasul, and Roland Vollgraf. Fashion-mnist: a novel image dataset for benchmarking machine learning algorithms. *arXiv preprint arXiv:1708.07747*, 2017.

Semih Yagli, Alex Dytso, and H Vincent Poor. Information-theoretic bounds on the generalization error and privacy leakage in federated learning. In *International Workshop on Signal Processing Advances in Wireless Communications (SPAWC)*, 2020.

Makoto Yamada, Masashi Sugiyama, and Tomoko Matsui. Semi-supervised speaker identification under covariate shift. *Signal Processing*, 90(8):2353–2361, 2010.

Makoto Yamada, Taiji Suzuki, Takafumi Kanamori, Hirotaka Hachiya, and Masashi Sugiyama. Relative density-ratio estimation for robust distribution comparison. In *Advances in Neural Information Processing Systems (NeurIPS)*, 2011.

Honglin Yuan, Warren Morningstar, Lin Ning, and Karan Singhal. What do we mean by generalization in federated learning? *arXiv preprint arXiv:2110.14216*, 2021.

Bianca Zadrozny. Learning and evaluating classifiers under sample selection bias. In *International Conference on Machine Learning (ICML)*, 2004.

Tianyi Zhang, Ikko Yamane, Nan Lu, and Masashi Sugiyama. A one-step approach to covariate shift adaptation. In *Asian Conference on Machine Learning*, 2020.

Aurick Zhou and Sergey Levine. Training on test data with bayesian adaptation for covariate shift. In *Advances in Neural Information Processing Systems (NeurIPS)*, 2021.

Ligeng Zhu, Zhijian Liu, and Song Han. Deep leakage from gradients. In *Advances in Neural Information Processing Systems (NeurIPS)*, 2019.

Difan Zou, Jingfeng Wu, Quanquan Gu, Dean P Foster, Sham Kakade, et al. The benefits of implicit regularization from SGD in least squares problems. In *Advances in Neural Information Processing Systems (NeurIPS)*, 2021.

A Appendix

The appendix is organized as follows:

- Examples of f for BD-based DRM are provided in Appendix A.
- Complete related work is provided in Appendix B.

Table 4: Examples of f for BD-based methods (Sugiyama et al., 2012; Kato & Teshima, 2021), LSIF = least-squares importance fitting, LR = logistic regression, BKL = binary Kullback–Leibler, UKL = unnormalized Kullback– Leibler, KLIEP = Kullback– Leibler importance estimation procedure, KMM = kernel mean matching , PULogLoss = positive and unlabeled learning with log Loss.

Reference	Algorithm	$f(z)$
Basu et al. (1998)	Robust	$\frac{z^{\alpha+1}-z}{\alpha},\ \alpha > 0$
Hastie et al. (2001)	LR (BKL)	$z\log(z) - (z+1)\log(z+1)$
Kanamori et al. (2009)	LSIF	$\frac{(z-1)^2}{2}$
Gretton et al. (2009)	KMM	$\frac{(z-1)^2}{2}$
Nguyen et al. (2010)	KLIEP	$z\log(z) - z$
Nguyen et al. (2010)	UKL	$z\log(z) - z$
Kato et al. (2019)	PULogLoss	$C\log(1-z) + Cz(\log(z) - \log(1-z)),\ z \in (0,1), C \leq \overline{r}$

- FIDEM with a focus on minmizing R_1 are provided in Appendix C.
- Details of density ratio estimation are provided in Appendix D.
- Communication costs of FIDEM and FIIDEM are analyzed in in Appendix E.
- UKL, LR, and PU variants of nnBD are provided in Appendix F.
- Convergence of $\tilde{r}$ and k-means clustering for HDRM are provided in Appendix G.
- UKL, LR, and PU variants of nnBD for multiple clients are provided in Appendix H.
- The proof of the core Theorem 1 exists in Appendix I.
- High-probability ratio estimation error bounds for multi-layer perceptron and multiple clients are established in Appendix J.
- Additional error due to estimation of $\overline{r}_k$ with HDRM is analyzed in Appendix K.
- Lemma 1 is proved in Appendix L.
- Theorem 2 is proved in Appendix M.
- A counterexample under which FIDEM cannot outperform ERM is provided in Appendix N.
- Additional experimental details are included in Appendix O.
- Computational complexity of Algorithm 1 is analyzed in Appendix P.
- The limitations of our work are described in Appendix Q.

B Complete related work

Federated learning. One well-known method in FL is FedAvg (McMahan et al., 2017). FedAvg and its variants are extensively studied in optimization with a focus on communication efficiency and partial participation of clients while preserving privacy.

Indeed, a host of techniques, such as gradient quantization, sparsification, and local updating rules, have been proposed to improve communication efficiency in FL (Alistarh et al., 2017). Furthermore, robust and secure aggregation schemes have been also proposed to provide robustness against training-time attacks launched by an adversary, and to compute aggregated values without being able to inspect the clients' local models and data, respectively (Li et al., 2020; Kairouz et al., 2021; Wang et al., 2021).

Taken together, these work largely focus on minimizing the empirical risk in the optimization objective, under the same training/test data distribution assumption over each client. Differences across clients are handled using personalization methods based on heuristics and currently do not have a statistical learning theoretical support (Smith et al., 2017; Khodak et al., 2019; Li et al., 2021b).

In contrast, we focus on learning and overall generalization performance under both intra-client and inter-client distribution shifts. Communication-efficient, robust, and secure aggregations can be viewed as complementary technologies, which can be used along with our proposed FIDEM method to improve the generalization performance. In our setting, clients can also all participate in every training iteration, such as cross-silo FL.

We note that (Hanzely et al., 2020; Gasanov et al., 2022) focus on minimizing the *empirical risk*, under the *same training/test data distribution assumption* over each client. Our formulation in FIDEM does not require specific assumptions on function F_k's for $k \in [K]$ to provide an unbiased estimate of true risk minimizer. Under strong convexity and smoothness assumptions w.r.t. model parameters, similar optimal algorithms to those proposed in (Hanzely et al., 2020; Gasanov et al., 2022) will be optimal for FIDEM.

Different from recent FL work by Duan et al. (2021) and Li et al. (2021c), our work introduces new FIDEM formulation and shows *statistical consistency*.

Importance-weighted ERM and density ratio matching. Density ratio estimation is an important step in various machine learning problems such as learning under covariate shift, learning under noisy labels, anomaly detection, two-sample testing, causal inference, change-pint detection, and classification from positive and unlabelled data (Qin, 1998; Shimodaira, 2000; Cheng & Chu, 2004; Keziou & Leoni-Aubin, 2005; Sugiyama et al., 2007; Kawahara & Sugiyama, 2009; Smola et al., 2009; Hido et al., 2011; Kanamori et al., 2011; Sugiyama et al., 2011; Yamada et al., 2011; Reddi et al., 2015; Liu & Tao, 2015; Kato et al., 2019; Fang et al., 2020; Uehara et al., 2020; Zhang et al., 2020; Kato & Teshima, 2021). In particular, covariate shift has been observed in real-world applications including brain-computer interfacing, emotion recognition, human activity recognition, spam filtering, and speaker identification (Bickel & Scheffer, 2007; Li et al., 2010; Yamada et al., 2010; Hachiya et al., 2012; Jirayucharoensak et al., 2014). Shimodaira (2000) introduced covariate shift where the input train and test distributions are different while the conditional distribution of the output variable given the input variable remains unchanged. Importance-weighted ERM is widely used to improve generalization performance under covariate shift (Zadrozny, 2004; Sugiyama & Müller, 2005; Huang et al., 2006; Sugiyama et al., 2007; Kanamori et al., 2009; Sugiyama et al., 2012; Fang et al., 2020; Zhang et al., 2020; Kato & Teshima, 2021). Zhang et al. (2020) proposed a one-step approach that jointly learns the predictive model and the corresponding weights in one optimization problem. Sugiyama et al. (2012) proposed a Bregman divergence-based DRM, which unifies various DRMs. Kato & Teshima (2021) proposed a non-negative Bregman divergence-based DRM to resolve the overfitting issue when using deep neural networks for density ratio estimation. While this line of work focuses on DRM with a single train and test distributions, we consider a federated setting with multiple clients in this paper.

Domain adaptation. Distribution shifts between a source and a target domain have been a prominent problem in machine learning for several decades (Wang & Deng, 2018; Kouw & Loog, 2019). The premise behind such shifts is that data is frequently biased, and this results in distribution shifts that can be estimated by assuming some (unlabelled) knowledge of the target distribution. The following categories of domain adaptation methods are most closely related to our work: a) sample-based, and b) feature-based methods. In feature-based methods, the goal is to find a transformation that maps the source samples to target samples (Ganin et al., 2016; Bousmalis et al., 2017; Das & Lee, 2018; Damodaran et al., 2018). Sample-based methods aim at minimizing the target risk through data in the source domain. Importance weighting is often used in sample-based methods (Shimodaira, 2000; Jiang & Zhai, 2007; Baktashmotlagh et al., 2014). However, the focus on domain adaptation has been mainly to adapt to a single target distribution, not the overall generalization performance on multiple clients, which is addressed in this paper.

Statistical generalization and excess risk bounds. Understanding generalization performance of learning algorithms is one essential topic in modern machine learning. Typical techniques to establish generalization guarantees include uniform convergence by Rademacher complexity (Bartlett, 1998), and its

Table 5: Details of scenarios described in Section 2.

Scenario	#Clients	Assumptions on Distributions	What client 1 Knows
No-CS in (C.1)	2	$p_1^{\mathrm{tr}}(\mathbf{x}) = p_1^{\mathrm{te}}(\mathbf{x}),\ \ p_1^{\mathrm{tr}}(\mathbf{x}) \neq p_2^{\mathrm{tr}}(\mathbf{x})$	$p_1^{\mathrm{tr}}(\mathbf{x})/p_2^{\mathrm{tr}}(\mathbf{x})$
CS on one in (C.2)	2	$p_1^{\mathrm{tr}}(\mathbf{x}) \neq p_1^{\mathrm{te}}(\mathbf{x}),\ \ p_2^{\mathrm{tr}}(\mathbf{x}) = p_2^{\mathrm{te}}(\mathbf{x})$	$p_1^{\mathrm{te}}(\mathbf{x})/p_1^{\mathrm{tr}}(\mathbf{x}),\ \ p_1^{\mathrm{te}}(\mathbf{x})/p_2^{\mathrm{tr}}(\mathbf{x})$
CS on both in (C.2)	2	$p_1^{\mathrm{tr}}(\mathbf{x}) \neq p_1^{\mathrm{te}}(\mathbf{x}),\ \ p_2^{\mathrm{tr}}(\mathbf{x}) \neq p_2^{\mathrm{te}}(\mathbf{x})$	$p_1^{\mathrm{te}}(\mathbf{x})/p_1^{\mathrm{tr}}(\mathbf{x}),\ \ p_1^{\mathrm{te}}(\mathbf{x})/p_2^{\mathrm{tr}}(\mathbf{x})$
CS on multi. in (C.3)	K	$p_k^{\mathrm{tr}}(\mathbf{x}) \neq p_1^{\mathrm{te}}(\mathbf{x})$ for all k	$p_1^{\mathrm{te}}(\mathbf{x})/p_k^{\mathrm{tr}}(\mathbf{x})$ for all k

variants (Bartlett et al., 2005), bias-variance decomposition (Geman et al., 1992; Adlam & Pennington, 2020), PAC-Bayes (McAllester, 1999), and stability-based analysis (Bousquet & Elisseeff, 2002; Shalev-Shwartz et al., 2010). Our work employs the first two techniques to analyze our density ratio estimation method in a federated setting and establish generalization guarantees for FIDEM, respectively. Rademacher complexity has been used in FL to obtain theoretical guarantees on the centralized model (Mohri et al., 2019) and personalized model (Mansour et al., 2020). Mohri et al. (2019) considered a scenario where a single target distribution is modeled as an unknown mixture of multiple domain distributions and obtained a global modal by minimizing the worst-case loss. This is different from our setting where we consider multiple test distributions for clients and focus on the overall test error. Mansour et al. (2020) studied personalization under the same training/test data distribution assumption over each client, which is different from our setting. Bias-variance decomposition provides a relatively refined characterization of generalization error (or excess risk), where a large bias indicates that a model is not flexible enough to learn from the data and a high variance indicates that the model performs unstably. Bias-variance decomposition is typically studied in two settings, i.e., the fixed and random design setting, which is categorized by whether the (training) data are fixed or random. This technique has been extensively applied in least squares (Hsu et al., 2012; Dieuleveut et al., 2017), analysis of SGD (Jain et al., 2018; Zou et al., 2021), and double descent (Adlam & Pennington, 2020).

Information-theoretic bounds on the generalization error and privacy leakage in federated settings were established in (Yagli et al., 2020). Under partial participation of clients, Yuan et al. (2021) proposed a framework, which distinguishes performance gaps due to unseen client data from performance gap due to unseen client distributions. Still, these work study FL under the same training/test data distribution assumption over each client.

C FIDEM with a focus on minmizing R_1

Without loss of generality and for simplicity of notation, in this section, we set $l = 1$. We consider four typical scenarios under various distribution shifts and formulate their FIDEM with a focus on minmizing R_1. The details of these scenarios are summarized in Table 5.

Remark 4. Covariance shift (as well as its assumption) is the *most commonly used and studied* in *theory* and *practice* in distribution shifts (Sugiyama et al., 2007; Kanamori et al., 2009; Kato & Teshima, 2021; Uehara et al., 2020; Tripuraneni et al., 2021; Zhou & Levine, 2021). Handling covariate shift is a challenging issue, especially in federated settings (Kairouz et al., 2021).

No intra-client covariate shift: (No-CS) For description simplicity, we assume that there are only 2 clients but our results can be directly extended to multiple clients. This scenario assumes $p_k^{\mathrm{tr}}(\mathbf{x}) = p_k^{\mathrm{te}}(\mathbf{x})$ for $k = 1, 2$. Client 1 aims to learn $h_{\mathbf{w}}$ assuming $\frac{p_1^{\mathrm{tr}}(x)}{p_2^{\mathrm{tr}}(x)}$ is given. We consider the following FIDEM that is proved to be consistent in terms of minimizing minimizing R_1:

$$\min_{\mathbf{w}\in\mathbb{R}^d} \frac{1}{n_1^{\mathrm{tr}}} \sum_{i=1}^{n_1^{\mathrm{tr}}} \ell(h_{\mathbf{w}}(\mathbf{x}_{1,i}^{\mathrm{tr}}), \mathbf{y}_{1,i}^{\mathrm{tr}}) + \frac{1}{n_2^{\mathrm{tr}}} \sum_{i=1}^{n_2^{\mathrm{tr}}} \frac{p_1^{\mathrm{tr}}(\mathbf{x}_{2,i}^{\mathrm{tr}})}{p_2^{\mathrm{tr}}(\mathbf{x}_{2,i}^{\mathrm{tr}})} \ell(h_{\mathbf{w}}(\mathbf{x}_{2,i}^{\mathrm{tr}}), \mathbf{y}_{2,i}^{\mathrm{tr}}). \tag{C.1}$$

Covariate shift only for client 1: (CS on one) We now consider covariate shift only for client 1, i.e., $p_1^{\mathrm{tr}}(\mathbf{x}) \neq p_1^{\mathrm{te}}(\mathbf{x})$ and $p_2^{\mathrm{tr}}(\mathbf{x}) = p_2^{\mathrm{te}}(\mathbf{x})$. We consider the following FIDEM

$$\min_{\mathbf{w}\in\mathbb{R}^d} \frac{1}{n_1^{\mathrm{tr}}} \sum_{i=1}^{n_1^{\mathrm{tr}}} \frac{p_1^{\mathrm{te}}(\mathbf{x}_{1,i}^{\mathrm{tr}})}{p_1^{\mathrm{tr}}(\mathbf{x}_{1,i}^{\mathrm{tr}})} \ell(h_{\mathbf{w}}(\mathbf{x}_{1,i}^{\mathrm{tr}}), \mathbf{y}_{1,i}^{\mathrm{tr}}) + \frac{1}{n_2^{\mathrm{tr}}} \sum_{i=1}^{n_2^{\mathrm{tr}}} \frac{p_1^{\mathrm{te}}(\mathbf{x}_{2,i}^{\mathrm{tr}})}{p_2^{\mathrm{tr}}(\mathbf{x}_{2,i}^{\mathrm{tr}})} \ell(h_{\mathbf{w}}(\mathbf{x}_{2,i}^{\mathrm{tr}}), \mathbf{y}_{2,i}^{\mathrm{tr}}). \tag{C.2}$$

Covariate shift for both clients: (CS on both) We assume $p_1^{\mathrm{tr}}(\mathbf{x}) \neq p_1^{\mathrm{te}}(\mathbf{x})$ and $p_2^{\mathrm{tr}}(\mathbf{x}) \neq p_2^{\mathrm{te}}(\mathbf{x})$, *i.e.,* covariate shift for both clients. The corresponding FIDEM is the same as Eq. (C.2).

Multiple clients: (CS on multi.) Finally, we consider a general scenario with K clients. We assume both intra-client and inter-client covariate shifts by the following FIDEM:

$$\min_{\mathbf{w}\in\mathbb{R}^d} \sum_{k=1}^{K} \frac{\lambda_k}{n_k^{\mathrm{tr}}} \sum_{i=1}^{n_k^{\mathrm{tr}}} \frac{p_1^{\mathrm{te}}(\mathbf{x}_{k,i}^{\mathrm{tr}})}{p_k^{\mathrm{tr}}(\mathbf{x}_{k,i}^{\mathrm{tr}})} \ell(h_{\mathbf{w}}(\mathbf{x}_{k,i}^{\mathrm{tr}}), \mathbf{y}_{k,i}^{\mathrm{tr}}) \tag{C.3}$$

where $\sum_{k=1}^{K} \lambda_k = 1$ and $\lambda_k \geq 0$.

Proposition 2. *Let $l \in [K]$. In above settings, FIDEM defined in Eqs. (C.1), (C.2), and (C.3) is consistent. i.e., the learned function converges in probability to the optimal function in terms of minimizing R_1.*

Proposition 2 implies that, under various settings, FIDEM outputs an unbiased estimate of a *minimizer of the true risk.*

Proof. For the scenario without intra-client covariate shift, FIDEM in Eq. (C.1) can be expressed as

$$\begin{aligned}
\frac{1}{n_2^{\mathrm{tr}}} \sum_{i=1}^{n_2^{\mathrm{tr}}} \frac{p_1^{\mathrm{tr}}(\mathbf{x}_{2,i}^{\mathrm{tr}})}{p_2^{\mathrm{tr}}(\mathbf{x}_{2,i}^{\mathrm{tr}})} \ell(h_{\mathbf{w}}(\mathbf{x}_{2,i}^{\mathrm{tr}}), \mathbf{y}_{2,i}^{\mathrm{tr}}) &\xrightarrow{n_2^{\mathrm{tr}}\to\infty} \mathbb{E}_{p_2^{\mathrm{tr}}(\mathbf{x},\mathbf{y})} \left[\frac{p_1^{\mathrm{tr}}(\mathbf{x})}{p_2^{\mathrm{tr}}(\mathbf{x})} \ell(h_{\mathbf{w}}(\mathbf{x}), \mathbf{y}) \right] \\
&= \int_{\mathcal{X}} \frac{p_1^{\mathrm{tr}}(\mathbf{x})}{p_2^{\mathrm{tr}}(\mathbf{x})} \mathbb{E}_{p(\mathbf{y}|\mathbf{x})} \left[\ell(h_{\mathbf{w}}(\mathbf{x}), \mathbf{y}) \right] p_2^{\mathrm{tr}}(\mathbf{x}) \, \mathrm{d}\mathbf{x} \\
&= \int_{\mathcal{X}} p_1^{\mathrm{tr}}(\mathbf{x}) \mathbb{E}_{p(\mathbf{y}|\mathbf{x})} \left[\ell(h_{\mathbf{w}}(\mathbf{x}), \mathbf{y}) \right] \mathrm{d}\mathbf{x} \\
&= \int_{\mathcal{X}} p_1^{\mathrm{te}}(\mathbf{x}) \mathbb{E}_{p(\mathbf{y}|\mathbf{x})} \left[\ell(h_{\mathbf{w}}(\mathbf{x}), \mathbf{y}) \right] \mathrm{d}\mathbf{x} \\
&= \mathbb{E}_{p_1^{\mathrm{te}}(\mathbf{x},\mathbf{y})} \left[\ell(h_{\mathbf{w}}(\mathbf{x}), \mathbf{y}) \right] \\
&= R_1(h_{\mathbf{w}}).
\end{aligned}$$

For the scenario with covariate shift only for client 1 or for both clients, FIDEM in Eq. (C.2) admits

$$\begin{aligned}
\frac{1}{n_2^{\mathrm{tr}}} \sum_{i=1}^{n_2^{\mathrm{tr}}} \frac{p_1^{\mathrm{te}}(\mathbf{x}_{2,i}^{\mathrm{tr}})}{p_2^{\mathrm{tr}}(\mathbf{x}_{2,i}^{\mathrm{tr}})} \ell(h_{\mathbf{w}}(\mathbf{x}_{2,i}^{\mathrm{tr}}), \mathbf{y}_{2,i}^{\mathrm{tr}}) &\xrightarrow{n_2^{\mathrm{tr}}\to\infty} \mathbb{E}_{p_2^{\mathrm{tr}}(\mathbf{x},\mathbf{y})} \left[\frac{p_1^{\mathrm{te}}(\mathbf{x})}{p_2^{\mathrm{tr}}(\mathbf{x})} \ell(h_{\mathbf{w}}(\mathbf{x}), \mathbf{y}) \right] \\
&= \int_{\mathcal{X}} \frac{p_1^{\mathrm{te}}(\mathbf{x})}{p_2^{\mathrm{tr}}(\mathbf{x})} \mathbb{E}_{p(\mathbf{y}|\mathbf{x})} \left[\ell(h_{\mathbf{w}}(\mathbf{x}), \mathbf{y}) \right] p_2^{\mathrm{tr}}(\mathbf{x}) \, \mathrm{d}\mathbf{x} \\
&= \int_{\mathcal{X}} p_1^{\mathrm{te}}(\mathbf{x}) \mathbb{E}_{p(\mathbf{y}|\mathbf{x})} \left[\ell(h_{\mathbf{w}}(\mathbf{x}), \mathbf{y}) \right] \mathrm{d}\mathbf{x} \\
&= \mathbb{E}_{p_1^{\mathrm{te}}(\mathbf{x},\mathbf{y})} \left[\ell(h_{\mathbf{w}}(\mathbf{x}), \mathbf{y}) \right] \\
&= R_1(h_{\mathbf{w}}).
\end{aligned}$$

We note that $\frac{p_1^{\mathrm{te}}(\mathbf{x})}{p_2^{\mathrm{tr}}(\mathbf{x})} = \frac{p_1^{\mathrm{te}}(\mathbf{x})}{p_1^{\mathrm{tr}}(\mathbf{x})} \frac{p_1^{\mathrm{tr}}(\mathbf{x})}{p_2^{\mathrm{tr}}(\mathbf{x})}$, which is the product of ratios due to intra-client covariate shift on client 1 and inter-client covariate shift.

For multiple clients, let $k \in [K]$. Similarly, we have

$$\frac{1}{n_k^{\text{tr}}} \sum_{i=1}^{n_k^{\text{tr}}} \frac{p_1^{\text{te}}(\mathbf{x}_{k,i}^{\text{tr}})}{p_k^{\text{tr}}(\mathbf{x}_{k,i}^{\text{tr}})} \ell(h_{\mathbf{w}}(\mathbf{x}_{k,i}^{\text{tr}}), \mathbf{y}_{k,i}^{\text{tr}}) \xrightarrow{n_k^{\text{tr}} \to \infty} R_1(h_{\mathbf{w}}).$$

Then we have

$$\sum_{k=1}^{K} \frac{\lambda_k}{n_k^{\text{tr}}} \sum_{i=1}^{n_k^{\text{tr}}} \frac{p_1^{\text{te}}(\mathbf{x}_{k,i}^{\text{tr}})}{p_k^{\text{tr}}(\mathbf{x}_{k,i}^{\text{tr}})} \ell(h_{\mathbf{w}}(\mathbf{x}_{k,i}^{\text{tr}}), \mathbf{y}_{k,i}^{\text{tr}}) \xrightarrow{n_1^{\text{tr}}, \ldots, n_K^{\text{tr}} \to \infty} R_1(h_{\mathbf{w}}).$$

The consistency of FIDEM, i.e., convergence in probability, is immediately followed the standard arguments in e.g., (Shimodaira, 2000)[Section 3] and (Sugiyama et al., 2007)[Section 2.2] using the law of large numbers. ■

Note that to solve Eq. (C.3), client 1 needs to estimate $\frac{p_1^{\text{te}}(\mathbf{x})}{p_k^{\text{tr}}(\mathbf{x})}$ for all clients k with $\lambda_k > 0$ in (C.3).

Remark 5. Scaling $\sum_{k=1}^{K} \lambda_k$ does not affect the optimal parameters in Eq. (C.3). For rotational simplicity, we set $\lambda_k = 1$ for $k \in [K]$.

C.1 No intra-client shift

In this section, we consider the important and special case of the setting described in Section 2.1 under no intra-client covariate shifts but inter-client covariate shifts. For simplicity, we consider a two clients with train/test distributions P and Q whose train/test densities are denoted by p and q, respectively. We also suppose that we have a sample $z \sim P$ and $z' \sim Q$ to learn with the goal is to find an unbiased estimate of the overall risk with the smallest variance. In this setting, the classical ERM (FedAvg) objective $\ell(z, \theta) + \ell(z', \theta)$ is an unbiased estimate for the overall risk $L(\theta) = \mathbb{E}_P[\ell(z, \theta)] + \mathbb{E}_Q[\ell(z', \theta)]$[5]. In this setting, the objective of FIDEM, i.e., $\frac{1}{2}(\hat{L}_P(\theta) + \hat{L}_Q(\theta))$ with $\hat{L}_P(\theta) = \big(1 + \frac{q(z)}{p(z)}\big)\ell(z, \theta)$ and $\hat{L}_Q(\theta) = \big(1 + \frac{p(z')}{q(z')}\big)\ell(z', \theta)$ is an unbiased estimate for the overall risk $L(\theta)$.

We now show that the our method (FIDEM) has a smaller variance than FedAvg under certain conditions. Let $\mathbb{E}_P[(\ell(z, \theta) - \mathbb{E}_P[\ell(z, \theta)])^2] = \sigma_P^2$ and $\mathbb{E}_Q[(\ell(z', \theta) - \mathbb{E}_Q[\ell(z', \theta)])^2] = \sigma_Q^2$.

For FedAvg, the variance is given by

$$\mathbb{E}_{P,Q}[(\ell(z, \theta) + \ell(z', \theta) - L(\theta))^2] = \sigma_P^2 + \sigma_Q^2.$$

For FIDEM, the variance is given by

$$\mathbb{E}_{P,Q}[(\frac{1}{2}(\hat{L}_P(\theta) + \hat{L}_Q(\theta)) - L(\theta))^2] = V_P + V_Q$$

where $V_P = \frac{1}{4}\mathbb{E}_P[(\hat{L}_P(\theta) - L(\theta))^2]$ and $V_Q = \frac{1}{4}\mathbb{E}_Q[(\hat{L}_Q(\theta) - L(\theta))^2]$.

We now expand each term V_P and V_Q. We can show that

$$V_P = \frac{1}{4}\mathbb{E}_P\Big[\Big((1 + \frac{q(z)}{p(z)})\ell(z, \theta) - \mathbb{E}_P[\ell(z, \theta)] - \mathbb{E}_Q[\ell(z', \theta)]\Big)^2\Big] = \frac{\sigma_P^2 + \tilde{\sigma}_P^2}{4}$$

where $\tilde{\sigma}_P^2 = \mathbb{E}_P\Big[\Big(\frac{q(z)}{p(z)}\ell(z, \theta) - \mathbb{E}_Q[\ell(z', \theta)]\Big)^2\Big] + 2\mathbb{E}_P\Big[\Big(\ell(z, \theta) - \mathbb{E}_P[\ell(z, \theta)]\Big)\Big(\frac{q(z)}{p(z)}\ell(z, \theta) - \mathbb{E}_Q[\ell(z', \theta)]\Big)\Big]$. Similarly, we have

$$V_Q = \frac{1}{4}\mathbb{E}_Q\Big[\Big((1 + \frac{p(z')}{q(z')})\ell(z', \theta) - \mathbb{E}_P[\ell(z, \theta)] - \mathbb{E}_Q[\ell(z', \theta)]\Big)^2\Big] = \frac{\sigma_Q^2 + \tilde{\sigma}_Q^2}{4}$$

[5]For notational simplicity, we overload $\ell(z, \theta)$ to denote the loss of model θ on example z.

where $\tilde{\sigma}_Q^2 = \mathbb{E}_Q\Big[\Big(\frac{p(z')}{q(z')}\ell(z',\theta) - \mathbb{E}_P[\ell(z,\theta)]\Big)^2\Big] + 2\mathbb{E}_Q\Big[\Big(\ell(z',\theta) - \mathbb{E}_Q[\ell(z',\theta)]\Big)\Big(\frac{p(z')}{q(z')}\ell(z',\theta) - \mathbb{E}_P[\ell(z,\theta)]\Big)\Big]$.

We note if $\tilde{\sigma}_P^2 + \tilde{\sigma}_Q^2 \leq 3(\sigma_P^2 + \sigma_Q^2)$ then, FIDEM will have smaller variance than FedAvg, i.e., $V_P + V_Q \leq \sigma_P^2 + \sigma_Q^2$. The exact condition depends on the loss and densities. To show a concrete example, for the more general and practical case with both intra/inter-client , in Section 4.2, we show that FIDEM results in smaller excess risk compared to FedAvg through a refined bias-variance decomposition. Given two distributions, considering the case of no intra-client shift is a special case, where it is true that FedAvg is an unbiased estimate of the overall risk. However, this unbiasedness breaks as soon as there is only one client whose test and train distributions are different, which is very common in theory and practice. Please note that FIDEM is an unbiased estimate of the overall risk in a general FL setting without requiring any prior knowledge/assumptions on the potential covariate shifts.

D Ratio estimation

D.1 nnBD DRM for a single client

For simplicity, we firstly focus on the problem of estimating $r(\mathbf{x}) = \frac{p^{\text{te}}(\mathbf{x})}{p^{\text{tr}}(\mathbf{x})}$ and then extend our consideration to the estimation of $r_k(\mathbf{x})$ in Eq. (3.1). Let r^* denote the true density ratio. Our goal is to estimate r^* by optimizing our ratio model r. The discrepancy between r and r^* is measured by $\mathbb{E}_{p^{\text{tr}}}[\text{BD}_f(r^*(\mathbf{x}) \parallel r(\mathbf{x}))]$. We note that $\mathbb{E}_{p^{\text{tr}}}[\text{BD}_f(r^*(\mathbf{x}) \parallel r(\mathbf{x}))] = \mathcal{E}_f(r) + \mathbb{E}_{p^{\text{tr}}}[f(r^*(\mathbf{x}))]$ where $\mathcal{E}_f(r) = \mathbb{E}_{p^{\text{tr}}}[\nabla f(r(\mathbf{x}))r(\mathbf{x}) - f(r(\mathbf{x}))] - \mathbb{E}_{p^{\text{te}}}[\nabla f(r(\mathbf{x}))]$. Note that $\mathbb{E}_{p^{\text{tr}}}[f(r^*(\mathbf{x}))]$ is constant w.r.t. r. Let $\{\mathbf{x}_i^{\text{tr}}\}_{i=1}^{n^{\text{tr}}}$ and $\{\mathbf{x}_j^{\text{te}}\}_{j=1}^{n^{\text{te}}}$ denote unlabelled samples drawn i.i.d from distributions p^{tr} and p^{te}, respectively. Let $\mathcal{H}_r \subset \{r : \mathcal{X} \to \mathcal{B}_f\}$ denote a hypothesis class for our model r. Using an empirical approximation of $\mathcal{E}_f(r^*(\mathbf{x}) \parallel r(\mathbf{x}))$, Sugiyama et al. (2012) formulated BD-based DRM problem as $\min_{r\in\mathcal{H}_r} \hat{\mathcal{E}}_f(r)$ where

$$\hat{\mathcal{E}}_f(r) = \frac{1}{n^{\text{tr}}}\sum_{i=1}^{n^{\text{tr}}}\Big(\nabla f(r(\mathbf{x}_i^{\text{tr}}))r(\mathbf{x}_i^{\text{tr}}) - f(r(\mathbf{x}_i^{\text{tr}}))\Big) - \frac{1}{n^{\text{te}}}\sum_{j=1}^{n^{\text{te}}}\nabla f(r(\mathbf{x}_j^{\text{te}})). \tag{D.1}$$

Sugiyama et al. (2012) showed that BD-based DRM unifies well-known density ratio estimation methods by substituting an appropriate f in (D.1). However, it is shown that solving BD-based DRM with highly flexible models such as neural networks typically leads to an over-fitting issue (Kato & Teshima, 2021; Kiryo et al., 2017). In particular, Kato & Teshima (2021) called such issue "train-loss hacking" where $-\frac{1}{n^{\text{te}}}\sum_{j=1}^{n^{\text{te}}}\nabla f(r(\mathbf{x}_j^{\text{te}}))$ in (D.1) diverges if there is no lower bound on this term. Even when there exists a lower bound, the model r tends to increase to the largest possible values of its output range at points $\{\mathbf{x}_j^{\text{te}}\}_{j=1}^{n^{\text{te}}}$. To resolve such issue, Kato & Teshima (2021) proposed to use non-negative BD (nnBD) DRM, i.e., $\min_{r\in\mathcal{H}_r} \hat{\mathcal{E}}_f^+(r)$ where

$$\hat{\mathcal{E}}_f^+(r) = \text{ReLU}\Big(\frac{1}{n^{\text{tr}}}\sum_{i=1}^{n^{\text{tr}}}\ell_1(r(\mathbf{x}_i^{\text{tr}})) - \frac{C}{n^{\text{te}}}\sum_{j=1}^{n^{\text{te}}}\ell_1(r(\mathbf{x}_j^{\text{te}}))\Big) + \frac{1}{n^{\text{te}}}\sum_{j=1}^{n^{\text{te}}}\ell_2(r(\mathbf{x}_j^{\text{te}})), \tag{D.2}$$

$\text{ReLU}(z) = \max\{0, z\}$, $0 < C < \frac{1}{\overline{r}}$, $\overline{r} = \sup_{\mathbf{x}\in\mathcal{X}^{\text{tr}}} r^*(\mathbf{x})$, $\ell_1(z) = \nabla f(z)z - f(z)$, and $\ell_2(z) = C(\nabla f(z)z - f(z)) - \nabla f(z)$. Substituting $f(z) = \frac{(z-1)^2}{2}$ into (D.2), the least-squares importance fitting (LSIF) variant of nnBD is given by

$$\hat{\mathcal{E}}_{\text{LSIF}}^+(r) = \text{ReLU}\Big(\frac{1}{2n^{\text{tr}}}\sum_{i=1}^{n^{\text{tr}}}r^2(\mathbf{x}_i^{\text{tr}}) - \frac{C}{2n^{\text{te}}}\sum_{j=1}^{n^{\text{te}}}r^2(\mathbf{x}_j^{\text{te}})\Big) - \frac{1}{n^{\text{te}}}\sum_{j=1}^{n^{\text{te}}}\big(r(\mathbf{x}_j^{\text{te}}) - \frac{C}{2}r^2(\mathbf{x}_j^{\text{te}})\big).$$

In Appendix F, we show explicit expressions for unnormalized Kullback–Leibler (UKL), logistic regression (LR), and positive and unlabeled learning (PU) variants of nnBD.

Estimating $\overline{r} = \sup_{\mathbf{x}\in\mathcal{X}^{\text{tr}}} r^*(\mathbf{x})$ is a key step for density ratio estimation. It is shown that underestimating C leads to significant performance degradation (Kato & Teshima, 2021, Section 5). Kato & Teshima (2021)

considered C as a hyper-parameter, which can be tuned. However, obtaining an efficient estimate of $\overline{r}$ is desirable, in particular when training a deep model.

Let $\mathcal{B} \subset \mathcal{X}^{\text{tr}}$. Assume p^{tr} and p^{te} are continuous. Since $\mathcal{B}$ is connected and Lebesgue-measurable with finite measure, by applying intermediate value theorem (Russ, 1980), there exist $\tilde{x}^{\text{tr}}$ and $\hat{x}^{\text{te}}$ such that $\Pr\{X^{\text{tr}} \in \mathcal{B}\} = p^{\text{tr}}(\tilde{x}^{\text{tr}})\text{Vol}(\mathcal{B})$ and $\Pr\{X^{\text{te}} \in \mathcal{B}\} = p^{\text{te}}(\hat{x}^{\text{te}})\text{Vol}(\mathcal{B})$ where $\text{Vol}(\mathcal{B}) = \int_{\mathbf{x}\in\mathcal{B}} \mathrm{d}\mathbf{x}$. We note that $\sup_{\mathbf{x}\in\mathcal{B}} r^*(\mathbf{x}) \leq \frac{\sup_{\mathbf{x}\in\mathcal{B}} p^{\text{te}}(\mathbf{x})}{\inf_{\mathbf{x}\in\mathcal{B}} p^{\text{tr}}(\mathbf{x})}$ and $\frac{p^{\text{te}}(\hat{x}^{\text{te}})}{p^{\text{tr}}(\tilde{x}^{\text{tr}})} \leq \frac{\sup_{\mathbf{x}\in\mathcal{B}} p^{\text{te}}(\mathbf{x})}{\inf_{\mathbf{x}\in\mathcal{B}} p^{\text{tr}}(\mathbf{x})}$. We partition $\mathcal{X}^{\text{tr}}$ into M bins where for each bin $\mathcal{B}_m$, if there exists some $\mathbf{x}_i^{\text{tr}} \in \mathcal{B}_m$, then we define $\tilde{r}_m := \frac{\Pr\{X^{\text{te}}\in\mathcal{B}_m\}}{\Pr\{X^{\text{tr}}\in\mathcal{B}_m\}} \simeq \frac{\frac{1}{n^{\text{te}}}\sum_{j=1}^{n^{\text{te}}} \mathbb{1}(\mathbf{x}_j^{\text{te}}\in\mathcal{B}_m)}{\frac{1}{n^{\text{tr}}}\sum_{i=1}^{n^{\text{tr}}} \mathbb{1}(\mathbf{x}_i^{\text{tr}}\in\mathcal{B}_m)}$ for $m \in [M]$. Otherwise, $\tilde{r}_m = 0$. Finally, we propose to use $C \leq \frac{1}{\tilde{r}}$ where $\tilde{r} = \max\{\tilde{r}_1, \ldots, \tilde{r}_M\}$. Convergence of $\tilde{r}$ to $\overline{r}$ is established in Appendix G.

Now, suppose there are K clients where each client provides n^{te} unlabelled test samples to the pool of samples. Our goal is to estimate r_k in Eq. (3.1) for $k = 1, \ldots, K$. The BD-based DRM for client k is given by $\min_{r_k\in\mathcal{H}_r} \hat{\mathcal{E}}_f(r_k)$ where $\hat{\mathcal{E}}_f(r_k) = \frac{1}{n_k^{\text{tr}}}\sum_{i=1}^{n_k^{\text{tr}}} \Big(\nabla f(r_k(\mathbf{x}_{k,i}^{\text{tr}}))r_k(\mathbf{x}_{k,i}^{\text{tr}}) - f(r_k(\mathbf{x}_{k,i}^{\text{tr}}))\Big) - \frac{1}{n^{\text{te}}}\sum_{j=1}^{n^{\text{te}}}\sum_{l=1}^{K} \nabla f(r_k(\mathbf{x}_{l,j}^{\text{te}}))$. The nnBD DRM problem for client k is $\min_{r_k\in\mathcal{H}_r} \hat{\mathcal{E}}_f^+(r_k)$ where

$$\hat{\mathcal{E}}_f^+(r_k) = \text{ReLU}(\hat{S}_{1,\ell_1}) + \frac{1}{n^{\text{te}}}\sum_{j=1}^{n^{\text{te}}}\sum_{l=1}^{K} \ell_2(r_k(\mathbf{x}_{l,j}^{\text{te}})), \tag{D.3}$$

$\hat{S}_{1,\ell_1} = \frac{1}{n_k^{\text{tr}}}\sum_{i=1}^{n_k^{\text{tr}}} \ell_1(r_k(\mathbf{x}_{k,i}^{\text{tr}})) - \frac{C_k}{n^{\text{te}}}\sum_{j=1}^{n^{\text{te}}}\sum_{l=1}^{K} \ell_1(r_k(\mathbf{x}_{l,j}^{\text{te}}))$, $0 < C_k < \frac{1}{\overline{r}_k}$, and $\overline{r}_k = \sup_{\mathbf{x}\in\mathcal{X}^{\text{tr}}} r_k^*(\mathbf{x})$. Substituting $f(z) = \frac{(z-1)^2}{2}$ into (D.3), the LSIF variant of nnBD for client k is given by $\min_{r_k\in\mathcal{H}_r} \hat{\mathcal{E}}_{\text{LSIF}}^+(r_k)$ where

$$\hat{\mathcal{E}}_{\text{LSIF}}^+(r_k) = \text{ReLU}(\hat{S}_{\text{LSIF}}) - \frac{1}{n^{\text{te}}}\sum_{j=1}^{n^{\text{te}}}\sum_{l=1}^{K} \big(r_k(\mathbf{x}_{l,j}^{\text{te}}) - \frac{C_k}{2} r_k^2(\mathbf{x}_{l,j}^{\text{te}})\big), \tag{D.4}$$

and $\hat{S}_{\text{LSIF}} = \frac{1}{2n_k^{\text{tr}}}\sum_{i=1}^{n_k^{\text{tr}}} r_k^2(\mathbf{x}_{k,i}^{\text{tr}}) - \frac{C_k}{2n^{\text{te}}}\sum_{j=1}^{n^{\text{te}}}\sum_{l=1}^{K} r_k^2(\mathbf{x}_{l,j}^{\text{te}})$. We provide explicit expressions for UKL, LR, and PU variants of nnBD for client k in Appendix H.

Our goal is to estimate $\overline{r}_k = \sup_{\mathbf{x}\in\mathcal{X}^{\text{tr}}} \frac{\sum_{l=1}^{K} p_l^{\text{te}}(\mathbf{x})}{p_k^{\text{tr}}(\mathbf{x})}$. For HDRM method, we first partition $\mathcal{X}^{\text{tr}}$ into M bins where for each bin $\mathcal{B}_m$, if there exists some $\mathbf{x}_{k,i}^{\text{tr}} \in \mathcal{B}_m$, then we define $\tilde{r}_{k,m} := \frac{\sum_{l=1}^{K}\Pr\{X_l^{\text{te}}\in\mathcal{B}_m\}}{\Pr\{X_k^{\text{tr}}\in\mathcal{B}_m\}} \simeq \frac{\frac{1}{n^{\text{te}}}\sum_{j=1}^{n^{\text{te}}}\sum_{l=1}^{K} \mathbb{1}(\mathbf{x}_{l,j}^{\text{te}}\in\mathcal{B}_m)}{\frac{1}{n_k^{\text{tr}}}\sum_{i=1}^{n_k^{\text{tr}}} \mathbb{1}(\mathbf{x}_{k,i}^{\text{tr}}\in\mathcal{B}_m)}$ for $m \in [M]$. Otherwise, $\tilde{r}_{k,m} = 0$. Finally, we propose to use $C_k = \frac{1}{\tilde{r}_k}$ where $\tilde{r}_k = \max\{\tilde{r}_{k,1}, \ldots, \tilde{r}_{k,M}\}$.

D.2 BD-based DRM for FL

Our goal is to estimate r_k by minimizing the discrepancy $\mathbb{E}_{p_k^{\text{tr}}}[\text{BD}_f(r_k^*(\mathbf{x}) \parallel r_k(\mathbf{x}))]$, which is equivalent to $\min_{r_k\in\mathcal{H}_r} \mathcal{E}_f(r_k)$ where

$$\mathcal{E}_f(r_k) = \mathbb{E}_{p_k^{\text{tr}}}[\nabla f(r_k(\mathbf{x}))r_k(\mathbf{x}) - f(r_k(\mathbf{x}))] - \sum_{l=1}^{K} \mathbb{E}_{p_l^{\text{te}}}[\nabla f(r_k(\mathbf{x}))], \tag{D.5}$$

since $\mathbb{E}_{p_k^{\text{tr}}}[\text{BD}_f(r_k^*(\mathbf{x}) \parallel r_k(\mathbf{x}))] = \mathcal{E}_f(r_k) + \mathbb{E}_{p_k^{\text{tr}}}[f(r_k^*(\mathbf{x}))]$ and $\mathbb{E}_{p_k^{\text{tr}}}[f(r_k^*(\mathbf{x}))]$ is constant w.r.t. r_k. Let $\{\mathbf{x}_{k,i}^{\text{tr}}\}_{i=1}^{n_k^{\text{tr}}}$ and $\{\mathbf{x}_{l,j}^{\text{te}}\}_{j=1}^{n^{\text{te}}}$ denote unlabelled samples drawn i.i.d from distributions p_k^{tr} and p_l^{te}, respectively, for $l \in [K]$. A natural way to solve $\min_{r_k\in\mathcal{H}_r} \mathcal{E}_f(r_k)$ is to substitute empirical averages in Eq. (D.5) (Sugiyama et al.,

2012), leading to BD-based DRM for FL: $\min_{r_k \in \mathcal{H}_r} \hat{\mathcal{E}}_f(r_k)$ where

$$\hat{\mathcal{E}}_f(r_k) = \frac{1}{n_k^{\mathrm{tr}}} \sum_{i=1}^{n_k^{\mathrm{tr}}} \Big(\nabla f(r_k(\mathbf{x}_{k,i}^{\mathrm{tr}})) r_k(\mathbf{x}_{k,i}^{\mathrm{tr}}) - f(r_k(\mathbf{x}_{k,i}^{\mathrm{tr}})) \Big) - \frac{1}{n^{\mathrm{te}}} \sum_{j=1}^{n^{\mathrm{te}}} \sum_{l=1}^{K} \nabla f(r_k(\mathbf{x}_{l,j}^{\mathrm{te}})).$$

E Communication costs and FIIDEM

To estimate density ratios for FIDEM, clients require to send a few unlabelled test samples *only once*. The server shuffles those samples and broadcasts the shuffled version to clients *only once*. The communication overhead to estimate ratios is negligible compared to the communication costs for sharing high-dimensional stochastic gradients over the course of training.

Consider the example of CIFAR10 consisting of 32 by 32 images with 3 channels represented by 8 bits. If one shares 1000 unlabelled images[6], the communication amounts to sharing roughly 3×10^6 values each with 8 bits, i.e., 25×10^6 total communication bits or 3.1MB. In contrast, during training, the network size alone easily surpasses this size (e.g. the common ResNet-18 has 11 million parameters, each represented by a 32-bit floating point). Standard training of ResNet-18 requires 8×10^4 iterations and aggregations, which amounts to 2.816×10^{13} total communicated bits per client, i.e., 3.5TB during training.

In other words, the number of communication bits needed during training in standard federated learning is usually many *orders of magnitudes* larger than the size of samples shared for estimating the ratios. To further reduce communication costs of density ratio estimation and gradient aggregation, compression methods such as quantization, sparsification, and local updating rules, can be used along with FIDEM *on the fly* (Alistarh et al., 2017).

Alternatively, to eliminate any privacy risks, clients may minimize the following surrogate objective, which we name FIIDEM:

$$\min_{\mathbf{w}} \tilde{F}(\mathbf{w}) := \sum_{k=1}^{K} \tilde{F}_k(\mathbf{w}) \tag{E.1}$$

where $\tilde{F}_k(\mathbf{w}) = \frac{1}{n_k^{\mathrm{tr}}} \sum_{i=1}^{n_k^{\mathrm{tr}}} \frac{p_k^{\mathrm{te}}(\mathbf{x}_{k,i}^{\mathrm{tr}})}{p_k^{\mathrm{tr}}(\mathbf{x}_{k,i}^{\mathrm{tr}})} \ell(h_{\mathbf{w}}(\mathbf{x}_{k,i}^{\mathrm{tr}}), \mathbf{y}_{k,i}^{\mathrm{tr}})$.

We note that privacy risks are eliminated by solving E.1. However, to exploit the entire data distributed among all clients and achieve the optimal global model in terms of overall test error, clients need to compromise some level of privacy and share unlabelled samples generated from their test distribution with the server. Hence, in this paper, we focus on the original objective $F(\mathbf{w})$ in FIDEM, which is different from $\tilde{F}(\mathbf{w})$.

F Variants of nnBD

In this section, we show explicit expressions for unnormalized Kullback–Leibler (UKL), logistic regression (LR), and positive and unlabeled learning (PU) variants of nnBD.

Substituting $f(z) = z\log(z) - z$ into Eq. (D.2), we have $\ell_1(z) = z$ and $\ell_2(z) = zC - \log(z)$, and the UKL variant of nnBD is given by

$$\begin{aligned} \hat{\mathcal{E}}_{\mathrm{UKL}}^{+}(r) = \mathrm{ReLU}\Big(& \frac{1}{n^{\mathrm{tr}}} \sum_{i=1}^{n^{\mathrm{tr}}} r(\mathbf{x}_i^{\mathrm{tr}}) - \frac{C}{n^{\mathrm{te}}} \sum_{j=1}^{n^{\mathrm{te}}} r(\mathbf{x}_j^{\mathrm{te}}) \Big) \\ & - \frac{1}{n^{\mathrm{te}}} \sum_{j=1}^{n^{\mathrm{te}}} \big(\log(r(\mathbf{x}_j^{\mathrm{te}})) - C r(\mathbf{x}_j^{\mathrm{te}}) \big). \end{aligned} \tag{F.1}$$

[6] A total number of 1000 images are shown to be sufficient to learn density ratios on CIFAR10 (Kato & Teshima, 2021)[10, Section 5.1].

Substituting $f(z) = z\log(z) - (z+1)\log(z+1)$ into Eq. (D.2), we have $\ell_1(z) = \log(z+1)$ and $\ell_2(z) = C\log(z+1) + \log\left(\frac{z+1}{z}\right)$, and the LR (BKL) variant of nnBD is given by

$$\begin{aligned}\hat{\mathcal{E}}^{+}_{\mathrm{LR}}(r) = \mathrm{ReLU}\Big(&\frac{1}{n^{\mathrm{tr}}}\sum_{i=1}^{n^{\mathrm{tr}}}\log(r(\mathbf{x}_i^{\mathrm{tr}})+1) - \frac{C}{n^{\mathrm{te}}}\sum_{j=1}^{n^{\mathrm{te}}}\log(r(\mathbf{x}_j^{\mathrm{te}})+1)\Big)\\ &- \frac{1}{n^{\mathrm{te}}}\sum_{j=1}^{n^{\mathrm{te}}}\left(\log\left(\frac{r(\mathbf{x}_j^{\mathrm{te}})}{r(\mathbf{x}_j^{\mathrm{te}})+1}\right) - C\log(r(\mathbf{x}_j^{\mathrm{te}})+1)\right).\end{aligned} \tag{F.2}$$

Substituting $f(z) = C\log(1-z) + Cz(\log(z) - \log(1-z))$ into Eq. (D.2), we have $\ell_1(z) = -C\log(1-z)$ and $\ell_2(z) = -C\log(z) + (C - C^2)\log(1-z)$, and the PU variant of nnBD is given by

$$\begin{aligned}\hat{\mathcal{E}}^{+}_{\mathrm{PU}}(r) = \mathrm{ReLU}\Big(&\frac{-C}{n^{\mathrm{tr}}}\sum_{i=1}^{n^{\mathrm{tr}}}\log(1-r(\mathbf{x}_i^{\mathrm{tr}})) + \frac{C^2}{n^{\mathrm{te}}}\sum_{j=1}^{n^{\mathrm{te}}}\log(1-r(\mathbf{x}_j^{\mathrm{te}}))\Big)\\ &- \frac{1}{n^{\mathrm{te}}}\sum_{j=1}^{n^{\mathrm{te}}}\left(C\log(r(\mathbf{x}_j^{\mathrm{te}})) - (C-C^2)\log(1-r(\mathbf{x}_j^{\mathrm{te}}))\right).\end{aligned} \tag{F.3}$$

G Convergence of $\tilde{r}$ and k-means clustering

Lemma 2. *If n_k^{tr}, n^{te}, and M go to infinity with $\sup_m \mathrm{Vol}(\mathcal{B}_m) \to 0$, then $\tilde{r}_k \to \overline{r}_k$.*

Proof. Let $\mathbf{x} \in \mathcal{X}^{\mathrm{tr}}$. Note that when n_k^{tr}, n^{te}, and M go to infinity, the numerator and denominator of $\tilde{r}_k$ become $\sum_{l=1}^{K} p_l^{\mathrm{te}}(\mathbf{x})\mathrm{Vol}(\mathcal{B}_m)$ and $p_k^{\mathrm{tr}}(\mathbf{x})\mathrm{Vol}(\mathcal{B}_m)$, respectively, where $\mathbf{x} \in \mathcal{B}_m$. ■

Please note that our density ratio in Eq. (3.1) is in the form of a sum of test densities over own train density. So even if one or a few number of ratios are poorly estimated, it will not impact the entire ratio in Eq. (3.1) as nested estimation errors. The error does not propagate in a multiplicative manner but in an additive way.

k-means clustering for HDRM. We note that partitioning the space and counting the number of samples in each bin is not necessarily an easy task when data is high dimensional. In practice, one simple method is to cluster train and test samples using an efficient implementation of k-means clustering with M clusters and count the number of train and test samples in each cluster (Lloyd, 1982). To estimate the ratios, we need a batch of samples from the test distribution of each client in addition to a batch of samples from the train distribution for each estimating client. The running time of Lloyd's algorithm with M clusters is $O(nd_{\mathbf{x}}M)$ where n is the total number of samples with dimension $d_{\mathbf{x}}$.

H UKL, LR, and PU variants of nnBD for multiple clients

In this section, we provide explicit expressions for UKL, LR, and PU variants of nnBD for client k.

The UKL variant of nnBD for client k is given by $\min_{r_k \in \mathcal{H}_r} \hat{\mathcal{E}}^{+}_{\mathrm{UKL}}(r_k)$ where

$$\begin{aligned}\hat{\mathcal{E}}^{+}_{\mathrm{UKL}}(r_k) = \mathrm{ReLU}\Big(&\frac{1}{n_k^{\mathrm{tr}}}\sum_{i=1}^{n_k^{\mathrm{tr}}} r_k(\mathbf{x}_{k,i}^{\mathrm{tr}}) - \frac{C_k}{n^{\mathrm{te}}}\sum_{j=1}^{n^{\mathrm{te}}}\sum_{l=1}^{K} r_k(\mathbf{x}_{l,j}^{\mathrm{te}})\Big)\\ &- \frac{1}{n^{\mathrm{te}}}\sum_{j=1}^{n^{\mathrm{te}}}\sum_{l=1}^{K}\left(\log(r_k(\mathbf{x}_{l,j}^{\mathrm{te}})) - C_k r_k(\mathbf{x}_{l,j}^{\mathrm{te}})\right).\end{aligned} \tag{H.1}$$

The LR variant of nnBD for client k is given by $\min_{r_k \in \mathcal{H}_r} \hat{\mathcal{E}}^+_{\mathrm{LR}}(r_k)$ where

$$\begin{aligned}\hat{\mathcal{E}}^+_{\mathrm{LR}}(r_k) = \mathrm{ReLU}\Big(&\frac{1}{n^{\mathrm{tr}}_k}\sum_{i=1}^{n^{\mathrm{tr}}_k}\log(r_k(\mathbf{x}^{\mathrm{tr}}_{k,i})+1) - \frac{C_k}{n^{\mathrm{te}}}\sum_{j=1}^{n^{\mathrm{te}}}\sum_{l=1}^{K}\log(r_k(\mathbf{x}^{\mathrm{te}}_{l,j})+1)\Big)\\ &- \frac{1}{n^{\mathrm{te}}}\sum_{j=1}^{n^{\mathrm{te}}}\sum_{l=1}^{K}\left(\log\left(\frac{r_k(\mathbf{x}^{\mathrm{te}}_{l,j})}{r_k(\mathbf{x}^{\mathrm{te}}_{l,j})+1}\right) - C_k\log(r_k(\mathbf{x}^{\mathrm{te}}_{l,j})+1)\right).\end{aligned} \tag{H.2}$$

The PU variant of nnBD for client k is given by $\min_{r_k \in \mathcal{H}_r} \hat{\mathcal{E}}^+_{\mathrm{PU}}(r_k)$ where

$$\begin{aligned}\hat{\mathcal{E}}^+_{\mathrm{PU}}(r_k) = \mathrm{ReLU}\Big(&\frac{-C_k}{n^{\mathrm{tr}}_k}\sum_{i=1}^{n^{\mathrm{tr}}_k}\log(1-r_k(\mathbf{x}^{\mathrm{tr}}_{k,i})) + \frac{C_k^2}{n^{\mathrm{te}}}\sum_{j=1}^{n^{\mathrm{te}}}\sum_{l=1}^{K}\log(1-r_k(\mathbf{x}^{\mathrm{te}}_{l,j}))\Big)\\ &- \frac{1}{n^{\mathrm{te}}}\sum_{j=1}^{n^{\mathrm{te}}}\sum_{l=1}^{K}\left(C_k\log(r_k(\mathbf{x}^{\mathrm{te}}_{l,j})) - (C_k - C_k^2)\log(1-r_k(\mathbf{x}^{\mathrm{te}}_{l,j}))\right).\end{aligned} \tag{H.3}$$

I Proof of Theorem 1

In this section, we prove Theorem 1, which establishes an upper bound on the ratio estimation error of nnBD DRM (HDRM method with an arbitrary f) for client k in terms of BD risk, which holds with high probability along the lines of (Kiryo et al., 2017; Lu et al., 2020; Kato & Teshima, 2021).

We remind that client k's goal is to estimate this ratio:

$$r_k(\mathbf{x}) = \frac{\sum_{l=1}^{K} p^{\mathrm{te}}_l(\mathbf{x})}{p^{\mathrm{tr}}_k(\mathbf{x})}. \tag{I.1}$$

For client k, the BD risk given by

$$\mathcal{E}_f(r_k) = \tilde{\mathbb{E}}_k(\mathbf{x})[\ell_1(r_k(\mathbf{x}))] + \sum_{l=1}^{K}\mathbb{E}_{p^{\mathrm{te}}_l}[\ell_2(r_k(\mathbf{x}))] \tag{I.2}$$

where $\tilde{\mathbb{E}}_k := \mathbb{E}_{p^{\mathrm{tr}}_k} - C_k\sum_{l=1}^{K}\mathbb{E}_{p^{\mathrm{te}}_l}$, $0 < C_k < \frac{1}{\overline{r}_k}$, $\overline{r}_k = \sup_{\mathbf{x}\in\mathcal{X}^{\mathrm{tr}}} = \frac{\sum_{l=1}^{K} p^{\mathrm{te}}_l(\mathbf{x})}{p^{\mathrm{tr}}_k(\mathbf{x})}$, $\ell_1(z) = \nabla f(z)z - f(z)$, and $\ell_2(z) = C(\nabla f(z)z - f(z)) - \nabla f(z)$. We note that the definition of C_k implies $\tilde{p}_k = p^{\mathrm{tr}}_k - C_k\sum_{l=1}^{K} p^{\mathrm{te}}_l > 0$. We remind that $f : \mathcal{B}_f \to \mathbb{R}$ is a strictly convex function with bounded gradient ∇f where $\mathcal{B}_f \subset [0,\infty)$, and $\mathcal{H}_r \subset \{r : \mathcal{X} \to \mathcal{B}_f\}$ denotes a hypothesis class for our model r.

The nnBD DRM problem for client k is $\min_{r_k\in\mathcal{H}_r} \hat{\mathcal{E}}^+_f(r_k)$ where

$$\hat{\mathcal{E}}^+_f(r_k) = \mathrm{ReLU}\Big((\hat{\mathbb{E}}_{p^{\mathrm{tr}}_k} - C_k\sum_{l=1}^{K}\hat{\mathbb{E}}_{p^{\mathrm{te}}_l})[\ell_1(r_k(\mathbf{x}))]\Big) + \sum_{l=1}^{K}\hat{\mathbb{E}}_{p^{\mathrm{te}}_l}[\ell_2(r_k(\mathbf{x}))] \tag{I.3}$$

with $\hat{\mathbb{E}}_{p^{\mathrm{tr}}_k}$ is the sample average over $\{\mathbf{x}^{\mathrm{tr}}_{k,i}\}_{i=1}^{n^{\mathrm{tr}}_k}$, and $\hat{\mathbb{E}}_{p^{\mathrm{te}}_l}$ is the sample average over $\{\mathbf{x}^{\mathrm{te}}_{l,j}\}_{j=1}^{n^{\mathrm{te}}}$. In the following, we denote $\hat{\mathbb{E}}_k := \hat{\mathbb{E}}_{p^{\mathrm{tr}}_k} - C_k\sum_{l=1}^{K}\hat{\mathbb{E}}_{p^{\mathrm{te}}_l}$ for notational simplicity.

Let $\hat{r}_k := \arg\min_{r_k\in\mathcal{H}_r}\hat{\mathcal{E}}^+_f(r_k)$ and $r^*_k := \arg\min_{r_k\in\mathcal{H}_r}\mathcal{E}_f(r_k)$. We first decompose the ratio estimation error into maximal deviation and bias terms:

$$\begin{aligned}\mathcal{E}_f(\hat{r}_k) - \mathcal{E}_f(r_k^*) &\leq \mathcal{E}_f(\hat{r}_k) - \hat{\mathcal{E}}_f^+(\hat{r}_k) + \hat{\mathcal{E}}_f^+(\hat{r}_k) - \mathcal{E}_f(r_k^*) \\ &\leq \mathcal{E}_f(\hat{r}_k) - \hat{\mathcal{E}}_f^+(\hat{r}_k) + \hat{\mathcal{E}}_f^+(r_k^*) - \mathcal{E}_f(r_k^*) \\ &\leq 2 \sup_{r_k \in \mathcal{H}_r} |\mathcal{E}_f(r_k) - \hat{\mathcal{E}}_f^+(r_k)| \\ &\leq 2 \sup_{r_k \in \mathcal{H}_r} |\hat{\mathcal{E}}_f^+(r_k) - \mathbb{E}[\hat{\mathcal{E}}_f^+(r_k)]| + 2 \sup_{r_k \in \mathcal{H}_r} |\mathbb{E}[\hat{\mathcal{E}}_f^+(r_k)] - \mathcal{E}_f(r_k)|\end{aligned} \tag{I.4}$$

where the second inequality holds since $\hat{r}_k := \arg\min_{r_k \in \mathcal{H}_r} \hat{\mathcal{E}}_f^+(r_k)$. The first term in the RHS of (I.4) is the maximal derivation and the second term is the bias.

In the following two lemmas, we find an upper bound on the maximal deviation $\sup_{r_k \in \mathcal{H}_r} |\hat{\mathcal{E}}_f^+(r_k) - \mathbb{E}[\hat{\mathcal{E}}_f^+(r_k)]|$ and bias $\sup_{r_k \in \mathcal{H}_r} |\mathbb{E}[\hat{\mathcal{E}}_f^+(r_k)] - \mathcal{E}_f(r_k)|$, respectively.

Lemma 3 (Maximal deviation bound)**.** *Denote $\Delta_\ell := \sup_{z \in \mathcal{B}_f} \max_{i \in \{1,2\}} |\ell_i(z)|$, then for any $0 < \delta < 1$, the maximal deviation term is upper bounded with probability at least $1 - \delta$*

$$\begin{aligned}\sup_{r_k \in \mathcal{H}_r} |\hat{\mathcal{E}}_f^+(r_k) - \mathbb{E}[\hat{\mathcal{E}}_f^+(r_k)]| \leq\ & 4L_1 R_{n_k^{\mathrm{tr}}}^{p_k^{\mathrm{tr}}}(\mathcal{H}_r) + 4(C_k L_1 + L_2) \sum_{l=1}^{K} R_{n^{\mathrm{te}}}^{p_l^{\mathrm{te}}}(\mathcal{H}_r) \\ & + \Delta_\ell \sqrt{2\Big(\frac{1}{n_k^{\mathrm{tr}}} + \frac{K(1+C_k)^2}{n^{\mathrm{te}}}\Big) \log \frac{1}{\delta}}.\end{aligned} \tag{I.5}$$

Proof. Denote $\Phi(\mathcal{S}_k) := \sup_{r_k \in \mathcal{H}_r} |\hat{\mathcal{E}}_f^+(r_k) - \mathbb{E}[\hat{\mathcal{E}}_f^+(r_k)]|$ with $\mathcal{S}_k = \{\mathbf{x}_{k,1}^{\mathrm{tr}}, \ldots, \mathbf{x}_{n_k^{\mathrm{tr}},1}^{\mathrm{tr}}, \mathbf{x}_{1,1}^{\mathrm{te}}, \ldots, \mathbf{x}_{K,n^{\mathrm{te}}}^{\mathrm{te}}\}$. Let $\mathcal{S}_k^{(i)}$ be obtained by replacing element i of set $\mathcal{S}_k$ by an independent data point taking values from the set $\mathcal{X}^{\mathrm{tr}}$. We now measure the absolute value of the difference caused by changing one data point in the maximal deviation term (I.5), i.e., $|\Phi(\mathcal{S}_k) - \Phi(\mathcal{S}_k^{(i)})|$. If the changed point is sampled from p_k^{tr}, then the absolute value of the difference caused in the maximal deviation term is upper bounded by $\frac{2\Delta_\ell}{n_k^{\mathrm{tr}}}$. If the changed point is sampled from p_l^{te}, the the absolute value of the difference caused in the maximal deviation term is upper bounded by $\frac{2\Delta_\ell(C_k+1)}{n^{\mathrm{te}}}$ for $l = 1, \ldots, K$. Applying McDiarmid's inequality (McDiarmid et al., 1989), with probability at least $1 - \delta$, we have

$$\begin{aligned}\sup_{r_k \in \mathcal{H}_r} |\hat{\mathcal{E}}_f^+(r_k) - \mathbb{E}[\hat{\mathcal{E}}_f^+(r_k)]| \leq\ & \mathbb{E}[\sup_{r_k \in \mathcal{H}_r} |\hat{\mathcal{E}}_f^+(r_k) - \mathbb{E}[\hat{\mathcal{E}}_f^+(r_k)]|] \\ & + \Delta_\ell \sqrt{2\Big(\frac{1}{n_k^{\mathrm{tr}}} + \frac{K(1+C_k)^2}{n^{\mathrm{te}}}\Big) \log \frac{1}{\delta}}.\end{aligned}$$

In the following, we establish an upper bound on the expected maximal deviation $\mathbb{E}[\sup_{r_k \in \mathcal{H}_r} |\hat{\mathcal{E}}_f^+(r_k) - \mathbb{E}[\hat{\mathcal{E}}_f^+(r_k)]|]$ by generalization the symmetrization argument in (Kiryo et al., 2017; Lu et al., 2020) followed by applying Talagrand's contraction lemma for two-sided Rademacher complexity.

Let $m \in [M]$ and $N_m \in \mathbb{Z}_+$ for $M \in \mathbb{Z}_+$. Let $g_m : \mathbb{R} \to \mathbb{R}$ be a L_{g_m}-Lipschitz function. Let $p_{m,p}$ denote a probability distribution over $\mathcal{X}^{\mathrm{tr}}$. Suppose that $\{\mathbf{x}_i\}_{i=1}^{n_{m,p}}$ are drawn i.i.d. from $p_{m,p}$ for $p \in [N_m]$ and $m \in [M]$. Let $\ell_{m,p} : \mathcal{B}_f \to \mathbb{R}_+$ be a $L_{m,p}$-Lipschitz function and $\tilde{C}_{m,p}$ be a constant $\forall\ m, p$. Consider the following stochastic process:

$$\hat{R}_k(r_k) := \sum_{m=1}^{M} g_m\Big(\sum_{p=1}^{N_m} \tilde{C}_{m,p} \hat{\mathbb{E}}_{m,p}[\ell_{(m,p)}(r_k(\mathbf{x}))]\Big)$$

where $\hat{\mathbb{E}}_{m,p}$ denotes sample average over $\{\mathbf{x}_i\}_{i=1}^{n_{m,p}}$. In the rest of the proof, we show that

$$\mathbb{E}[\sup_{r_k \in \mathcal{H}_r} |\hat{R}_k(r_k) - \mathbb{E}[\hat{R}_k(r_k)]|] \leq 4 \sum_{m=1}^{M} \sum_{p=1}^{N_m} L_{g_m} |\tilde{C}_{m,p}| L_{m,p} R_{n_{m,p}}^{p_{m,p}}(\mathcal{H}_r). \tag{I.6}$$

To prove (I.6), we consider a continuous extension of $\ell_{(m,p)}$ defined on the origin. We note that such extension does not change $\hat{R}_k(r_k)$ since $\ell_{(m,p)}$ takes values only in $\mathcal{B}_f$. If $\mathcal{B}_f = \{(z_1, z_2)\}$ for some $0 \leq z_1 < z_2$, then for any $z \in [0, z_1]$, we define $\ell_{(m,p)}(z) = \lim_{z \downarrow z_1} \ell_{(m,p)}(z)$ where $\lim_{z \downarrow z_1} \ell_{(m,p)}(z)$ exists since $\ell_{(m,p)}$ is uniformly continuous due to Lipschitz continuity. Then $\ell_{(m,p)}$ will be $L_{m,p}$-Lipschitz on $z \in [0, z_2]$. Let $\{\tilde{\mathbf{x}}_i\}_{i=1}^{n_{m,p}}$ be an independent copy of $\{\mathbf{x}_i\}_{i=1}^{n_{m,p}}$. Let denote $\delta_{\hat{R}} := \mathbb{E}[\sup_{r_k \in \mathcal{H}_r} |\hat{R}_k(r_k) - \mathbb{E}[\hat{R}_k(r_k)]|]$. Following a symmetrization argument (Vapnik, 1999), an upper bound on the symmetrized process can be established by Rademacher complexity:

$$
\begin{aligned}
\delta_{\hat{R}} &\leq \mathbb{E}\left[\sup_{r_k \in \mathcal{H}_r} \sum_{m=1}^{M} \left| g_m\Big(\sum_{p=1}^{N_m} \tilde{C}_{m,p} \hat{\mathbb{E}}_{m,p}[\ell_{(m,p)}(r_k(\mathbf{x}))]\Big) - \tilde{\mathbb{E}}\Big[g_m\Big(\sum_{p=1}^{N_m} \tilde{C}_{m,p} \hat{\tilde{\mathbb{E}}}_{m,p}[\ell_{(m,p)}(r_k(\mathbf{x}))]\Big)\Big] \right|\right] \\
&\leq \mathbb{E}\tilde{\mathbb{E}}\left[\sup_{r_k \in \mathcal{H}_r} \sum_{m=1}^{M} \left| g_m\Big(\sum_{p=1}^{N_m} \tilde{C}_{m,p} \hat{\mathbb{E}}_{m,p}[\ell_{(m,p)}(r_k(\mathbf{x}))]\Big) - g_m\Big(\sum_{p=1}^{N_m} \tilde{C}_{m,p} \hat{\tilde{\mathbb{E}}}_{m,p}[\ell_{(m,p)}(r_k(\mathbf{x}))]\Big) \right|\right] \\
&\leq \sum_{m=1}^{M} L_{g_m} \sum_{p=1}^{N_m} |\tilde{C}_{m,p}| \mathbb{E}\tilde{\mathbb{E}}\left[\sup_{r_k \in \mathcal{H}_r} \left| \hat{\mathbb{E}}_{m,p}[\ell_{(m,p)}(r_k(\mathbf{x}))] - \hat{\tilde{\mathbb{E}}}_{m,p}[\ell_{(m,p)}(r_k(\mathbf{x}))] \right|\right] \\
&= \sum_{m=1}^{M} L_{g_m} \sum_{p=1}^{N_m} |\tilde{C}_{m,p}| \mathbb{E}\tilde{\mathbb{E}}\Big[\sup_{r_k \in \mathcal{H}_r} \Big|\hat{\mathbb{E}}_{m,p}[\ell_{(m,p)}(r_k(\mathbf{x})) - \ell_{(m,p)}(0)] - \hat{\tilde{\mathbb{E}}}_{m,p}[\ell_{(m,p)}(r_k(\mathbf{x})) - \ell_{(m,p)}(0)]\Big|\Big] \\
&\leq 4 \sum_{m=1}^{M} L_{g_m} \sum_{p=1}^{N_m} |\tilde{C}_{m,p}| \mathbb{E}\left[\sup_{r_k \in \mathcal{H}_r} \left|\hat{\mathbb{E}}_{m,p}[\sigma_{m,p}(\ell_{(m,p)}(r_k(\mathbf{x})) - \ell_{(m,p)}(0))]\right|\right] \\
&\leq 4 \sum_{m=1}^{M} L_{g_m} \sum_{p=1}^{N_m} |\tilde{C}_{m,p}| R_{n_{m,p}}^{p_{m,p}}(\mathcal{H}_r)
\end{aligned}
\tag{I.7}
$$

where $\sigma_{m,p}$ are Rademacher variables uniformly chosen from $\{-1, 1\}$, $\tilde{\mathbb{E}}$ and $\hat{\tilde{\mathbb{E}}}_{m,p}$ denote the expectation and sample average over data distribution $p_{m,p}$ and the independent copy $\{\tilde{\mathbf{x}}_i\}_{i=1}^{n_{m,p}}$, respectively, the third inequality holds by the Lipschitz continuous property of g_m, and the last inequality is obtained by applying Talagrand's contraction lemma for two-sided Rademacher complexity (Ledoux & Talagrand, 1991; Bartlett & Mendelson, 2002).

Applying (I.6), we can show that

$$
\mathbb{E}[\sup_{r_k \in \mathcal{H}_r} |\hat{\mathcal{E}}_f^+(r_k) - \mathbb{E}[\hat{\mathcal{E}}_f^+(r_k)]|] \leq 4L_1 R_{n_k^{\mathrm{tr}}}^{p_k^{\mathrm{tr}}}(\mathcal{H}_r) + 4(C_k L_1 + L_2) \sum_{l=1}^{K} R_{n^{\mathrm{te}}}^{p_l^{\mathrm{te}}}(\mathcal{H}_r),
$$

which completes the proof. ■

Next we find an upper bound on the bias $\sup_{r_k \in \mathcal{H}_r} |\mathbb{E}[\hat{\mathcal{E}}_f^+(r_k)] - \mathcal{E}_f(r_k)|$.

Lemma 4 (Bias bound)**.** *Denote* $\Delta_\ell := \sup_{z \in \mathcal{B}_f} \max_{i \in \{1,2\}} |\ell_i(z)|$. *Assume* $\inf_{r \in \mathcal{H}_r} \mathbb{E}[\hat{\mathbb{E}}_k[\ell_1(r_k(\mathbf{x}))]] > 0$ *for* $k \in [K]$. *Then, an upper bound on the bias term is given by*

$$
\sup_{r_k \in \mathcal{H}_r} |\mathbb{E}[\hat{\mathcal{E}}_f^+(r_k)] - \mathcal{E}_f(r_k)| \leq (1 + KC_k)\Delta_\ell \exp\left(\frac{-2\eta_k^2}{\Delta_\ell^2/n_k^{\mathrm{tr}} + KC_k^2 \Delta_\ell^2/n^{\mathrm{te}}}\right) \tag{I.8}
$$

for some constant $\eta_k > 0$.

Proof. Let $\hat{\tilde{\mathbb{E}}}_k := \hat{\mathbb{E}}_{p_k^{\text{tr}}} - C_k \sum_{l=1}^{K} \hat{\mathbb{E}}_{p_l^{\text{te}}}$. We first note that

$$\begin{aligned}
|\mathbb{E}[\hat{\mathcal{E}}_f^+(r_k)] - \mathcal{E}_f(r_k)| &= |\mathbb{E}[\hat{\mathcal{E}}_f^+(r_k) - \hat{\mathcal{E}}_f(r_k)]| \\
&= \left|\mathbb{E}\left[\text{ReLU}\left(\hat{\tilde{\mathbb{E}}}_k[\ell_1(r_k(\mathbf{x}))]\right) - \hat{\tilde{\mathbb{E}}}_k[\ell_1(r_k(\mathbf{x}))]\right]\right| \\
&\leq \mathbb{E}\left[\left|\text{ReLU}\left(\hat{\tilde{\mathbb{E}}}_k[\ell_1(r_k(\mathbf{x}))]\right) - \hat{\tilde{\mathbb{E}}}_k[\ell_1(r_k(\mathbf{x}))]\right|\right] \\
&= \mathbb{E}\left[1\left\{\text{ReLU}\left(\hat{\tilde{\mathbb{E}}}_k[\ell_1(r_k(\mathbf{x}))]\right) \neq \hat{\tilde{\mathbb{E}}}_k[\ell_1(r_k(\mathbf{x}))]\right\}\right] \\
&\quad \cdot \left|\text{ReLU}\left(\hat{\tilde{\mathbb{E}}}_k[\ell_1(r_k(\mathbf{x}))]\right) - \hat{\tilde{\mathbb{E}}}_k[\ell_1(r_k(\mathbf{x}))]\right| \\
&= \mathbb{E}\left[1\left\{\text{ReLU}\left(\hat{\tilde{\mathbb{E}}}_k[\ell_1(r_k(\mathbf{x}))]\right) \neq \hat{\tilde{\mathbb{E}}}_k[\ell_1(r_k(\mathbf{x}))]\right\}\right] \sup_{z:|z|\leq(1+KC_k)\Delta_\ell} (\text{ReLU}(z) - z)
\end{aligned}$$

where the third inequality holds due to Jensen's inequality.

We note that $\hat{\tilde{\mathbb{E}}}_k[\ell_1(r_k(\mathbf{x}))] \leq (1 + KC_k)\Delta_\ell$ implies

$$\sup_{z:|z|\leq(1+KC_k)\Delta_\ell} (\text{ReLU}(z) - z) \leq (1 + KC_k)\Delta_\ell.$$

Due to the assumption $\inf_{r\in\mathcal{H}_r} \mathbb{E}[\hat{\mathbb{E}}_k[\ell_1(r_k(\mathbf{x}))]] > 0$, there exists an $\eta_k > 0$ such that $\mathbb{E}[\hat{\mathbb{E}}_k[\ell_1(r_k(\mathbf{x}))]] \geq \eta_k$ for all $r_k \in \mathcal{H}_r$. Then we have

$$\begin{aligned}
\mathbb{E}\left[1\left\{\text{ReLU}\left(\hat{\tilde{\mathbb{E}}}_k[\ell_1(r_k(\mathbf{x}))]\right) \neq \hat{\tilde{\mathbb{E}}}_k[\ell_1(r_k(\mathbf{x}))]\right\}\right] &= \Pr\left\{\hat{\tilde{\mathbb{E}}}_k[\ell_1(r_k(\mathbf{x}))] \in \text{supp}(\widetilde{\text{ReLU}})\right\} \\
&= \Pr\left\{\hat{\tilde{\mathbb{E}}}_k[\ell_1(r_k(\mathbf{x}))] < 0\right\} \\
&= \Pr\left\{\hat{\tilde{\mathbb{E}}}_k[\ell_1(r_k(\mathbf{x}))] < \mathbb{E}[\hat{\tilde{\mathbb{E}}}_k[\ell_1(r_k(\mathbf{x}))]] - \eta_k\right\}
\end{aligned}$$

where $\widetilde{\text{ReLU}}(z) = \text{ReLU}(z) - z$.

Denote $\tilde{\Phi}(\mathcal{S}_k) := \hat{\tilde{\mathbb{E}}}_k[\ell_1(r_k(\mathbf{x}))]$ where $\mathcal{S}_k = \{\mathbf{x}_{k,1}^{\text{tr}}, \ldots, \mathbf{x}_{n_k^{\text{tr}},1}^{\text{tr}}, \mathbf{x}_{1,1}^{\text{te}}, \ldots, \mathbf{x}_{K,n^{\text{te}}}^{\text{te}}\}$. Let $\mathcal{S}_k^{(i)}$ be obtained by replacing element i of set $\mathcal{S}_k$ by an independent data point taking values from the set $\mathcal{X}^{\text{tr}}$. We now measure the absolute value of the difference caused by changing one data point in $|\tilde{\Phi}(\mathcal{S}_k) - \tilde{\Phi}(\mathcal{S}_k^{(i)})|$. If the changed point is sampled from p_k^{tr}, the the absolute value of the difference caused in the maximal deviation term is upper bounded by $\frac{\Delta_\ell}{n_k^{\text{tr}}}$. If the changed point is sampled from p_l^{te}, the the absolute value of the difference caused in the maximal deviation term is upper bounded by $\frac{\Delta_\ell C_k}{n^{\text{te}}}$ for $l = 1, \ldots, K$. Finally, McDiarmid's inequality (McDiarmid et al., 1989) implies:

$$\Pr\left\{\hat{\tilde{\mathbb{E}}}_k[\ell_1(r_k(\mathbf{x}))] < \mathbb{E}[\hat{\tilde{\mathbb{E}}}_k[\ell_1(r_k(\mathbf{x}))]] - \eta_k\right\} \leq \exp\left(\frac{-2\eta_k^2}{\Delta_\ell^2/n_k^{\text{tr}} + KC_k^2\Delta_\ell^2/n^{\text{te}}}\right),$$

which completes the proof. ■

Substituting the upper bounds in (I.5) and (I.8) into (I.4), with probability at least $1 - \delta$, we have

$$\mathcal{E}_f(\hat{r}_k) - \mathcal{E}_f(r_k^*) \leq 8L_1 R_{n_k^{\text{tr}}}^{p_k^{\text{tr}}}(\mathcal{H}_r) + \Psi(\delta, \Delta_\ell, n_k^{\text{tr}}, n^{\text{te}}) + 8(C_k L_1 + L_2) \sum_{l=1}^{K} R_{n^{\text{te}}}^{p_l^{\text{te}}}(\mathcal{H}_r) \tag{I.9}$$

where $\Psi = \Delta_\ell \sqrt{8(\frac{1}{n_k^{\text{tr}}} + \frac{K(1+C_k)^2}{n^{\text{te}}}) \log \frac{1}{\delta}} + 2(1 + KC_k)\Delta_\ell \exp\left(\frac{-2\eta_k^2}{\Delta_\ell^2/n_k^{\text{tr}} + KC_k^2\Delta_\ell^2/n^{\text{te}}}\right)$ for some constant $\eta_k > 0$. This completes the proof.

J Ratio estimation error bound for multi-layer perceptron and multiple clients

Our high-probability ratio estimation error bound for client k depends on the Rademacher complexity of the hypothesis class for our density ratio model $\mathcal{H}_r \subset \{r : \mathcal{X} \to \mathcal{B}_f\}$ w.r.t. client k train distribution p_k^{tr} and all client's test distributions p_l^{te} for $l \in [K]$. By restricting a function class for density ratios and substituting an upper bounds on its Rademacher complexity, we can obtain explicit ratio estimation error bounds in terms of $n_k^{\text{tr}}, n^{\text{te}}$ in a special case. As an example, the following corollary establishes a ratio estimation error bound for multi-layer perceptron density ratio models in terms of the Frobenius norms of weight matrices.

Example J.1 (Complexity for multi-layer perceptron class (Golowich et al., 2018))**.** Assume that distribution p has a bounded support $S_p := \sup_{\mathbf{x} \in \text{supp}(p)} \|\mathbf{x}\| < \infty$. Let $\mathcal{H}$ be the class of real-valued neural networks with depth L over the domain $\mathcal{X}^{\text{tr}}$, $\mathbf{W}_i$ be the network weight matrix i. Suppose that each weight matrix has a bounded Frobenius norm $\|\mathbf{W}_i\|_F \leq \Delta_{\mathbf{W}_i}$ for $i \in [L]$ and the activation ϕ is 1-Lipschitz, and positive-homogeneous function, *i.e.,* $\phi(\alpha z) = \alpha\phi(z)$, which is applied element-wise. Then we have

$$R_n^p(\mathcal{H}) \leq \frac{S_p(\sqrt{2L\log 2} + 1)\prod_{i=1}^L \Delta_{\mathbf{W}_i}}{\sqrt{n}}.$$

Remark 6. To control the upper bound $\Delta_{\mathbf{W}_i}$ for $i \in [L]$, it is natural to employ the sparsity of the weights, *e.g.,* (Golowich et al., 2018, Section 4) and (Hanin & Rolnick, 2019). We consider a special network architecture where $\text{diag}(\mathbf{W}_i)$'s are close to 1-sparse unit vectors for $i \in [L]$, which implies that the matrices $\mathbf{W}_i$'s will be *almost* rank-1. Then $\|\mathbf{W}_i\|_F$ is upper bounded by 1 for $i \in [L]$.

Corollary 1 (High-probability ratio estimation error bound under Example J.1)**.** *For Example J.1 and loss functions described in Theorem 1, with probability at least* $1 - \delta$*, we have*

$$\mathcal{E}_f(\hat{r}_k) - \mathcal{E}_f(r_k^*) \leq \frac{K_k^{\text{tr}}}{\sqrt{n_k^{\text{tr}}}} + \sum_{l=1}^K \frac{K_l^{\text{te}}}{\sqrt{n^{\text{te}}}} + \Psi(\delta, \Delta_\ell, n_k^{\text{tr}}, n^{\text{te}})$$

where $K_k^{\text{tr}} = O(L_1 S_{p_k^{\text{tr}}} \sqrt{L} \prod_{i=1}^L \Delta_{\mathbf{W}_i})$, $K_l^{\text{te}} = O(\max\{L_1, L_2\} S_{p_l^{\text{te}}} \sqrt{L} \prod_{i=1}^L \Delta_{\mathbf{W}_i})$, *and* $\Psi = \Delta_\ell \sqrt{8(\frac{1}{n_k^{\text{tr}}} + \frac{K(1+C_k)^2}{n^{\text{te}}}) \log \frac{1}{\delta}} + 2(1 + KC_k)\Delta_\ell \exp\left(\frac{-2\eta_k^2}{\Delta_\ell^2/n_k^{\text{tr}} + KC_k^2 \Delta_\ell^2/n^{\text{te}}}\right)$ *for some constant* $\eta_k > 0$.

Finally, we apply union bound and obtain a global ratio estimation error bound that holds for all clients:

Corollary 2 (High-probability ratio estimation error bound for multiple clients)**.** *Let* $0 < \delta_k < 1$ *for* $k \in [K]$*. Let* $\overline{K}^{\text{tr}} = \max_{k \in [K]} K_k^{\text{tr}}$*. For Example J.1 and loss functions described in Theorem 1, with probability at least* $1 - \sum_{k=1}^K \delta_k$*, we have*

$$\max_{k \in [K]} \{\mathcal{E}_f(\hat{r}_k) - \mathcal{E}_f(r_k^*)\} \leq \frac{\overline{K}^{\text{tr}}}{\sqrt{\underline{n}^{\text{tr}}}} + \sum_{l=1}^K \frac{K_l^{\text{te}}}{\sqrt{n^{\text{te}}}} + \overline{\Psi}(\delta, \Delta_\ell, \underline{n}^{\text{tr}}, n^{\text{te}})$$

where $\overline{\Psi} = \Delta_\ell \sqrt{8(\frac{1}{\underline{n}^{\text{tr}}} + \frac{K(1+\overline{C})^2}{n^{\text{te}}}) \log \frac{1}{\underline{\delta}}} + 2(1 + K\overline{C})\Delta_\ell \exp\left(\frac{-2\underline{\eta}^2}{\Delta_\ell^2/\underline{n}^{\text{tr}} + K\overline{C}^2 \Delta_\ell^2/n^{\text{te}}}\right)$, $\overline{C} = \max_{k \in [K]} C_k$, $\underline{n}^{\text{tr}} = \min_{k \in [K]} n_k^{\text{tr}}$, $\underline{\delta} = \min_{k \in [K]} \delta_k$, *and* $\underline{\eta} = \min_{k \in [K]} \eta_k$.

The rates match the optimal minimax rates for example for a density estimation problem when the density belongs to the Hölder function class (Tsybakov, 2008)[Section 2] with a sufficiently large β based on Definition 1.2 of Tsybakov (2008). The $\Omega(1/\sqrt{n})$ lower bounds are obtained for important problems including nonparametric regression, estimation of functionals, nonparametric testing, and finding a linear combination of M functions to be as close as the target data generating function (Nemirovski, 1998)[Section 5.3].

K Additional error due to estimation of $\overline{r}_k$

In this section, we consider a practical scenario where we have access to only in imperfect estimate of $\overline{r}_k = \sup_{\mathbf{x} \in \mathcal{X}^{\text{tr}}} r_k^*(\mathbf{x})$ to find C_k in Eq. (3.2). In particular, we find additional error when using $\tilde{C}_k = \frac{1}{\tilde{r}_k}$ where

$\tilde{r}_k$ is obtained by HDRM in Section 3. The nnBD DRM problem for client k using $\tilde{C}_k$ is $\min_{r_k \in \mathcal{H}_r} \hat{\mathcal{E}}_f^+(r_k)$ where

$$\hat{\mathcal{E}}_f^+(r_k) = \mathrm{ReLU}\Big((\hat{\mathbb{E}}_{p_k^{\mathrm{tr}}} - \tilde{C}_k \sum_{l=1}^{K} \hat{\mathbb{E}}_{p_l^{\mathrm{te}}})[\ell_1(r_k(\mathbf{x}))]\Big) + \sum_{l=1}^{K} \hat{\mathbb{E}}_{p_l^{\mathrm{te}}}[\ell_2(r_k(\mathbf{x}))]. \tag{K.1}$$

Along the lines of the proof of Lemma 3, we can show that the maximal deviation term using $\tilde{C}_k$ is upper bounded with probability at least $1-\delta$:

$$\begin{aligned}\sup_{r_k \in \mathcal{H}_r} |\hat{\mathcal{E}}_f^+(r_k) - \mathbb{E}[\hat{\mathcal{E}}_f^+(r_k)]| \leq 4L_1 R_{n_k^{\mathrm{tr}}}^{p_k^{\mathrm{tr}}}(\mathcal{H}_r) + 4(\tilde{C}_k L_1 + L_2) \sum_{l=1}^{K} R_{n^{\mathrm{te}}}^{p_l^{\mathrm{te}}}(\mathcal{H}_r) \\ + \Delta_\ell \sqrt{2\Big(\frac{1}{n_k^{\mathrm{tr}}} + \frac{K(1+\tilde{C}_k)^2}{n^{\mathrm{te}}}\Big) \log \frac{1}{\delta}}.\end{aligned} \tag{K.2}$$

Under perfect estimate of $\overline{r}_k = \sup_{\mathbf{x} \in \mathcal{X}^{\mathrm{tr}}} r_k^*(\mathbf{x})$ with $C_k = \frac{1}{\overline{r}_k}$, the nnBD DRM problem for client k is $\min_{r_k \in \mathcal{H}_r} \hat{\mathcal{E}}_f^{++}(r_k)$ where

$$\hat{\mathcal{E}}_f^{++}(r_k) = \mathrm{ReLU}\Big((\hat{\mathbb{E}}_{p_k^{\mathrm{tr}}} - C_k \sum_{l=1}^{K} \hat{\mathbb{E}}_{p_l^{\mathrm{te}}})[\ell_1(r_k(\mathbf{x}))]\Big) + \sum_{l=1}^{K} \hat{\mathbb{E}}_{p_l^{\mathrm{te}}}[\ell_2(r_k(\mathbf{x}))]. \tag{K.3}$$

Applying triangle inequality, we first decompose the bias term

$$\begin{aligned}\sup_{r_k \in \mathcal{H}_r} |\mathbb{E}[\hat{\mathcal{E}}_f^+(r_k)] - \mathcal{E}_f(r_k)| \leq \sup_{r_k \in \mathcal{H}_r} |\mathbb{E}[\hat{\mathcal{E}}_f^+(r_k) - \hat{\mathcal{E}}_f^{++}(r_k)]| \\ + \sup_{r_k \in \mathcal{H}_r} |\mathbb{E}[\hat{\mathcal{E}}_f^{++}(r_k)] - \mathcal{E}_f(r_k)|.\end{aligned} \tag{K.4}$$

An upper bound on $\sup_{r_k \in \mathcal{H}_r} |\mathbb{E}[\hat{\mathcal{E}}_f^{++}(r_k)] - \mathcal{E}_f(r_k)|$ is established similar to the proof of Lemma 4:

$$\sup_{r_k \in \mathcal{H}_r} |\mathbb{E}[\hat{\mathcal{E}}_f^{++}(r_k)] - \mathcal{E}_f(r_k)| \leq (1 + KC_k)\Delta_\ell \exp\Big(\frac{-2\eta_k^2}{\Delta_\ell^2/n_k^{\mathrm{tr}} + KC_k^2 \Delta_\ell^2/n^{\mathrm{te}}}\Big).$$

Substituting Eq. (K.1) and Eq. (K.3) into $|\mathbb{E}[\hat{\mathcal{E}}_f^+(r_k) - \hat{\mathcal{E}}_f^{++}(r_k)]|$, we have

$$\begin{aligned}&|\mathbb{E}[\hat{\mathcal{E}}_f^+(r_k) - \hat{\mathcal{E}}_f^{++}(r_k)]| \\ &= |\mathbb{E}[\mathrm{ReLU}((\hat{\mathbb{E}}_{p_k^{\mathrm{tr}}} - \tilde{C}_k \sum_{l=1}^{K} \hat{\mathbb{E}}_{p_l^{\mathrm{te}}})[\ell_1(r_k(\mathbf{x}))]) - \mathrm{ReLU}((\hat{\mathbb{E}}_{p_k^{\mathrm{tr}}} - C_k \sum_{l=1}^{K} \hat{\mathbb{E}}_{p_l^{\mathrm{te}}})[\ell_1(r_k(\mathbf{x}))])]|\,,\end{aligned}$$

which together with $\mathrm{ReLU}(a) - \mathrm{ReLU}(b) \leq |a-b|$ is used to establish the following upper bound:

$$\Big|\mathbb{E}\Big[\hat{\mathcal{E}}_f^+(r_k) - \hat{\mathcal{E}}_f^{++}(r_k)\Big]\Big| \leq K\Delta_\ell |\tilde{C}_k - C_k|. \tag{K.5}$$

Let $m^* = \arg\max_{m \in [M]} \tilde{r}_{k,m}$. We note that by the construction of HDRM, there is a constant lower bound on the numerator of $\tilde{r}_k$, i.e., $\frac{1}{n^{\mathrm{te}}} \sum_{j=1}^{n^{\mathrm{te}}} \sum_{l=1}^{K} \mathbb{1}(\mathbf{x}_{l,j}^{\mathrm{te}} \in \mathcal{B}_{m^*}) \geq \overline{c}$, that is achieved when $\{\mathbf{x}_{l,j}^{\mathrm{te}}\}_{j=1}^{n^{\mathrm{te}}}$ are distributed uniformly across M bins. Let $\mathbf{x} \in \mathcal{X}$ and let $\hat{p}_k^{\mathrm{tr}}(\mathbf{x}; M)$ denote a histogram-based density estimate of $p_k^{\mathrm{tr}}(\mathbf{x})$ with M bins. The maximum value of $\tilde{C}_k$ is attained when $\frac{1}{n^{\mathrm{te}}} \sum_{j=1}^{n^{\mathrm{te}}} \sum_{l=1}^{K} \mathbb{1}(\mathbf{x}_{l,j}^{\mathrm{te}} \in \mathcal{B}_{m^*})$ meets its lower bound, which leads to the maximum deviation from $C_k \leq \tilde{C}_k$. Assuming $p_k^{\mathrm{tr}}(\mathbf{x})$ is L_k-Lipschitz with $\sup_{\mathbf{x} \in \mathcal{X}} p_k^{\mathrm{tr}}(\mathbf{x}) < \infty$, the mean squared error of a histogram-based density estimate with M bins is upper

bounded by (Wasserman, 2006, Section 6): $\mathbb{E}|\hat{p}_k^{\mathrm{tr}}(\mathbf{x}; M) - p_k^{\mathrm{tr}}(\mathbf{x})|^2 = \mathcal{O}(L_k^2/M^2 + M/n_k^{\mathrm{tr}})$. Putting together with a constant lower bound on the numerator of $\tilde{r}_k$ and applying Jensen's inequality, we have:

$$\mathbb{E}[|\tilde{C}_k - C_k|] \lesssim \frac{1}{M} + \sqrt{\frac{M}{n_k^{\mathrm{tr}}}}\,.$$

L Proof of Lemma 1

We first note that

$$\mathbb{E}[L(\hat{\boldsymbol{\theta}})] - L(\boldsymbol{\theta}_*) = \mathbb{E}\|\hat{\boldsymbol{\theta}} - \boldsymbol{\theta}_*\|_{\boldsymbol{\Sigma}^{\mathrm{te}}}^2 = \text{Bias} + \text{Variance}\,.$$

We first find the expression for $\hat{\boldsymbol{\theta}}$ considering the ridge regression problem assuming $\frac{p^{\mathrm{te}}(\mathbf{x})}{p^{\mathrm{tr}}(\mathbf{x})}$ is given. FIDEM problem with Tikhonov regularization is given by

$$\hat{\boldsymbol{\theta}} = \arg\min_{\boldsymbol{\theta}} \sum_{i=1}^{n} w_i(\boldsymbol{\theta}^\top \mathbf{x}_i - y_i)^2 + \lambda\|\boldsymbol{\theta}\|_2^2$$

where $w_i = \frac{p^{\mathrm{te}}(\mathbf{x}_i)}{p^{\mathrm{tr}}(\mathbf{x}_i)}$ and λ is the regularization parameter. This is a reweighted least squares problem.

The objective function above is strongly convex and differentiable. Applying the fist-order condition, the unique minimum is as follows:

$$\hat{\boldsymbol{\theta}} = \left(\mathbf{X}^\top \mathbf{W}\mathbf{X} + \lambda \mathbf{I}_d\right)^{-1} \mathbf{X}^\top \mathbf{W}\mathbf{y} \tag{L.1}$$

where $\mathbf{W} = \mathrm{diag}(w_1, \ldots, w_n)$.

Substituting $\mathbf{y} = \mathbf{X}\boldsymbol{\theta}_* + \boldsymbol{\epsilon}$ into (L.1), we note that

$$\hat{\boldsymbol{\theta}} = \left(\mathbf{X}^\top \mathbf{W}\mathbf{X} + \lambda \mathbf{I}_d\right)^{-1} \mathbf{X}^\top \mathbf{W}\mathbf{X}\boldsymbol{\theta}_* + \left(\mathbf{X}^\top \mathbf{W}\mathbf{X} + \lambda \mathbf{I}_d\right)^{-1} \mathbf{X}^\top \mathbf{W}\boldsymbol{\epsilon}$$

and

$$\mathbb{E}_{\mathbf{X},\boldsymbol{\epsilon}}[\hat{\boldsymbol{\theta}}] = \mathbb{E}_{\mathbf{X}}\left[\left(\mathbf{X}^\top \mathbf{W}\mathbf{X} + \lambda \mathbf{I}_d\right)^{-1} \mathbf{X}^\top \mathbf{W}\mathbf{X}\boldsymbol{\theta}_*\right].$$

We now characterize the bias $\mathtt{B}(\hat{\boldsymbol{\theta}})$ and variance $\mathtt{V}(\hat{\boldsymbol{\theta}})$ terms when the model estimate is given by (L.1).

Let $\|\mathbf{x}\|_{\mathbf{A}}^2 := \mathbf{x}^\top \mathbf{A}\mathbf{x}$. Substituting the expression for $\hat{\boldsymbol{\theta}}$ into $R(\hat{\boldsymbol{\theta}})$, the excess risk can be decomposed into a bias and a variance term as follows:

$$\begin{aligned}
R(\hat{\boldsymbol{\theta}}) &= \mathbb{E}_{\mathbf{X},\boldsymbol{\epsilon},\mathbf{x},\epsilon_{\mathrm{te}}}[(y - \hat{\boldsymbol{\theta}}^\top \mathbf{x})^2 - (y - \boldsymbol{\theta}_*^\top \mathbf{x})^2] \\
&= \mathbb{E}_{\mathbf{X},\boldsymbol{\epsilon},\mathbf{x},\epsilon_{\mathrm{te}}}[\left(y - \boldsymbol{\theta}_*^\top \mathbf{x} + (\boldsymbol{\theta}_* - \hat{\boldsymbol{\theta}})^\top \mathbf{x}\right)^2 - (y - \boldsymbol{\theta}_*^\top \mathbf{x})^2] \\
&= \mathbb{E}_{\mathbf{X},\boldsymbol{\epsilon},\mathbf{x}}\left[\left((\boldsymbol{\theta}_* - \hat{\boldsymbol{\theta}})^\top \mathbf{x}\right)^2\right] \\
&= \mathbb{E}_{\mathbf{X},\boldsymbol{\epsilon}}[\|\boldsymbol{\theta}_* - \hat{\boldsymbol{\theta}}\|_{\boldsymbol{\Sigma}^{\mathrm{te}}}^2] \\
&= \mathtt{B} + \mathtt{V}
\end{aligned}$$

where the bias is given by

$$\begin{aligned}
\mathtt{B} &= \mathbb{E}_{\mathbf{X},\boldsymbol{\epsilon}}\left[\left\|\left(\mathbf{X}^\top \mathbf{W}\mathbf{X} + \lambda \mathbf{I}_d\right)^{-1} \mathbf{X}^\top \mathbf{W}\mathbf{X}\boldsymbol{\theta}_* - \boldsymbol{\theta}_*\right\|_{\boldsymbol{\Sigma}^{\mathrm{te}}}^2\right] \\
&= \mathbb{E}_{\mathbf{X}}\left[\left\|\left(\mathbf{X}^\top \mathbf{W}\mathbf{X} + \lambda \mathbf{I}_d\right)^{-1} \lambda\boldsymbol{\theta}_*\right\|_{\boldsymbol{\Sigma}^{\mathrm{te}}}^2\right]. \\
&= \lambda^2 \boldsymbol{\theta}_*^\top \mathbb{E}_{\mathbf{X}}[\boldsymbol{\Delta}_{\mathbf{W},\lambda}\boldsymbol{\Sigma}^{\mathrm{te}}\boldsymbol{\Delta}_{\mathbf{W},\lambda}]\boldsymbol{\theta}_*
\end{aligned}$$

with

$$\boldsymbol{\Delta}_{\mathbf{W},\lambda} = \left[\left(\mathbf{X}^\top \mathbf{W}\mathbf{X} + \lambda \mathbf{I}_d\right)^{-1}\right],$$

and the variance is given by

$$\begin{aligned}\mathtt{V} &= \mathbb{E}_{\mathbf{X},\boldsymbol{\epsilon}}\left[\left\|\left(\mathbf{X}^\top \mathbf{W}\mathbf{X} + \lambda \mathbf{I}_d\right)^{-1}\mathbf{X}^\top \mathbf{W}\boldsymbol{\epsilon}\right\|^2_{\boldsymbol{\Sigma}^{\mathrm{te}}}\right] \\ &= \sigma_\epsilon^2 \mathbb{E}_{\mathbf{X}}\left[\mathrm{tr}\left(\Phi_V\right)\right].\end{aligned}$$

where $\Phi_V = \left(\mathbf{X}^\top \mathbf{W}\mathbf{X} + \lambda \mathbf{I}_d\right)^{-1}\mathbf{X}^\top \mathbf{W}^2\mathbf{X}\left(\mathbf{X}^\top \mathbf{W}\mathbf{X} + \lambda \mathbf{I}_d\right)^{-1}\boldsymbol{\Sigma}^{\mathrm{te}}$.

M Proof of Theorem 2

In the one-hot case, it is clear that $\mathbf{X}^\top\mathbf{X} = \sum_{i=1}^n \mathbf{x}_i\mathbf{x}_i^\top$ and $\mathbf{X}^\top\mathbf{W}\mathbf{X} = \sum_{i=1}^n w_i\mathbf{x}_i\mathbf{x}_i^\top$ are diagonal matrices. For bias in the one-hot setting, we have

$$\begin{aligned}\mathtt{B}(\hat{\boldsymbol{\theta}}) &= \lambda^2\left[\boldsymbol{\theta}_*^\top\left(\mathbf{X}^\top\mathbf{W}\mathbf{X} + \lambda\mathbf{I}\right)^{-1}\boldsymbol{\Sigma}^{\mathrm{te}}\left(\mathbf{X}^\top\mathbf{W}\mathbf{X} + \lambda\mathbf{I}\right)^{-1}\boldsymbol{\theta}_*\right] \\ &= \lambda^2\sum_{i=1}^d \frac{[(\boldsymbol{\theta}_*)_i]^2\lambda_i'}{\left(\lambda_i(\mathbf{X}^\top\mathbf{W}\mathbf{X}) + \lambda\right)^2} \\ &= \lambda^2\sum_{i=1}^d \frac{[(\boldsymbol{\theta}_*)_i]^2\lambda_i'}{\left[\mu_i w_i + \lambda\right]^2}\end{aligned}$$

where the equation holds by the fact that, all matrices are diagonal including $\mathbf{X}^\top\mathbf{X}$, $\mathbf{X}^\top\mathbf{W}\mathbf{X}$, and $\boldsymbol{\Sigma}^{\mathrm{te}}$. Accordingly, we have $\lambda_i(\mathbf{X}^\top\mathbf{W}\mathbf{X}) = \lambda_i(\mathbf{X}^\top\mathbf{X})\lambda_i(\mathbf{W})$ with $i \in [d]$. For the classical ERM, the bias is

$$\mathtt{B}(\boldsymbol{\theta}^{\mathrm{v}}) = \lambda^2\sum_{i=1}^d \frac{[(\boldsymbol{\theta}_*)_i]^2\lambda_i}{\left[\mu_i + \lambda\right]^2}$$

where λ_i is the eigenvalue of $\boldsymbol{\Sigma}^{\mathrm{tr}}$. To achieve $\mathtt{B}(\hat{\boldsymbol{\theta}}) \leqslant \mathtt{B}(\boldsymbol{\theta}^{\mathrm{v}})$, we have to make some assumptions on the relationship between λ_i, λ_i' and w_i. Our analysis of error bound requires

$$\frac{\lambda_i'}{\left[\mu_i w_i + \lambda\right]^2} \leqslant \frac{\lambda_i}{\left[\mu_i + \lambda\right]^2} \Leftrightarrow \frac{\mu_i + \lambda}{\mu_i w_i + \lambda} \leqslant \sqrt{\frac{\lambda_i}{\lambda_i'}}, \tag{M.1}$$

which implies

$$w_i \geqslant \sqrt{\frac{\lambda_i'}{\lambda_i}} - 1, \tag{M.2}$$

such that Eq. (M.1) holds where we use the inequality $\frac{a+c}{b+c} \leqslant \frac{a}{b} + 1$ for any $a, b, c > 0$.

For the vanilla ERM, the variance is

$$\mathtt{V}(\boldsymbol{\theta}^{\mathrm{v}}) = \sigma_\epsilon^2\sum_{i=1}^d \frac{\lambda_i\mu_i}{\left[\mu_i + \lambda\right]^2}.$$

For FIDEM, the variance is

$$\begin{aligned}\mathtt{V}(\hat{\boldsymbol{\theta}}) &= \sigma_\epsilon^2\left[\left(\mathbf{X}^\top\mathbf{W}\mathbf{X} + \lambda\mathbf{I}\right)^{-1}\mathbf{X}^\top\mathbf{W}^2\mathbf{X}\left(\mathbf{X}^\top\mathbf{W}\mathbf{X} + \lambda\mathbf{I}\right)^{-1}\boldsymbol{\Sigma}^{\mathrm{te}}\right] \\ &= \sigma_\epsilon^2\sum_{i=1}^d \frac{\lambda_i'\lambda_i(\mathbf{X}^\top\mathbf{W}^2\mathbf{X})}{\left(\lambda_i(\mathbf{X}^\top\mathbf{W}\mathbf{X}) + \lambda\right)^2} \\ &= \sigma_\epsilon^2\sum_{i=1}^d \frac{\lambda_i'\mu_i w_i^2}{\left[\mu_i w_i + \lambda\right]^2}.\end{aligned}$$

We note that $\mathtt{V}(\hat{\boldsymbol{\theta}}) \leq \mathtt{V}(\boldsymbol{\theta}^{\mathrm{v}})$ can be achieved by

$$\frac{\lambda_i \mu_i}{[\mu_i + \lambda]^2} \geq \frac{\lambda_i' \mu_i w_i^2}{[\mu_i w_i + \lambda]^2}\,.$$

This can be obtained by

$$\frac{\mu_i + \frac{\lambda}{w_i}}{\mu_i + \lambda} \geq \frac{\frac{\lambda}{w_i}}{\mu_i + \lambda} \geq \sqrt{\frac{\lambda_i'}{\lambda_i}}\,, \tag{M.3}$$

which implies $w_i \leqslant \xi_i \sqrt{\frac{\lambda_i}{\lambda_i'}}$. Combining Eqs. (M.2) and (M.3), the proof is complete.

N When FIDEM cannot outperform ERM

In this section, we provide a counterexample to show that, under which certain case, FIDEM cannot provably outperform ERM.

Proposition 3. *Under the same setting of Theorem 2, i.e., the fixed-design setting and label noise assumption, under the following condition*

$$\sqrt{\frac{\lambda_i'}{\lambda_i}} \geqslant \max\{\xi, 1-\xi\}\,.$$

If the ratio satisfies

$$w_i \leqslant \min\left\{\frac{1}{\frac{\sqrt{\lambda_i'/\lambda_i}-1}{\xi}+1}, \sqrt{\frac{\lambda_i'}{\lambda_i}} + \frac{\lambda}{\mu_i}\sqrt{\frac{\lambda_i'}{\lambda_i}} - \frac{\lambda}{\mu_i}\right\}, \tag{N.1}$$

then we have

$$R(\boldsymbol{\theta}^{\mathrm{v}}) \leqslant R(\hat{\boldsymbol{\theta}})\,.$$

Proof. According to Eq. (M.1), $\mathtt{B}(\boldsymbol{\theta}^{\mathrm{v}}) \leqslant \mathtt{B}(\hat{\boldsymbol{\theta}})$ holds by

$$\frac{\mu_i + \lambda}{\mu_i w_i + \lambda} \geqslant \sqrt{\frac{\lambda_i}{\lambda_i'}}\,,$$

which is equivalent to

$$w_i \leqslant \sqrt{\frac{\lambda_i'}{\lambda_i}} + \frac{\lambda}{\mu_i}\sqrt{\frac{\lambda_i'}{\lambda_i}} - \frac{\lambda}{\mu_i}\,. \tag{N.2}$$

According to Eq. (M.3), $\mathtt{V}(\boldsymbol{\theta}^{\mathrm{v}}) \leqslant \mathtt{V}(\hat{\boldsymbol{\theta}})$ holds by

$$\frac{\mu_i + \frac{\lambda}{w_i}}{\mu_i + \lambda} \leq \sqrt{\frac{\lambda_i'}{\lambda_i}}\,,$$

which is equivalent to

$$w_i \leqslant \frac{1}{\frac{\sqrt{\frac{\lambda_i'}{\lambda_i}}-1}{\xi}+1}\,. \tag{N.3}$$

Combining Eqs. (N.2) and (N.3), the proof is complete. To validate the condition in Eq. (N.1), we require each term in the RHS to be nonnegative. That implies

$$\sqrt{\frac{\lambda_i'}{\lambda_i}} \geqslant \max\{\xi, 1-\xi\}\,,$$

which is our condition in Proposition 3.

By checking Eqs. (N.2) and (N.3), in both cases $\sqrt{\frac{\lambda_i'}{\lambda_i}} \geq 1$ and $\sqrt{\frac{\lambda_i'}{\lambda_i}} \leq 1$, we have

$$w_i \leqslant 1\,.$$

■

O Experimental details and additional experiments

Datasets: We make use of three datasets in the experiments: *MNIST* (LeCun et al., 1998), *Fashion MNIST*[7] (Xiao et al., 2017), and *CIFAR10* (Krizhevsky et al., 2009). *MNIST* consists of images depicting handwritten digits from 0 to 9. The resolution of each image is 28×28. The dataset includes $60,000$ images for training. Similarly *Fashion MNIST* includes grayscale images of clothing of resolution 28×28. The training set consists of $60,000$ examples, and the test set of $10,000$ examples. *CIFAR10* consists of colored images with a resolution of 32×32. The training set contains $50,000$ examples while the test set contains $10,000$ examples.

Experimental setup: For all experiments we use the cross entropy loss. The stochastic gradient for each of the clients are computed with a batch size of 64 and aggregated on the server, which uses the Adam optimizer. Experiments on *MNIST* and *Fashion MNIST* uses a LeNet (LeCun et al., 1998), a learning rate of 0.001, no weight decay, and runs for $5,000$ iterations. For *CIFAR10* experiments we use the larger ResNet-18 (He et al., 2016). Batch normalization in ResNet-18 is treated by averaging the statistics on the server and subsequently broadcasting to the workers. A learning rate of 0.0001 and weight decay of 0.0001 are used. We report the best iterate in terms of average test accuracy after $20,000$ iterations. All reported mean and standard deviations are computed over 5 independent runs except for CIFAR10 which uses 3 independent runs. For target shift the randomisation is also over the realization of the class distributions to ensure that the conclusions are not due to the particularities of the sub-sampled images. All experiments are carried out on an internal cluster using one GPU.

O.1 Target shift

For the target shift experiments on *Fashion MNIST* in Table 1, we summarize the different number of data points for each dataset split in Table 9. A similar distribution across clients is used for the additional experiments for FIDEM and FedAvg on *CIFAR10* (Table 8). *CIFAR10* differs from *Fashion MNIST* in the number of examples due to the training set being smaller. The results for *CIFAR10* in Table 7 shows that FIDEM uniformly improves the accuracy over FedAvg on this difficult target shift instance. We additionally include a two-client setting in Table 10 with the associated distribution described in Table 11.

To compute the exact ratio $r(\mathbf{x})$ we will assume that the distributions are separable.

Definition 3 (Separability)**.** *A distribution over $\mathcal{X} \times \mathcal{Y}$ is separable if there exists a partition $(\mathcal{X}_i)_{i=1}^m$ of $\mathcal{X}$ such that $p(y_i|\mathcal{X}_i) = 1$ for some $y_i \in \mathcal{Y}$ and all $i \in [m]$. We denote the associated deterministic label assignment as $g : \mathcal{X} \to \mathcal{Y}$.*

Proposition 4. *Assume that the distributions $p^{\mathrm{te}}(\mathbf{x}, y)$ and $p^{\mathrm{tr}}(\mathbf{x}, y)$ are both separable. Then the ratio can be computed based on the associated label $y := g(\mathbf{x})$ as follows,*

$$r(x) = \frac{p^{\mathrm{te}}(y)}{p^{\mathrm{tr}}(y)}. \tag{O.1}$$

Proof. Due to separability, $p^{\mathrm{te}}(y|x) = p^{\mathrm{tr}}(y|\mathbf{x})$. So

$$r(\mathbf{x}) := \frac{p^{\mathrm{te}}(\mathbf{x})}{p^{\mathrm{tr}}(\mathbf{x})} = \frac{p^{\mathrm{te}}(\mathbf{x})p^{\mathrm{te}}(y|\mathbf{x})}{p^{\mathrm{tr}}(\mathbf{x})p^{\mathrm{tr}}(y|\mathbf{x})} = \frac{p^{\mathrm{te}}(\mathbf{x}, y)}{p^{\mathrm{tr}}(\mathbf{x}, y)}. \tag{O.2}$$

[7] *Fashion MNIST* is provided under the MIT license.

Table 6: CIFAR10 target shift distribution across 100 clients where groups of 10 clients shares the same distribution.

		Class									
		0	1	2	3	4	5	6	7	8	9
Client 1-10	Train	$^{95}/_{100}$	$^{5}/_{9}$	$^{5}/_{9}$	$^{5}/_{9}$	$^{5}/_{9}$	$^{5}/_{9}$	$^{5}/_{9}$	$^{5}/_{9}$	$^{5}/_{9}$	$^{5}/_{9}$
	Test	$^{5}/_{9}$	$^{5}/_{9}$	$^{5}/_{9}$	$^{5}/_{9}$	$^{5}/_{9}$	$^{5}/_{9}$	$^{5}/_{9}$	$^{5}/_{9}$	$^{5}/_{9}$	$^{95}/_{100}$
Client 11-20	Train	$^{5}/_{9}$	$^{95}/_{100}$	$^{5}/_{9}$	$^{5}/_{9}$	$^{5}/_{9}$	$^{5}/_{9}$	$^{5}/_{9}$	$^{5}/_{9}$	$^{5}/_{9}$	$^{5}/_{9}$
	Test	$^{5}/_{9}$	$^{5}/_{9}$	$^{5}/_{9}$	$^{5}/_{9}$	$^{5}/_{9}$	$^{5}/_{9}$	$^{5}/_{9}$	$^{5}/_{9}$	$^{95}/_{100}$	$^{5}/_{9}$
Client 21-30	Train	$^{5}/_{9}$	$^{5}/_{9}$	$^{95}/_{100}$	$^{5}/_{9}$	$^{5}/_{9}$	$^{5}/_{9}$	$^{5}/_{9}$	$^{5}/_{9}$	$^{5}/_{9}$	$^{5}/_{9}$
	Test	$^{5}/_{9}$	$^{5}/_{9}$	$^{5}/_{9}$	$^{5}/_{9}$	$^{5}/_{9}$	$^{5}/_{9}$	$^{5}/_{9}$	$^{95}/_{100}$	$^{5}/_{9}$	$^{5}/_{9}$
Client 31-40	Train	$^{5}/_{9}$	$^{5}/_{9}$	$^{5}/_{9}$	$^{95}/_{100}$	$^{5}/_{9}$	$^{5}/_{9}$	$^{5}/_{9}$	$^{5}/_{9}$	$^{5}/_{9}$	$^{5}/_{9}$
	Test	$^{5}/_{9}$	$^{5}/_{9}$	$^{5}/_{9}$	$^{5}/_{9}$	$^{5}/_{9}$	$^{5}/_{9}$	$^{95}/_{100}$	$^{5}/_{9}$	$^{5}/_{9}$	$^{5}/_{9}$
Client 41-50	Train	$^{5}/_{9}$	$^{5}/_{9}$	$^{5}/_{9}$	$^{5}/_{9}$	$^{95}/_{100}$	$^{5}/_{9}$	$^{5}/_{9}$	$^{5}/_{9}$	$^{5}/_{9}$	$^{5}/_{9}$
	Test	$^{5}/_{9}$	$^{5}/_{9}$	$^{5}/_{9}$	$^{5}/_{9}$	$^{5}/_{9}$	$^{95}/_{100}$	$^{5}/_{9}$	$^{5}/_{9}$	$^{5}/_{9}$	$^{5}/_{9}$
Client 51-60	Train	$^{5}/_{9}$	$^{5}/_{9}$	$^{5}/_{9}$	$^{5}/_{9}$	$^{5}/_{9}$	$^{95}/_{100}$	$^{5}/_{9}$	$^{5}/_{9}$	$^{5}/_{9}$	$^{5}/_{9}$
	Test	$^{5}/_{9}$	$^{5}/_{9}$	$^{5}/_{9}$	$^{5}/_{9}$	$^{95}/_{100}$	$^{5}/_{9}$	$^{5}/_{9}$	$^{5}/_{9}$	$^{5}/_{9}$	$^{5}/_{9}$
Client 61-70	Train	$^{5}/_{9}$	$^{5}/_{9}$	$^{5}/_{9}$	$^{5}/_{9}$	$^{5}/_{9}$	$^{5}/_{9}$	$^{95}/_{100}$	$^{5}/_{9}$	$^{5}/_{9}$	$^{5}/_{9}$
	Test	$^{5}/_{9}$	$^{5}/_{9}$	$^{5}/_{9}$	$^{95}/_{100}$	$^{5}/_{9}$	$^{5}/_{9}$	$^{5}/_{9}$	$^{5}/_{9}$	$^{5}/_{9}$	$^{5}/_{9}$
Client 71-80	Train	$^{5}/_{9}$	$^{5}/_{9}$	$^{5}/_{9}$	$^{5}/_{9}$	$^{5}/_{9}$	$^{5}/_{9}$	$^{5}/_{9}$	$^{95}/_{100}$	$^{5}/_{9}$	$^{5}/_{9}$
	Test	$^{5}/_{9}$	$^{5}/_{9}$	$^{95}/_{100}$	$^{5}/_{9}$	$^{5}/_{9}$	$^{5}/_{9}$	$^{5}/_{9}$	$^{5}/_{9}$	$^{5}/_{9}$	$^{5}/_{9}$
Client 81-90	Train	$^{5}/_{9}$	$^{5}/_{9}$	$^{5}/_{9}$	$^{5}/_{9}$	$^{5}/_{9}$	$^{5}/_{9}$	$^{5}/_{9}$	$^{5}/_{9}$	$^{95}/_{100}$	$^{5}/_{9}$
	Test	$^{5}/_{9}$	$^{95}/_{100}$	$^{5}/_{9}$	$^{5}/_{9}$	$^{5}/_{9}$	$^{5}/_{9}$	$^{5}/_{9}$	$^{5}/_{9}$	$^{5}/_{9}$	$^{5}/_{9}$
Client 91-100	Train	$^{5}/_{9}$	$^{5}/_{9}$	$^{5}/_{9}$	$^{5}/_{9}$	$^{5}/_{9}$	$^{5}/_{9}$	$^{5}/_{9}$	$^{5}/_{9}$	$^{5}/_{9}$	$^{95}/_{100}$
	Test	$^{95}/_{100}$	$^{5}/_{9}$	$^{5}/_{9}$	$^{5}/_{9}$	$^{5}/_{9}$	$^{5}/_{9}$	$^{5}/_{9}$	$^{5}/_{9}$	$^{5}/_{9}$	$^{5}/_{9}$

Table 7: Target shift on CIFAR10 with ResNet-18.

	FIDEM	**FedAvg**
Average accuracy	**0.6004** $\pm$ 0.0076	0.4426 $\pm$ 0.0291
Client 1 accuracy	**0.6714** $\pm$ 0.0153	0.3984 $\pm$ 0.1497
Client 2 accuracy	**0.8196** $\pm$ 0.0962	0.7307 $\pm$ 0.1533
Client 3 accuracy	**0.5412** $\pm$ 0.0776	0.3333 $\pm$ 0.2251
Client 4 accuracy	**0.5087** $\pm$ 0.0827	0.3030 $\pm$ 0.1106
Client 5 accuracy	**0.4610** $\pm$ 0.0508	0.4476 $\pm$ 0.3649

It follows that,

$$\frac{p^{\text{te}}(\mathbf{x}, y)}{p^{\text{tr}}(\mathbf{x}, y)} = \frac{p^{\text{te}}(\mathbf{x}|y)p^{\text{te}}(y)}{p^{\text{tr}}(\mathbf{x}|y)p^{\text{tr}}(y)}. \tag{O.3}$$

Using the definition of the target shift assumption, $p^{\text{te}}(\mathbf{x}|y) = p^{\text{tr}}(\mathbf{x}|y)$, the conditional distributions cancel and we obtain the claim. ■

Proposition 4 provides a way to compute the ratio $r(\mathbf{x})$ when the labels are available and the shift is known.

O.2 Covariate shift

The color flipping probability used to generate each of the colored MNIST datasets for the covariate shift experiment can be found in Table 12. We consider an asymmetric client setup where client 1 in addition has 40 times less training examples than client 2.

Table 8: CIFAR10 target shift distribution.

		Class									
		0	1	2	3	4	5	6	7	8	9
Client 1	Train	28	28	28	28	28	4885	28	28	28	28
	Test	977	5	5	5	5	5	5	5	5	5
Client 2	Train	28	28	28	28	28	28	4885	28	28	28
	Test	5	977	5	5	5	5	5	5	5	5
Client 3	Train	28	28	28	28	28	28	28	4885	28	28
	Test	5	5	977	5	5	5	5	5	5	5
Client 4	Train	28	28	28	28	28	28	28	28	4885	28
	Test	5	5	5	977	5	5	5	5	5	5
Client 5	Train	28	28	28	28	28	28	28	28	28	4885
	Test	5	5	5	5	977	5	5	5	5	5

Table 9: Fashion MNIST target shift distribution.

		Class									
		0	1	2	3	4	5	6	7	8	9
Client 1	Train	34	34	34	34	34	5862	34	34	34	34
	Test	977	5	5	5	5	5	5	5	5	5
Client 2	Train	34	34	34	34	34	34	5862	34	34	34
	Test	5	977	5	5	5	5	5	5	5	5
Client 3	Train	34	34	34	34	34	34	34	5862	34	34
	Test	5	5	977	5	5	5	5	5	5	5
Client 4	Train	34	34	34	34	34	34	34	34	5862	34
	Test	5	5	5	977	5	5	5	5	5	5
Client 5	Train	34	34	34	34	34	34	34	34	34	5862
	Test	5	5	5	5	977	5	5	5	5	5

Table 10: Fashion MNIST with target shift across two clients.

	FIDEM	**FIIDEM**	**FedAvg**
Average accuracy	**0.82** $\pm$ 0.00	0.76 $\pm$ 0.01	0.76 $\pm$ 0.01
Client 1 accuracy	0.89 $\pm$ 0.01	0.80 $\pm$ 0.02	**0.94** $\pm$ 0.00
Client 2 accuracy	**0.74** $\pm$ 0.01	0.71 $\pm$ 0.02	0.58 $\pm$ 0.01

P Computational complexity of Algorithm 1

We note that clients compute the ratios *in parallel* where each client needs to estimate one ratio. To estimate density ratios for FIDEM, clients require to send a few unlabelled test samples *only once*. The server shuffles those samples and broadcasts the shuffled version to clients *only once*. Compared to FedAvg, the additional computational cost per client is $\mathcal{O}(TN_k)$ where T is the number of iterations for Algorithm 1 to converge and N_k is the number of batches for ratio estimation. Compared to baseline FedAvg, the additional computation of FIDEM is negligible but leads to substantial improvements of the overall generalization in settings under challenging distribution shifts.

Table 11: Two-client Fashion MNIST. The number of samples for each class across the different datasets.

		Class									
		0	1	2	3	4	5	6	7	8	9
Client 1	Train	100	100	100	100	100	100	100	100	100	100
	Test	9	9	9	9	9	990	990	990	990	990
Client 2	Train	39	39	39	39	39	3986	3986	3986	3986	3986
	Test	990	990	990	990	990	9	9	9	9	9

Table 12: For covariate shift the datasets for each of the client are constructed using different probabilities.

	$p_1^{\text{tr}}(\mathbf{x})$	$p_1^{\text{te}}(\mathbf{x})$	$p_2^{\text{tr}}(\mathbf{x})$	$p_2^{\text{te}}(\mathbf{x})$
Probability of flipping color	0.5	0.2	0.2	0.8

Table 13: Estimating ratio upper bound with k-means clustering. We consider the target shift setup, such that a tight upper bound is known, and construct a single client variant for simplicity. We specifically consider MNIST with a label distribution during training and testing to be $q^{\text{tr}} \propto (1/20, 1/20, 1/20, 1/20, 1/20, 1, 1, 1, 1, 1)^\top$ and $q^{\text{te}} \propto (1, 1, 1, 1, 1, 1/20, 1/20, 1/20, 1/20, 1/20)^\top$ respectively. The table shows the estimated upper bound on the ratio ($\tilde{r}$) for a range of clustering sizes. A reasonable estimate of the true maximal ratio of 20 is obtained for a wide range of clustering sizes. Whereas naively binning the space can be problematic due to division by zero, the clustering approach is less prone to this issue as long as #(clusters) $\ll$ #(datapoints).

#(clusters)	10	20	40	50	100	200	500
$\tilde{r}$	10.31	15.48	19.08	27.41	31.47	32.84	206.76

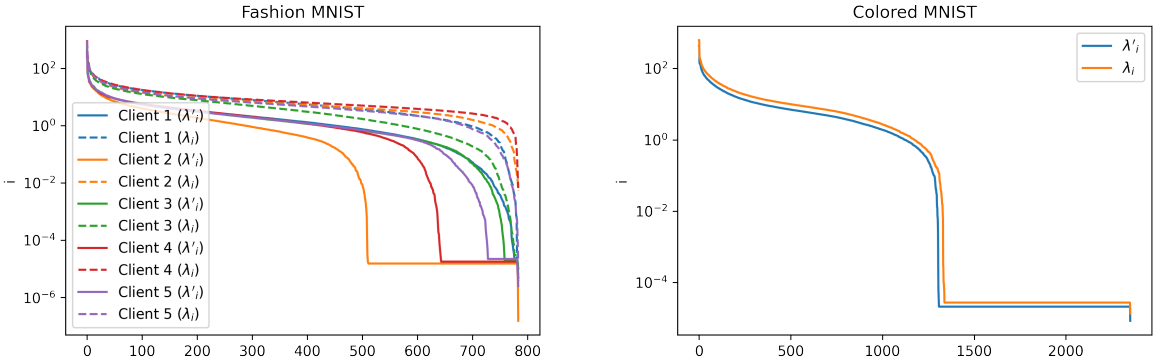

Figure 3: The sudden increase in the eigenvalue ratio observed in for i larger than 780 and 1300 in Fashion MNIST and CMNIST respectively is most likely due to numerical error. We plot the eigenvalues under the test distributions (λ') and under the training distribution (λ) and observe that indeed the eigenvalues suddenly drop very close to zero.

Q Limitations

In this paper, we focus on settings where ratio estimation is required *once* prior to model training. Handling distribution shifts in complex non-stationary settings where ratio estimation is an ongoing process is an interesting problem for future work.

In addition, various personalization methods have been proposed to improve fairness in terms of uniformity of model performance across clients (Li et al., 2021a;b). To meet specific requirements of each client, our global model can be combined with a personalized model on each client. Developing new variants of FIDEM with a focus on fairness is an interesting problem for future work.

To estimate $\{r_k(\mathbf{x})\}_{k=1}^K$, clients need to send unlabelled samples $\mathbf{x}_{l,j}^{\mathrm{te}}$ for $l \in [K]$ and $j \in [n^{\mathrm{te}}]$ from their test distributions. We note that instead of their true samples, clients can alternatively send samples generated from a *generative model* (Goodfellow et al., 2020).

Note that training GANs may be computationally extensive due to required computational resources and availability of representative samples. However, we propose to use GANs as an alternative method with clear caveats, only when 1) clients have sufficient computational resources and 2) they are unwilling to share unlabelled data with the server.

As a partial mitigation of privacy risks, we introduced FIIDEM. FIIDEM does not require any data sharing among clients and does not require any GAN training. In this paper, we focus on FIDEM since it outputs an unbiased estimate of a minimizer of the overall *true risk*, and enables us to theoretically show the benefit of importance weighting in generalization.

One particular challenge in real-world cross-device FL is to estimate ratios on real-world datasets such as WILDS (Koh et al., 2021) and LEAF (Caldas et al., 2019). WILDS has been mostly used for domain generalization, where the setting is not similar to ours. We still have to decide on an arbitrary test/train split. LEAF mainly captures inter-client distribution shifts and settings where different clients have different numbers of examples over thousands of clients. This work is not about scalability to thousands of clients experimentally using our single GPU simulated setup. While we anticipate efficient ratio estimation will improve over time, our FIDEM and FIIDEM formulations along with improved ratio estimates will provide reasonable solutions to learn an effective global model in real-world cross-device FL under covariate shifts.